AN INVESTIGATION OF MINERALS USING MICROWAVE MEASUREMENT OF COMPLEX PERMITTIVITY

Graeme Pendock

Dissertation submitted as a Half-Thesis to the Department of Electrical and Electronic Engineering, University of Cape Town, in partial fulfillment of the degree of Master of Engineering.

April 1990

SYNOPSIS

Microwave measurement techniques have found many industrial and commercial applications. This measurement potential of microwaves, together with observations that different minerals show different microwave heating characteristics, suggests the possibility of applying microwave techniques to various forms of mineral analysis. Simple, low cost, on-line mineral analysis techniques are of interest to the mining industry.

The objectives of this research project were to cover the background theory of microwave interaction with minerals and to investigate different microwave measurement techniques that could possibly be applied to mineral measurement. Measurements were then to be performed on selected minerals in order to observe any differences between them. Finally, to comment on the feasibility of using microwave measurement techniques for the differentiation, identification and analysis of minerals.

This thesis begins by explaining how minerals can very often be considered as dielectrics and how their electrical properties can thus be fully characterised by their complex permittivity. Microwave methods of measuring complex permittivity and possible problems in applying these to mineral measurement are covered. Two methods, the short circuited coaxial line method and cavity perturbation, were selected for testing on the various minerals chosen for this study. The minerals measured in this study were all in powdered form, as this is how they would occur in most industrial applications. Problems with repeatability resulting from using powders are addressed.

The short circuited coaxial line technique was considered suitable since it enables wide bandwidth permittivity measurements to be made. The theory, equations and measurement method are described. Unfortunately, testing of the experimental system showed the method was prone to large errors that limited the success of the experiment. The sources of these errors are explained. Tests did, however, show that there were no

significantly large variations in the mineral dielectric constants over the 1 GHz to 8 GHz frequency range covered.

The second measurement method investigated is a cavity perturbation technique using a 1 GHz cylindrical cavity operating in a TM_{010} mode. Cavity perturbation techniques provide a high sensitivity in measuring dielectric loss. The theory behind cavity perturbation and the measurement system used is described. The system was very successful with tests showing that the complex permittivities of dielectrics could be measured repeatedly with a high degree of accuracy. The results of the measured mineral powders are presented and discussed. The minerals showed substantial variation in both dielectric constant and loss factor. The results are plotted on a plane of complex permittivity that clearly illustrates the potential of using cavity perturbation techniques for mineral differentiation and sorting. Possible application of the cavity perturbation technique in crude composition analysis was briefly investigated. This was done by varying the composition of a binary mixture and observing the changes in permittivity.

Although microwave measurement techniques will not offer the accuracy and versatility of existing sophisticated analysis techniques (eg. X-ray spectroscopy, NMR, ESR), they show potential as simple, low cost measurement systems in certain applications.

ACKNOWLEDGEMENTS

I would like to thank my supervisor, Professor B.J. Downing, for his guidance and support during this thesis. His helpfulness, willingness to listen and sound advice were very much appreciated.

I am also extremely grateful to the South African Council of Mineral Technology (MINTEK) for their support.

TABLE OF CONTENTS

1. INTRODUCTION

It is of great importance to the mining industry to be able to perform on-line analysis on the mined product. This allows the gold mining industry to determine the gold concentration in a slurry, and it enables the diamond mines to detect and sort diamonds from their native rock. These processes usually work on x-ray fluoroscopy, which is expensive and potentially hazardous.

Other techniques that have been investigated for mineral analysis are nuclear magnetic resonance (NMR) and electron spin resonance (ESR) [1]. These are very sophisticated techniques, and although successfully tested on a laboratory scale, have seldom been applied to on-line industrial processes due to their high costs.

Heating using microwave power has been used in various industrial and commercial processes. These have usually centred on the drying and heating of materials [2], heating for chemical processes [3] and enhancing mineral extraction [4]. More recently, the measurement of microwave attenuation has been applied to moisture measurement [5], on-line rock sorting [6] and fruit weighing [7]. The potential for using microwave techniques to provide simple non-contact, on-line (or just off-line) measurement systems is becoming evident.

This measurement potential of microwaves, together with observations that show different minerals heat up at substantially different rates under microwave power [8], suggest the possibility of applying microwave techniques to various forms of mineral analysis. There have been several studies investigating these possibilities [9], [10], [11] and [12]. These have generally been limited in their application, technique or frequency range.

Based on these observations, the objectives of this research project were to :

1) Investigate the background theory on interaction of microwave signals with different materials in order to understand why different minerals absorb microwave energy at different rates.

2) Investigate different microwave measurement techniques that could possibly be applied to mineral measurement.

3) Then, using measurement techniques selected in 2) above, to take measurements on various minerals and observe any difference in their characteristics.

4) Comment on the feasibility of using microwave measurement techniques for the differentiation, identification and analysis of minerals.

Simple forms of microwave analysis on minerals have relied on placing samples of them in a microwave oven, and noting their different rates of temperature increase [8]. The rate at which these different minerals heat up depends on the product of two properties of the minerals :

1) The absorptivity of microwave radiation by the mineral. This determines the rate at which energy is absorbed by the mineral.

2) The specific heat capacity of the mineral. This determines the rate at which the mineral heats up for its specific rate of energy absorption.

Obviously heating up the minerals, and noting their rate of temperature increases, is not a very suitable method of analysing or identifying the mineral types. This is unsuitable for several reasons :

1) It is slow, and thus not suited for on-line or just-off-line processing.

2) Temperature measurement is difficult, dependent on the specific point of measurement within the sample, and not very repeatable.

3) As explained above, the heating rates depend on both the mineral's microwave absorbtivity and its specific heat capacity. Since this a combination of two factors, it is more difficult to characterise minerals uniquely by their heating rates.

4) To obtain significant heating rates a powerful, and expensive, microwave power source is necessary. Such power levels are also potentially hazardous.

5) Only one parameter (the rate of temperature increase) is being measured. There may be other factors which are easily measured, and help characterise the mineral type, but cannot be determined from heating effects.

From the first four points above, it would seem obvious that the next best method for analysis would be to measure the microwave attenuation of the minerals at a low power level (eg. as in [6]). This eliminates most of the problems associated with the heating method. Measurements can now be made far more quickly, more accurately and with greater repeatability. However, this is still not optimum since, referring to point 5) above, there may be electrical properties of minerals that provide more information than attenuation alone. This will become apparent later.

Since microwave signals are electromagnetic waves, any interaction with matter depends on only the individual interactions of both the electric and magnetic fields. The only parameters which characterise any interaction of electric and magnetic fields with matter are the electric permittivity (ϵ_r) and magnetic permeability (μ_r), respectively. Since most minerals are non-ferromagnetic (with some exceptions, eg. those

containing Fe, Ni and Co), their relative magnetic permeabilities are essentially that of free-space, ie. $\mu_r \approx 1$, and are hence essentially dielectrics.

It was thus decided to investigate the dielectric properties of the minerals concerned. In order to understand dielectric properties and microwave interactions within them, chapter 2 gives a brief overview of dielectric polarisation, and how complex permittivity fully characterises dielectrics. The advantages of measuring complex permittivity rather than attenuation are explained.

Some properties of minerals that may complicate measurement of their permittivity are discussed in chapter 3. Steps to avoid these potential complications are suggested. The specific minerals chosen for study are then presented.

Chapter 4 gives a summary on some of the existing microwave techniques used to measure complex permittivity, followed by a recommendation on those most suited to mineral measurement.

Chapter 5 and 6, the main chapters, describe the two measurement techniques chosen for investigation, experimental procedures, results obtained, and discussions and conclusions.

Finally, based on the findings of this investigation, the thesis concludes by commenting on the feasibility of using microwaves for mineral analysis, and presents future proposals and recommendations.

2. DIELECTRIC MATERIALS AND COMPLEX PERMITTIVITY

2.1. INTRODUCTION TO DIELECTRIC MATERIALS

As explained in the previous chapter, since minerals are very often non-ferromagnetic, they behave as dielectrics. To help understand the behaviour and properties of dielectric materials in microwave fields, this chapter briefly describes dielectric materials, polarisation, mechanism of power loss within dielectrics, and how these properties are completely modelled by their complex permittivities.

2.2. POLARISATION IN DIELECTRICS

If a dielectric is inserted between the plates of a parallel capacitor, its capacitance is seen to increase by a factor ϵ_r due to the increased electric field energy being stored in the dielectric. This factor, ϵ_r, is called the relative permittivity, or dielectric constant, of the dielectric. In reality ϵ_r is generally complex, since it not only accounts for stored energy within the dielectric, but energy losses as well. This is explained by polarisation.

Since dielectrics are insulators they have no free charges to allow for DC conduction. However, transient electric fields do result in the movement of bound charge, and hence transient conduction [13]. The following simple model helps explain this: The electrically neutral dielectric consists of positive and negative charges which are bound together and not free to separate (eg. a symmetric neutral atom consisting of a nucleus within an electron cloud - figure 2.1.a). However, application of an electric field **E** will distort the atom, moving positive and negative charge centres apart. This displacement in the relative positions of these opposite bound charges results in a small dipole moment **p** being induced (figure 2.1.b).

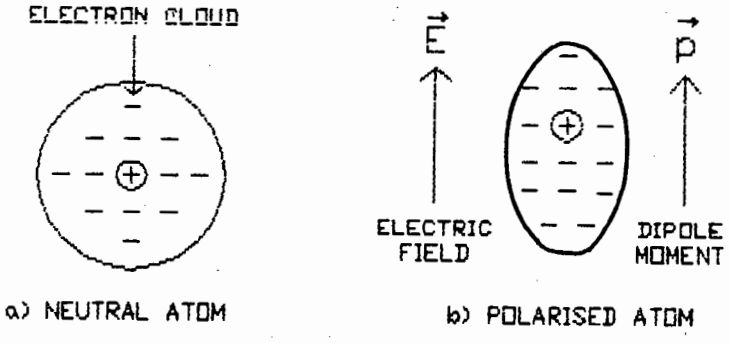

Figure 2.1. Inducement of Polarisation in a Neutral (Symmetric) Atom

For N such atoms (or molecules), the total polarisation **P** of the dielectric is then

$$\mathbf{P} = N\mathbf{p}.$$

Polarisation **P** is also proportional to the electric field intensity **E**. The constant of proportionality depends on the ease with which dipole moments are induced for that specific material [14]. The proportionality may be written as

$$\mathbf{P} = \chi \epsilon_o \mathbf{E},$$

where χ is the dielectric susceptibilty of the material, and ϵ_o is the absolute permittivity of free space.

The relative permittivity ϵ_r is related to the dielectric susceptibility χ by :

$$\epsilon_r = 1 + \chi$$

Thus, the more easily the material polarises, the larger ϵ_r. The mechanism of polarisation is not limited to the above example. Two of the most common forms of polarisation [15] are briefly described below :

2.2.1. Electronic Polarisation

This occurs for non-polar molecules, as in the above example. Here polarisation is due to induced dipole moments caused by the relative shifting of the oppositely charged nucleus and electron cloud. This is a fairly weak effect, and hence non-polar molecules tend to have low permittivities.

2.2.2. Orientation Polarisation

This occurs for polar molecules (eg. water). Although polar molecules possess individual dipole moments, the average polarisation of the material under absence of an electric field is zero, due to their random orientations. On application of an electric field the moments become aligned resulting in a strong net polarisation. Permittivities for polar molecules can thus be high (eg. for water, ϵ_r = 73 to 77).

2.3. COMPLEX PERMITTIVITY AND POWER LOSS IN DIELECTRICS

The mechanism of power loss in a dielectric, due to an alternating electric field, will now be explained. The concept of complex permittivity, which is used to account for these losses, is introduced. Since the dielectric permittivity is of more interest than the electric susceptibility, it is more convenient to work with the electric displacement vector **D**, rather than polarisation **P**, where $\mathbf{D} = \epsilon_o\mathbf{E} + \mathbf{P}$.

When the polarising electric field is sinusoidal $\mathbf{E} = \mathbf{E}_o\cos(\omega t)$ (eg. for an electromagnetic wave), the dipole moment will oscillate in orientation in an attempt to stay aligned with the field. However, due to the inertial moments and restoring forces of the molecules, the polarisation will lag behind the electric field [16] :

$$\mathbf{D} = \epsilon^*\mathbf{E}\cos(\omega t - \Phi) \qquad ,\Phi>0 \text{ since lag.}$$

or $\mathbf{D} = \epsilon^* e^{-i\Phi}\mathbf{E}\cdot\exp(j\omega t)$,using phasor notation

where $\epsilon^* e^{-i\Phi}$ is a complex factor accounting for this phase difference. Thus complex permittivity ϵ can now be defined as

$$\epsilon = \epsilon^* e^{-j\Phi} = \epsilon_o\cdot(\epsilon' - j\epsilon'')$$

where $\epsilon' = \dfrac{\epsilon^*\cos\Phi}{\epsilon_o}$ & $\epsilon'' = \dfrac{\epsilon^*\sin\Phi}{\epsilon_o}$

From electromagnetic theory, energy change (per unit volume) is given by the expression $\mathbf{E}\cdot d\mathbf{D}$

The energy loss rate L in the dielectric is thus given by

$$L = \frac{\omega}{2c}\int_0^{2\pi/\omega} \mathbf{E}\frac{\delta \mathbf{D}}{\delta t}\,dt$$

Inserting the expression $\mathbf{D} = \epsilon_o\mathbf{E}\{\epsilon'\cos(\omega t) - \epsilon''\sin(\omega t)\}$ and $\mathbf{E} = \mathbf{E}_o\cos(\omega t)$ into the above and integrating, the formula for the mean energy loss rate L in a dielectric is obtained :

$$L = \frac{\epsilon_o\epsilon''\mathbf{E}_o^2\omega}{2}$$

The real part of the complex permittivity (ϵ') can now be recognised as the familiar dielectric constant (since $\cos\Phi\approx 1$ as Φ is small), whereas the imaginary part (ϵ'') is termed the dielectric loss factor. It is this loss factor (ϵ'') that accounts for energy losses within dielectrics, and hence heating by electromagnetic waves. The ratio (ϵ''/ϵ') is often termed the loss tangent, since $\tan\Phi = (\epsilon''/\epsilon')$.

2.4. LOSS DUE TO CONDUCTIVITY

A dielectric may also have a small, non-zero conductivity which will also result in energy losses. Thus energy losses within a dielectric may be due to both polarisation and resistive loss mechanisms. But as far as

external effects are concerned, these mechanisms are indistinguishable. The the conductivity loss can therefore be modeled into the dielectric loss factor ϵ'' [16].

This can be seen from Maxwell's equation

$$\text{curl } \mathbf{H} = j\omega\mathbf{D} + \mathbf{J} \qquad \text{(for sinusoidal fields)}$$

$$\Rightarrow \quad \text{curl } \mathbf{H} = j\omega\epsilon\mathbf{E} + \sigma\mathbf{E}$$

$$\Rightarrow \quad \text{curl } \mathbf{H} = j\omega\epsilon_o\{\epsilon' - j\epsilon'' - j\sigma/(\omega\epsilon_o)\}\mathbf{E}$$

The new loss factor may now be thought of as consisting of the old loss factor (resulting from polarisation loss) plus a new term $\sigma/\omega\epsilon_o$ caused by resistive loss mechanisms.

Thus, even for a dielectric of zero conductivity, the power loss may be thought of as a result of an effective dielectric conductivity $\sigma = \epsilon_o\epsilon''\omega$, instead of as a polarisation loss.

2.5. ELECTROMAGNETIC WAVES IN LOSSY DIELECTRICS

The advantages of measuring complex permittivity directly, rather than attenuation alone is evident when the expression for an electromagnetic wave in a lossy dielectric is studied. This is now done below.

The form of an electromagnetic wave in a lossy dielectric can easily be obtained by replacing ϵ_r in the wave solution of Maxwell's equation, for a lossless dielectric, by the complex permittivity value $\epsilon' - j\epsilon''$.

The form of the electric field component of a plane wave travelling in the x direction in a dielectric is

$$\mathbf{E}_y = \mathbf{E}_o \cdot \exp[j(\omega t - kx)] \qquad (1)$$

where $k = 2\pi/\lambda = \omega\sqrt{\epsilon_r}/c$

and $\sqrt{\epsilon_r} = \sqrt{\epsilon'} \cdot \sqrt{1 - j\epsilon''/\epsilon'}$

Typically $\epsilon''/\epsilon' \ll 1$, and thus the binomial expansion may be used to get

$$\sqrt{\epsilon_r} \approx \sqrt{\epsilon'} \cdot \{1 - j\epsilon'/(2\epsilon'')\} \qquad (2)$$

Substituting this expression into (1) above, the expression for an electromagnetic wave in a lossy dielectric medium [14] is obtained :

$$E_y = E_o \cdot \exp[j\omega\{t - x\sqrt{\epsilon'}/c\}] \cdot \exp[-\omega x \epsilon''/2c\sqrt{\epsilon'}] \qquad (3)$$

This expression is that of an exponentially decaying wave (see figure 2.2.). The wave has a velocity $v = c/\sqrt{\epsilon'}$ and an exponential attenuation $e^{-\alpha}$ where $\alpha = \omega x \epsilon''/2c\sqrt{\epsilon'}$.

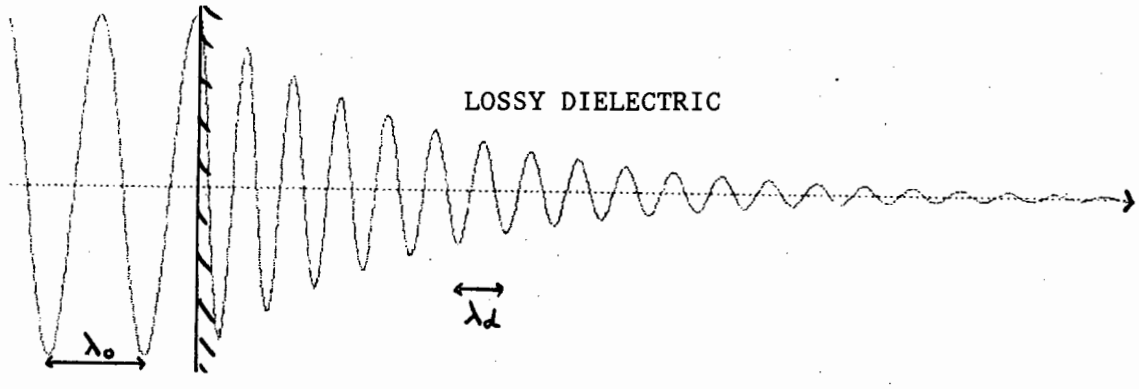

Figure 2.2. Decay of an Electromagnetic Wave in a Lossy Dielectric

The above observation shows that, as suggested in the introduction, measurement of the attenuation is not optimum, as it will only indicate the ratio $\epsilon''/\sqrt{\epsilon'}$. It would be better to measure both the dielectric constant ϵ' and loss factor ϵ'' independently. This could be achieved by additional measurement of the wave's phase displacement through the material (and comparing it to its free space wavelength) in order to obtain the factor $\sqrt{\epsilon'}$.

2.6. CONCLUSION ON DIELECTRICS

This chapter has shown how the complex permittivity completely models the behaviour of a dielectric under influence of electromagnetic waves. Thus, by measuring the complex permittivity of different minerals, it is hoped that this will help in their differentiation, identification and analysis. Several researchers have done permittivity measurements on minerals (eg.[9], [10], & [17]), but have generally been somewhat restricted. For instance, Parkomenko [17] gives a fairly comprehensive collection of results on dielectric constants for minerals, but these exclude loss factors and are restricted to frequencies well below the microwave region. Measuring complex permittivity, (instead of heating, attenuation, or dielectric constant alone) has the advantage that two parameters (and hence two degrees of classification) are being used.

Before methods of measuring complex permittivity are discussed, the following chapter presents a brief review of some of the properties of minerals that may complicate permittivity measurement, and how these can be avoided.

3. ELECTRICAL PROPERTIES OF MINERALS

This chapter highlights some of the problems that may occur in measuring the permittivities of minerals, and how these can be overcome. The chapter concludes by presenting the minerals chosen for this study.

3.1. ANISOTROPY

In the formation of rocks, crystals will often show preference in their orientation. This results in rocks that are anisotropic, therefore exhibit different values of permittivity along different axes. Results [17] have shown that values of permittivity for rocks may differ by up to a factor of four depending on the axis of measurement.

Powdering the rock (or solid) will destroy this grain orientation and hence eliminate its anisotropy. However, the powdered form will have a lower permittivity, as it is now effectively a mineral/air mixture. The packing density of the powder will also affect this resultant permittivity.

3.2. WATER CONTENT

Minerals have a natural water content that varies from 0.1% - 50% [17]. Since water has a very high permittivity (about 73 to 77), compared to a typical mineral permittivity of about 2 - 12, any permittivity measurements of moist minerals will be dominated by the effect of the water. Water content will also vary substantially between samples of the same mineral, giving inconsistent readings.

Water also has a very high dielectric loss factor. This may further be enhanced by the water forming a fairly conductive aqueous solution of ions from the mineral salts. The loss of the water may probably be several hundred times higher than that of the actual mineral alone.

Thus in order to achieve accurate, consistent permittivity measurements of any minerals, they must be rid of all water content. This can be achieved by drying the mineral samples in a thermal oven.

3.3. MIXTURES

Rocks are a complex composition of one or more mineral constituents. The electrical properties are thus a product of the individual constituent minerals, their proportions, and, most importantly, their microstructure.

To help in understanding the resultant permittivity of such polymineralic rocks, the rock's microstrucure may be considered as either a matrix or a mixture [17]. In a matrix one of the constituents occurs as a continuous host material, while the other component occurs as isolated particles within this matrix. A mixture is simply an unordered mixture of the two constituents. See figure 3.1.

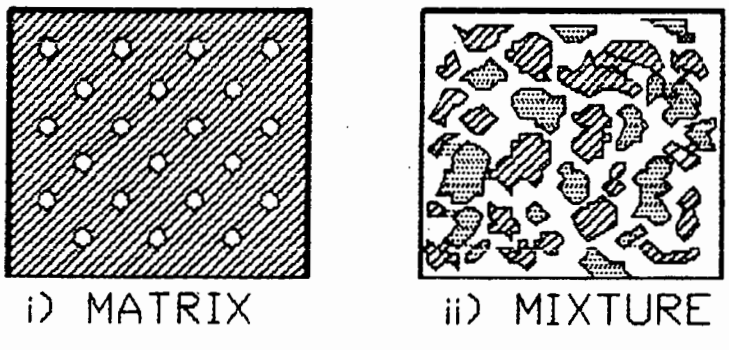

Figure 3.1. Differences between a Matrix and a Mixture

Many formulae, both empirical and theoretical, attempting to predict the properties of composite materials may be found in the literature. Two common formulae [17] for the simple cases of binary mixtures and matrices are briefly given below.

If the material is a matrix in which the inclusions are spherical, and their separation distances greater than their diameters, Maxwell's equation may be used to predict the resulting permittivity :

$$\epsilon = \epsilon_1 \cdot \frac{2\epsilon_1 + \epsilon_2 - 2\theta(\epsilon_1 - \epsilon_2)}{2\epsilon_1 + \epsilon_2 + \theta(\epsilon_1 - \epsilon_2)}$$

where ϵ_1 and ϵ_2 are the dielectric permittivities of the matrix and the inclusions respectively, and θ is the volume ratio for the inclusions.

If the system is an unordered mixture of two components the resulting dielectric constant can be predicted from Lichteniker's formula

$$\log \epsilon = \theta_1 \cdot \log \epsilon_1 + \theta_2 \cdot \log \epsilon_2$$

where ϵ_1 and ϵ_2 are the component permittivities, and θ_1 and θ_2 are their volume fractions, with $\theta_1 + \theta_2 = 1$.

Finely powdering a rock that is of a matrix form, will generally result in a powder that is essentially an unordered mixture.

3.4. FERROMAGNETIC MINERALS

Although minerals are generally non-ferromagnetic, there are some (especially those containing Fe) that are highly ferromagnetic. For such minerals, their magnetic permeability μ_r may be several hundred, and they can be extremely lossy due to their magnetic hysteresis. As with dielectrics, ferromagnetic material properties can be completely modelled by their complex permeability, $\mu_r = \mu' + j\mu''$. Treating ferromagnetic minerals as pure dielectrics, and attempting to measure their permittivities will now no longer give their true values of permittivity, but a reading that is the combination of both permittivity and permeability. This, however, remains useful since it still allows comparisons and differentiations to be made between the minerals.

3.5. MINERALS SELECTED FOR STUDY

Although minerals in a powdered form are far easier to work with than solids (they easily fill any shape container) and no longer have any anisotropy, they are effectively an air/mineral mixture. This means that the measured permittivity is no longer that of the true mineral, but a reduced value due to the added air.

It was, however, decided that the mineral samples to be measured should be in powdered form. This was for several reasons:

1) Minerals in their powdered form would be far easier to work with. Solids would have to be machined.

2) Minerals in powdered form are more easily obtained.

3) Minerals are generally encountered in their powdered form in industry, eg. slurries.

The minerals were to be finely ground in order to achieve a high packing density. This would greatly reduce the proportion of air in them than if they were coarsely ground, and also helps achieve a more consistent packing density between different samples. Methods for obtaining uniform packing densities, and eliminating the problem of air, will be discussed later.

The minerals chosen for study were supplied by MINTEK and various other sources. They are listed in **Appendix A** together with an analysis of their compositions. The choice attempted to obtain a balanced selection of some of the more common minerals. Red Oxide (Fe_2O_3) and Pyrite will obviously exhibit some ferromagnetic properties.

In order to investigate the feasibility of using microwaves as a crude analysis technique, SiO_2 was to be used as a base mineral into which various other single minerals could be mixed in different proportions.

The permittivities of the resulting mixtures were then to be measured in order to try and detect any changes.

Now that dielectrics and problems in mineral measurement have been studied, it is appropriate to investigate microwave methods of measuring complex permittivity. This is done in the next section.

4. MICROWAVE MEASUREMENT OF COMPLEX PERMITTIVITY

4.1. INTRODUCTION TO MEASUREMENT TECHNIQUES

Numerous methods for measuring the complex permittivity of dielectrics at microwave frequencies exist. In order to select a method which is suited for this investigation, several of the major techniques were investigated and are briefly described below. Their advantages and disadvantages , with respect to mineral measurement, are presented and compared. The chapter concludes on a recommendation of method(s) considered most appropriate.

The various measurement techniques may be broadly classified into two groups :

a) Transmission line or Waveguide methods.
b) Cavity Perturbation methods.

These are discussed under their respective headings below.

4.2. TRANSMISSION LINE / WAVEGUIDE METHODS

In these methods, a section of transmission line or waveguide is filled with the dielectric, and variations in the line parameters (eg. VSWR, reflection coefficient, impedance, s-parameters, etc.) are measured. The complex permittivity can then be calculated from these measurements.

Either hollow waveguides (rectangular or cylindrical) or coaxial transmission lines can be used. The choice may depend on the following advantages and disadvantages of each :

a) Hollow waveguides are mechanically far simpler than coaxial line, especially if the dielectric sample is solid.

b) Coaxial line is suitable for broad-band frequency use since, unlike waveguide, it does not have a cut-off frequency.

c) Microwave test equipment generally has coaxial connectors, which make it easier to match into a coaxial line. Coaxial to waveguide transitions can be matched for narrow bandwidths only.

Other microwave transmission line structures, such as microstrip, strip line, slot line, fin line, coplanar waveguide, etc., could theoretically be used; however, these are far less practical.

The most popular variations of these methods are now presented.

4.2.1. Short-Circuited Line Method

This is one of the earliest methods, and mathematical details can be found in [18]. The dielectric sample to be measured is placed at the short-circuited end of the waveguide/coaxial line (figure 4.1.). The reflection coefficient at the sample/air interface is then measured using a network analyser or slotted line. From the reflection coefficient and the sample and line dimensions, the complex permittivity can be calculated.

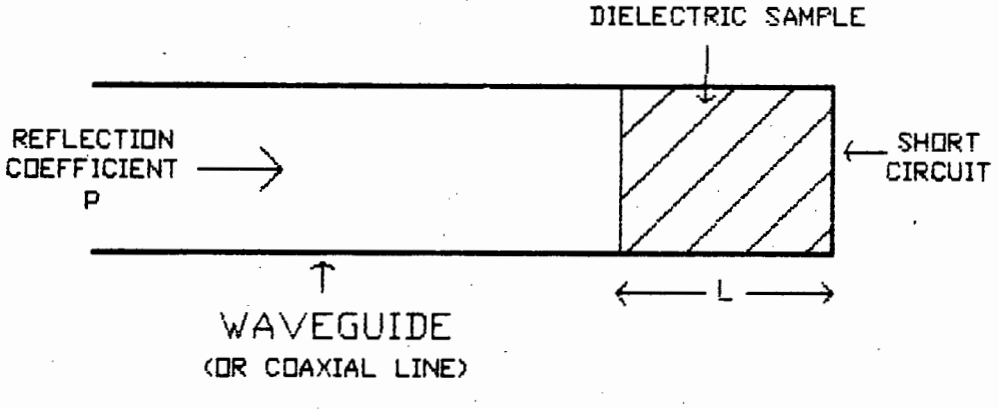

Figure 4.1. Permittivity Measurement using a Short Circuited Waveguide

A major problem with this method is the equation to be solved; it is a complex transcendental equation and must therefore be solved numerically. Since it contains trigonometric functions, it yields multiple solutions for permittivity. The correct solution can very often be identified from the expected dielectric constant (the others being unrealistic), or else multiple measurements must be made on samples of different lengths in order to remove this ambiguity.

4.2.2. Two-Port Measurement

In this method, the dielectric fills a section of the wave-guide/coaxial line, but instead of a short-circuit, measurements are made at both ports (figure 4.2.). From the reflection coefficient s_{11} (or s_{22}) and transmission coefficient s_{12} (or s_{21}), and the physical dimensions, the complex permittivity can be calculated. This is a simple calculation and yields a unique solution.

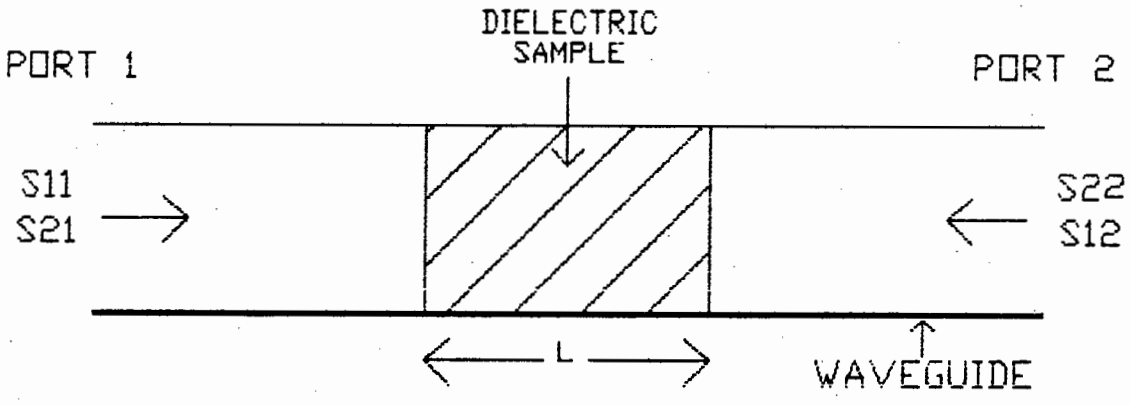

Figure 4.2. Transmission Measurement of Permittivity

Errors in measurements are likely to be higher than the short-circuited line method, since two connections and measurements are now being made. More details on this method can be found in [19] and [20].

4.2.3. Infinite Sample Method

If the dielectric sample in the short-circuited line method is either very long or very lossy, then negligible energy will be reflected by the short-circuit. The sample length can then be assumed to be infinite. This greatly simplifies the mathematics and yields a unique solution. This method is only suitable for very lossy materials and has poor accuracy. Details may be found in [19].

4.2.4. Open-Ended Termination

In this method, a flanged open ended wave-guide or coaxial line terminates on the flat surface of a large sample of the dielectric (see figure 4.3.). The reflection coefficient is then used to calculate the permittivity. This method has the advantage that it is non-intrusive.

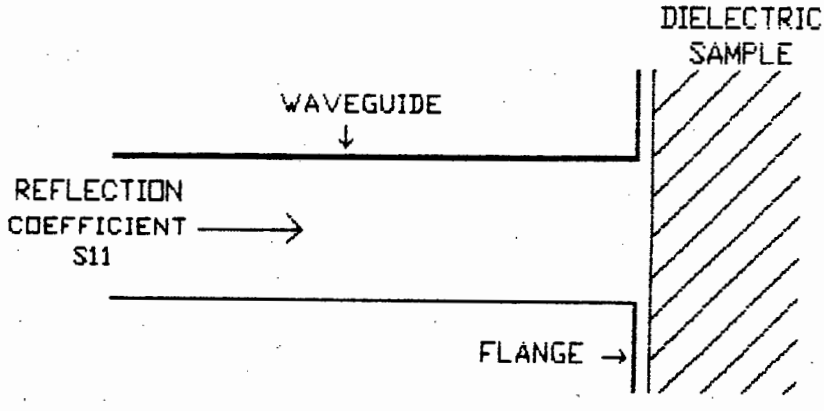

Figure 4.3. Measurement of Permittivity using an Open Ended Termination

Since this method assumes that the sample is infinite in extent, it is most suited to lossy materials. The computations are complicated and rely on approximations of the penetrating field. Thus the accuracy may not be very good. Details of this method are given in [21] and [22].

4.3. CAVITY PERTURBATION TECHNIQUES

Cavity techniques involve the measurement of the resonant frequency and Q (quality factor) of a hollow metallic resonant cavity with, and without, a small dielectric sample enclosed. For example, figure 4.4. shows a rectangular cavity containing a dielectric rod.

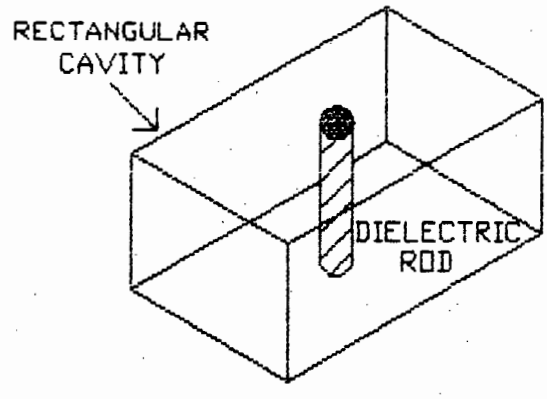

Figure 4.4. Cavity Perturbation using a Rectangular Cavity with Dielectric Rod

The introduction of the dielectric sample into the cavity has two effects :

1) The resonant frequency decreases. This is due to the wavelength becoming shortened in the dielectric sample. The amount of frequency decrease is mainly a function of the dielectric constant ϵ'.

2) The Q decreases. The dielectric sample increases the amount of energy lost, and hence the Q decreases. The decrease in Q is thus mainly a function of the dielectric loss factor ϵ''.

This change in resonance is shown in figure 4.5. From the measured shifts in resonant frequency and Q (and the cavity, field and sample geometry), the complex permittivity can be calculated.

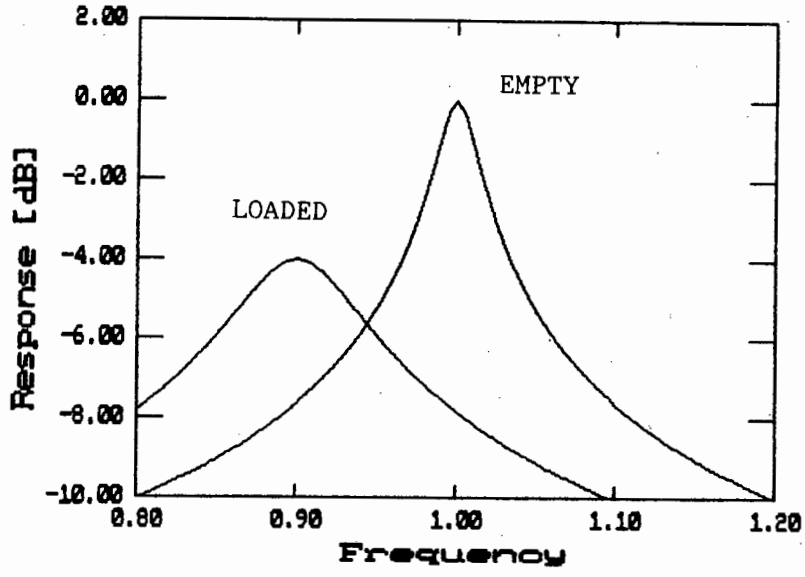

Figure 4.5. Change in Cavity Resonant Response due to Dielectric Perturbation

Because these methods rely on resonant structures they are restricted to measurement at the resonant frequency only. Since very high Q's are obtained in microwave cavities, cavity perturbation techniques are highly sensitive to measuring variations in loss.

There are many variations on cavity perturbation techniques. These depend on some of the following different configurations :

1) Type of resonant cavity used, eg. rectangular, cylindrical, re-entrant, etc.

2) Mode of resonance and hence electric field configuration, eg. TM_{010}, TE_{121}, etc.

3) Shape and positioning of dielectric sample within the cavity.

Further details of cavity perturbation techniques can be found in [19], [23], and [24].

4.4. RECOMMENDATIONS ON MEASUREMENT TECHNIQUE

Following this investigation on microwave permittivity measurement techniques, it was decided to use two methods for the study :

1) The short-circuited coaxial line method as a first study. This should allow medium accuracy, broad-band measurements to made over 100 MHz to 10 GHz using the available HP 8410 network analyser. A broad-band measurement technique would help show if there are any substantial variations in complex permittivity with frequency.

2) A cavity perturbation technique. This a more sensitive technique and may help show differences between the minerals.

The short-circuited line method and results are covered in the following chapter. The cavity perturbation technique is then covered in chapter 6.

5. SHORT-CIRCUITED COAXIAL LINE METHOD

5.1. INTRODUCTION

As explained in the previous chapter, this method is suitable for taking wide-band permittivity measurements, and is thus appropriate as an initial investigation technique. This chapter begins by introducing the theoretical equation used to calculate the permittivity from the measured reflection coefficient. The experimental setup used for taking measurements is then described. Calibration tests and a discussion on sensitivity and error are presented. Selected results from the measurements on the chosen minerals are presented. These results and the success of the experiment are discussed in the conclusion.

5.2. THEORY

In this method, originally developed by Roberts and von Hippel [18], the dielectric sample (length d) is placed at the short circuited end of the coaxial line (figure 5.1.).

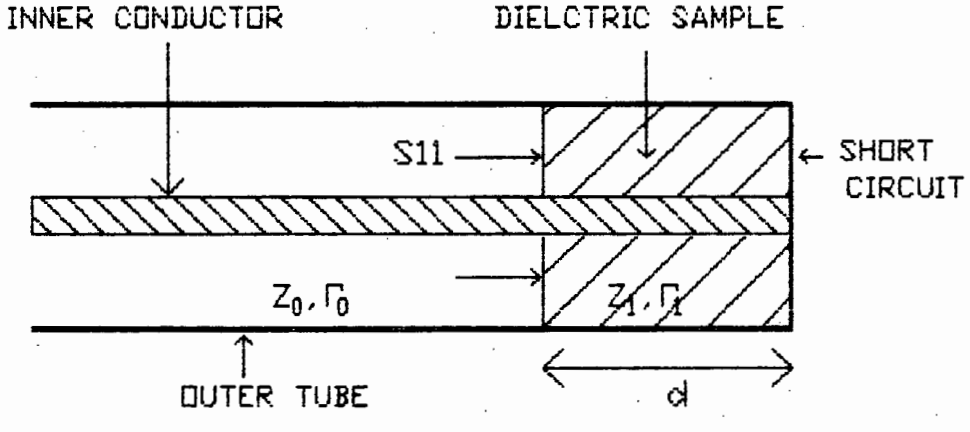

Figure 5.1. Short Circuited Coaxial Line Containing Dielectric Sample

If the unfilled section of the coaxial line has a propagation constant Γ_o (or characteristic impedance Z_o), the dielectrically filled section will then have a different propagation constant $\Gamma = \Gamma_o \cdot \sqrt{\epsilon_r}$. Now by the use of simple transmission line theory the reflection coefficient ρ at the air-dielectric interface looking towards the short circuit can be shown to be :

$$\rho = \frac{\Gamma o \cdot \tanh(\Gamma d) - \Gamma}{\Gamma o \cdot \tanh(\Gamma d) + \Gamma} \qquad (1)$$

Complete derivations of this equation may be found in the references [18], [19], [25], or [10].

Once the reflection coefficient ρ has been measured, eg. using a network analyser, this equation must be solved for Γ, where Γ_o and d are known. Once Γ is determined, the complex permittivity ϵ_r can then be calculated since

$$\Gamma = \omega\sqrt{\epsilon_r}/c \qquad (2)$$

where ω is the angular frequency and c the speed of light.

Solving the characteristic equation (1) for Γ is not easy. Since it is a transcendental equation (has no analytical solution) it must be solved numerically. Because Γ is complex, tanh exhibits periodicity and the equation yields multiple solutions for permittivity. The correct solution can usually be selected by inspection - the other solutions being improbable. Several methods of solving this equation were tried before a successful one was found. Details of the method used, together with its implementation in a computer program, are given in **Appendix B**.

5.3. EXPERIMENTAL SET-UP

Since the characteristic impedance of an air-filled coaxial line is given by

$$Z_o = 60 \cdot \ln(b/a)$$

and an impedance of 50Ω is desirable to match the test equipment, a ratio of inner to outer diameter of b/a = 2.3 for the coaxial line is necessary. The diameter of the tube should not be too large, otherwise unwanted waveguide modes may propagate. The cut-off frequency of the lowest order coaxial waveguide mode is given by [26] :

$$f_c = c/1.475(a+b).$$

Thus to ensure only TEM waves up to 10 GHz (the upper limit of the network analyser) will propagate, the outer diameter must have a maximum dimension b = 14.7 mm. It must also be remembered that these dimensions and cut-off frequencies will be reduced by a factor equal to $\sqrt{\epsilon_r}$ when dielectrically loaded. To best fit the coaxial tube to a standard N-type male connector (to facilitate connection to the test equipment) the dimensions a = 3 mm and b = 6.9 mm were chosen. Two similar coaxial-line test cells of these dimensions were machined from brass and are shown (simplified) in figure 5.2.. A screw-on cap provided the short circuit. The test-cell could easily be unscrewed and dismantled to allow loading of the sample and cleaning.

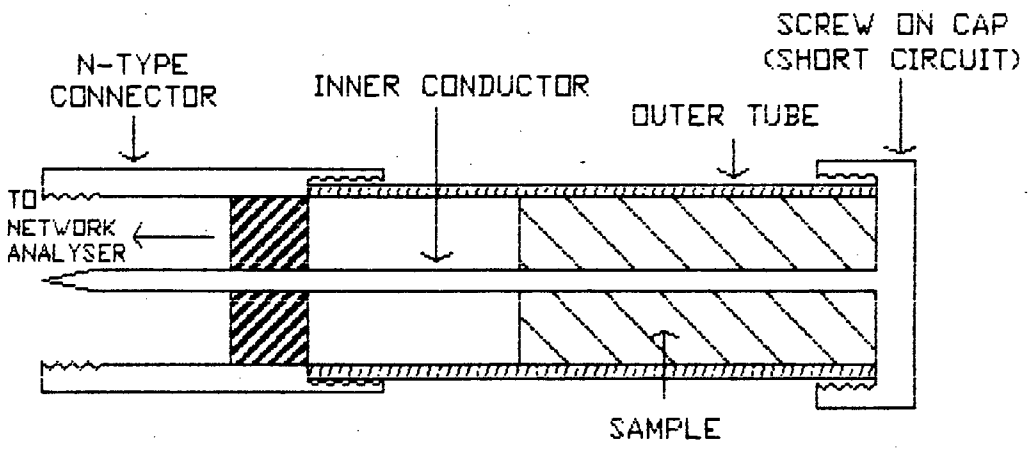

Figure 5.2. Coaxial Test Cell

The equipment set-up consisted of the HP 8410 network analyser (and associated components) interfaced to a PC computer. The computer allowed automatic control and measurement of the system and subsequent data processing. A schematic diagram of the equipment set-up is given below in figure 5.3.

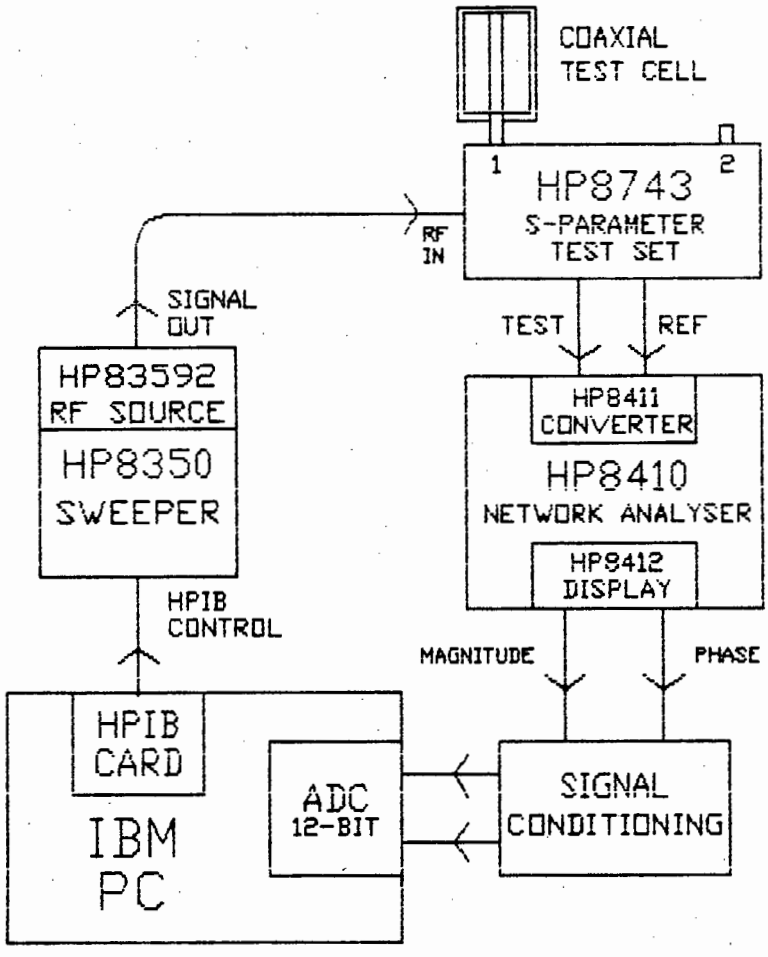

Figure 5.3. Measurement System for the Short Circuit Coaxial Line

A brief description of the measurement system and its operation is given below :

Software running on the PC controls the microwave signal generator via an HPIB interface card and bus. This allows automatic control of the signal generators sweep range and rate, and power level. The microwave signal is fed to the s-parameter test set, onto which the coaxial test cell is connected. The reflection coefficient is measured and displayed on the phase/magnitude display of the network analyser. To provide accurate and automatic measurements of the reflection coefficient, the analogue outputs of the magnitude and phase display are sampled by a 12-

bit ADC on-board the PC. This completes the system loop. The overall system has a frequency range of about 500 MHz to 10 GHz.

The user sets (at the PC) the frequency range to be measured, eg 4 GHz to 6 GHz in 100 MHz steps. Measurements are then made on the empty test cell to allow for later correction of system errors. These errors are due to imperfections in the network analyser and reflections in the connectors. The sample is then loaded and reflection measurements taken over the range. The computer then calculates the permittivities of the sample and displays these on a graph against frequency. More complete details of the system interface and operation can be found in **Appendix C**.

5.4. TESTING AND SENSITIVITY ANALYSIS

To evaluate the system, measurements were performed on plugs of teflon, polyethylene and nylon, and compared against their known permittivity values. Readings were taken for frequencies from 1 GHz to 8 GHz in 100 MHz steps. Plots of these results are shown in figures 5.4.. The solid line represents the dielectric constant, and the dashed line the loss factor.

There are erratic variations in these curves for the measured data, particularly in loss factor. These are <u>not</u> due to the characteristics of the materials, but are errors. The fluctuations in the dielectric constant (solid line) are about 10 - 15%, whereas they are far larger for the loss factor (dotted line) making this reading meaningless. Apart from the fluctuations in the measured dielectric constant, their <u>average</u> measured values are realistic : teflon 2.0, polyethylene 2.3, and nylon 3.0. These average measured values of dielectric constant compare favourably against their referenced values - see table 1 below. However, since a wide range of mineral powders are to be measured and compared, measurement repeatability and absence of fluctuations is of more importance than absolute accuracy.

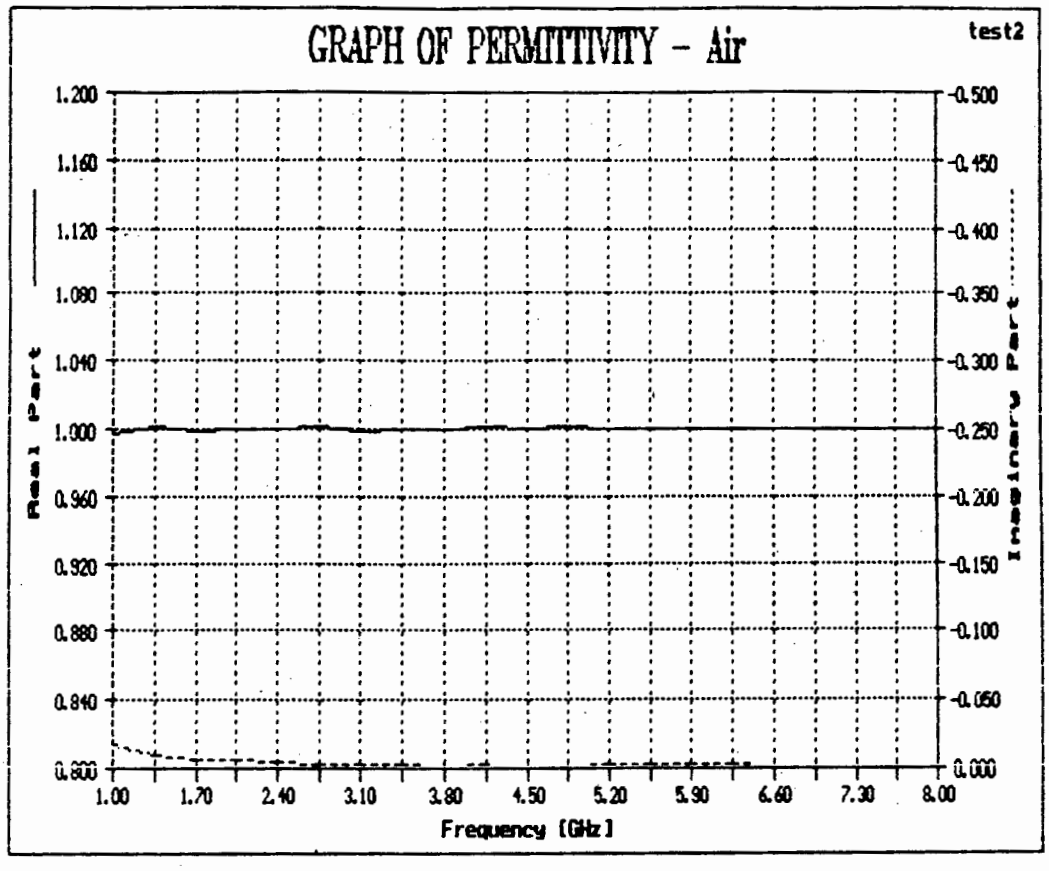

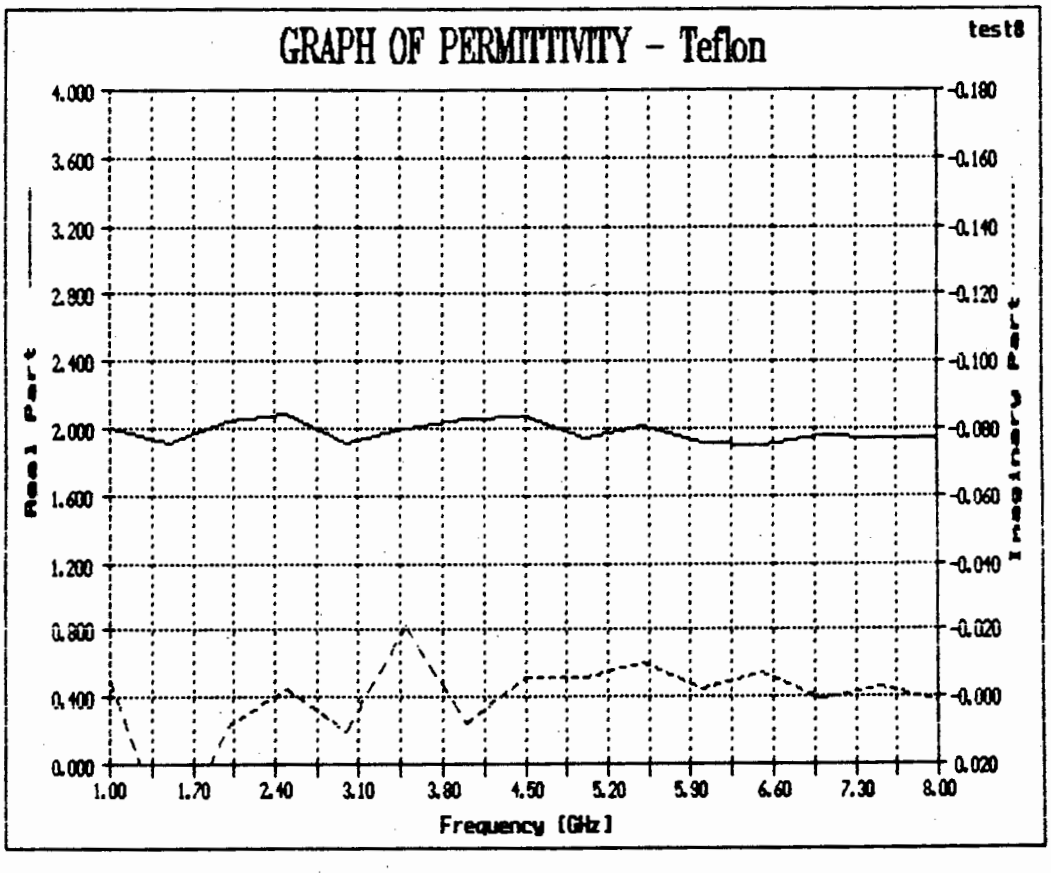

Figure 5.4.i) Permittivity Test Results on Known Plastics

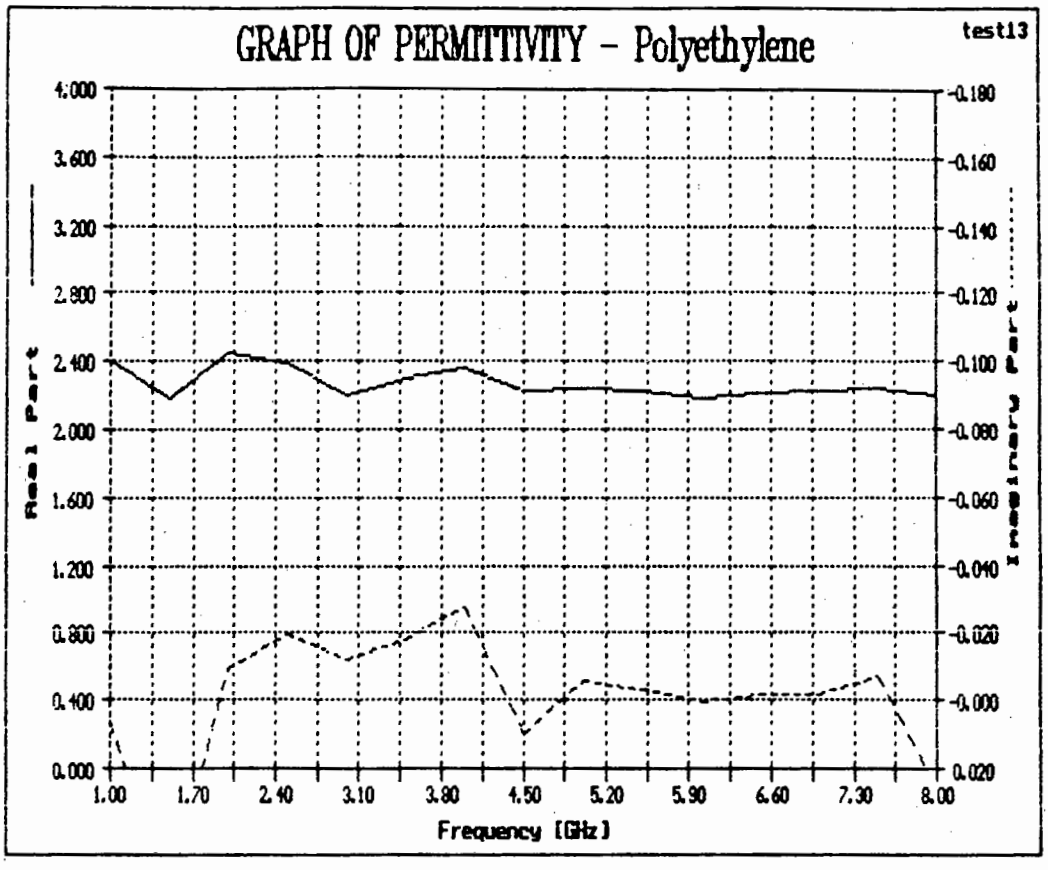

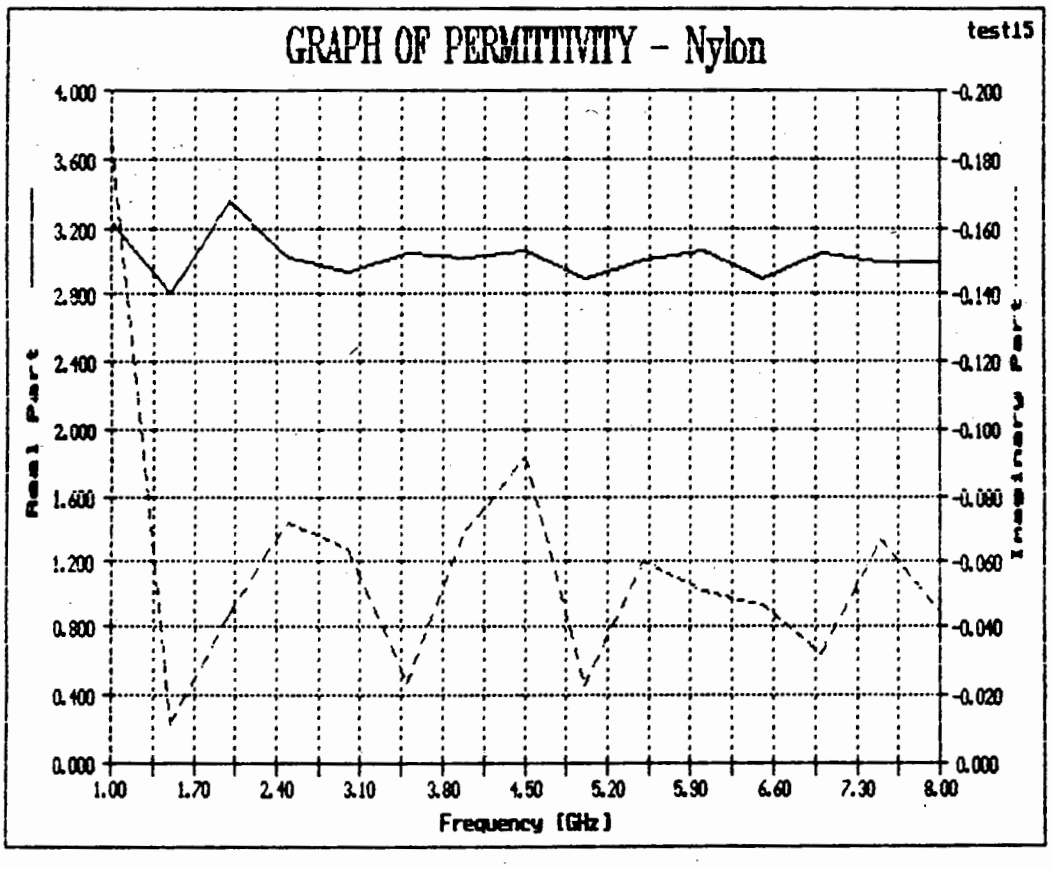

Figure 5.4.ii) Permittivity Test Results on Known Plastics

MATERIAL	MEASURED ϵ	REFERENCE ϵ [27]
Air	1.0	1.0
Teflon	2.0	2.1
Polyethylene	2.3	2.33
Nylon	3.0	3.00 - 3.4

Table 1. Comparison of Measured and Referenced Values of Dielectric Constants for the Solid Plastics Measured

There are three main sources responsible for these large fluctuations and errors : i) Inaccuracies in the Network Analyser, ii) Imperfect Transitions, Connections and Short Circuit, and iii) Poor Sensitivity in the Characteristic Equation. These sources are briefly explained below :

5.4.i). Inaccuracies in the Network Analyser

The couplers in the s-parameter test set, used to separate reference and test signals, are obviously not perfect. Instead of providing a constant fraction of coupling over the bandwidth their response has a small amount of ripple. This contributes as an error to the measured reflection coefficient. Error correction using the correction models described in [28], [29] and [30] were tried but provided little improvement, mainly because they did not seem to successfully model the errors with the test cell included. Other possible sources of error in the network analyser system were random fluctuations in the analogue output and instability in the frequency of the sweep generator.

5.4.ii). Imperfect Transitions, Connections and Short Circuit

The coaxial test cell needed to be connected to the network analyser via a series of connectors : APC7-SMA[F], SMA[M]-N[F]

Right Angle, N[M]-Test Cell. Each connector has a non-zero VSWR that contributes to, and corrupts, the measured reflection coefficient. There is little that can be done about this. Error correction (as mentioned above) would help reduce these connector errors, but not those of the coaxial cell connector and the cell's short circuit. The imperfect short circuit in the test cell was also a major source of error.

5.4.iii). Poor Sensitivity in the Characteristic Equation

The measurement of the reflection coefficient will obviously (due to the above reasons) be in some error, ie. $\rho+\delta\rho$ instead of ρ. Subsequently, the calculated permittivity ϵ_r will also be in error, $\epsilon_r+\delta\epsilon_r$. The resulting percentage error in calculated permittivity $(\delta\epsilon_r/\epsilon_r)\%$ will depend on the measurement error $\delta\rho$, and more importantly, on the sensitivity of the characteristic equation from which ϵ_r was derived (equation 1, section 5.2.). Due to the cyclic and hyperbolic tangent functions in this equation, it shows large variations in sensitivity depending on the argument Γd which is proportional to d/λ, where λ is the wavelength. This behaviour can be studied only numerically, and has been done so by Chao [25]. These results can be briefly summarised by the two graphs in figure 5.5.

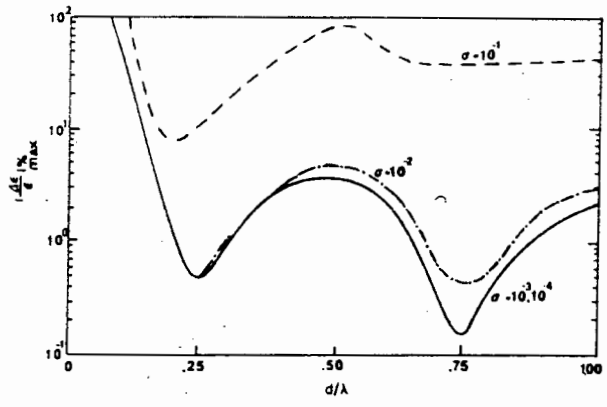

The maximum percentage uncertainty of dielectric constant for $\sigma = 10^{-4}$ to 1.0/Ω · cm and $\epsilon_r = 10$.

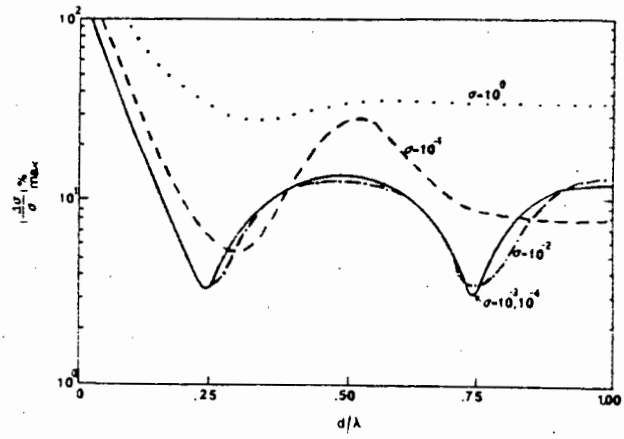

The maximum percentage uncertainty of conductivity for $\sigma = 10^{-4}$ to 1.0/Ω · cm and $\epsilon_r = 10$.

Figure 5.5. Graphs Showing Sensitivity of ϵ' and ϵ'' (or σ) against d/λ

The main points of interest are :

i) The loss factor is more sensitive than the dielectric constant.

ii) There are points of minimum sensitivity where $d/\lambda = n/4$, n odd.

iii) For the region $d/\lambda < 0.2$ the sensitivity, and hence the error, increases rapidly.

iv) The larger the loss factor, the poorer is its sensitivity.

Point ii) cannot always be satisfied since wide band sweeps are being made. The only thing that can be done is to ensure point iii) is satisfied by using long enough samples.

Although the accuracy and sensitivity of this method were disappointing, measurements on the powdered minerals were performed. These results are presented in the next section.

5.5. MINERAL TESTS AND RESULTS

The powdered minerals were measured using the short circuited coaxial test cell. Some of these permittivity responses are shown in figures 5.6.

As explained from the test results and discussion on sensitivity, the error in the dielectric constant was about ±10-15 %, whereas the loss factor was very poor. The range in the dielectric constant for the different non-ferromagnetic minerals measured was about 2.0 to 3.2. It could be seen that, within the bounds of the fluctuation errors, there was no noticeable variation in dielectric constant over the frequency range measured. This could not be determined for the loss factor. For the two ferromagnetic minerals shown, red oxide and iron pyrites, their "effective dielectric constant" could be seen to be far larger (about 4.0 to 6.4) and they were very lossy ($\epsilon'' \approx -0.6$). This is as expected.

Conclusions on this method, together with suggestions for possible improvements, are now given.

5.6. CONCLUSION ON SHORT-CIRCUITED LINE METHOD

Although the success of this experiment was limited by the accuracy obtained, the tests did show that there were no noticeable large variations in dielectric constant over the frequency range covered. There was ,therefore, no good reason for choosing a specific frequency (within this range) for later mineral analysis using cavity perturbation. The choice of resonant frequency for cavity perturbation is justified in section 6.2.1.

Work by Church [10], using a similar technique on mineral powders but at a lower frequency range 300 MHz to 1 GHz, showed little variation in dielectric constant but substantial variations in loss factor. These variations were as large as 10:1. The validity of these results remains

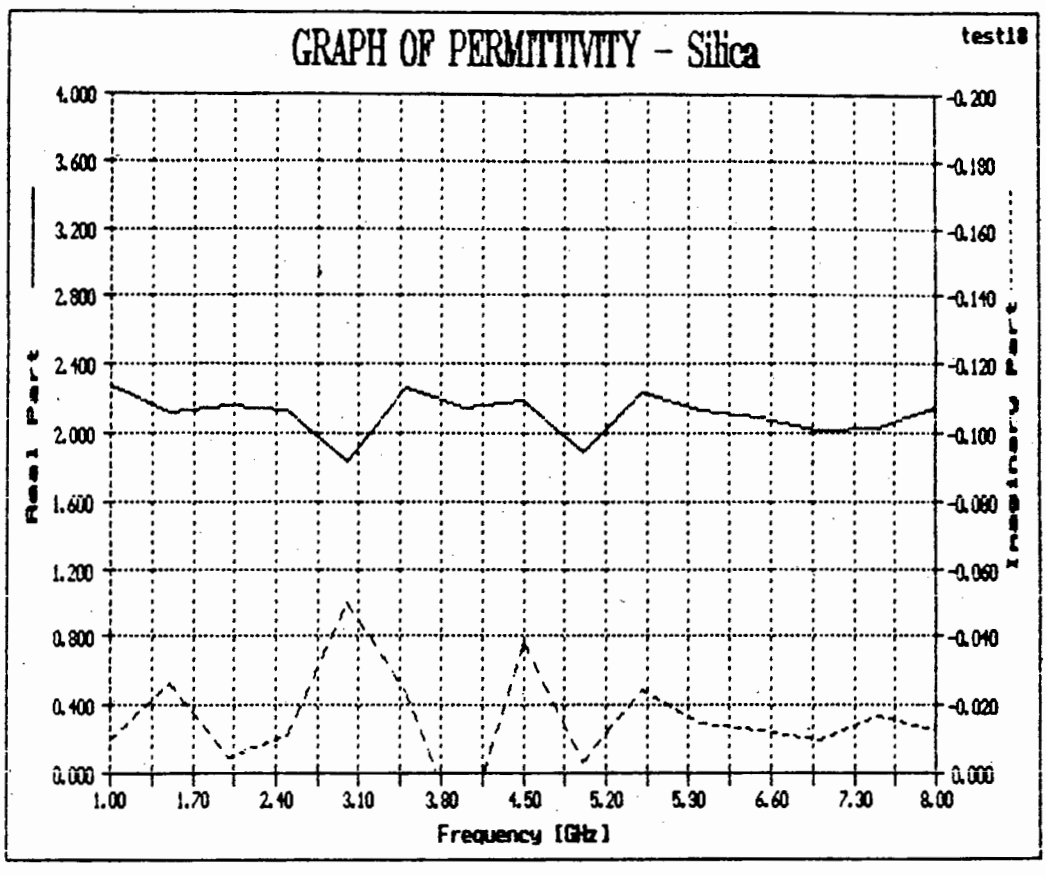

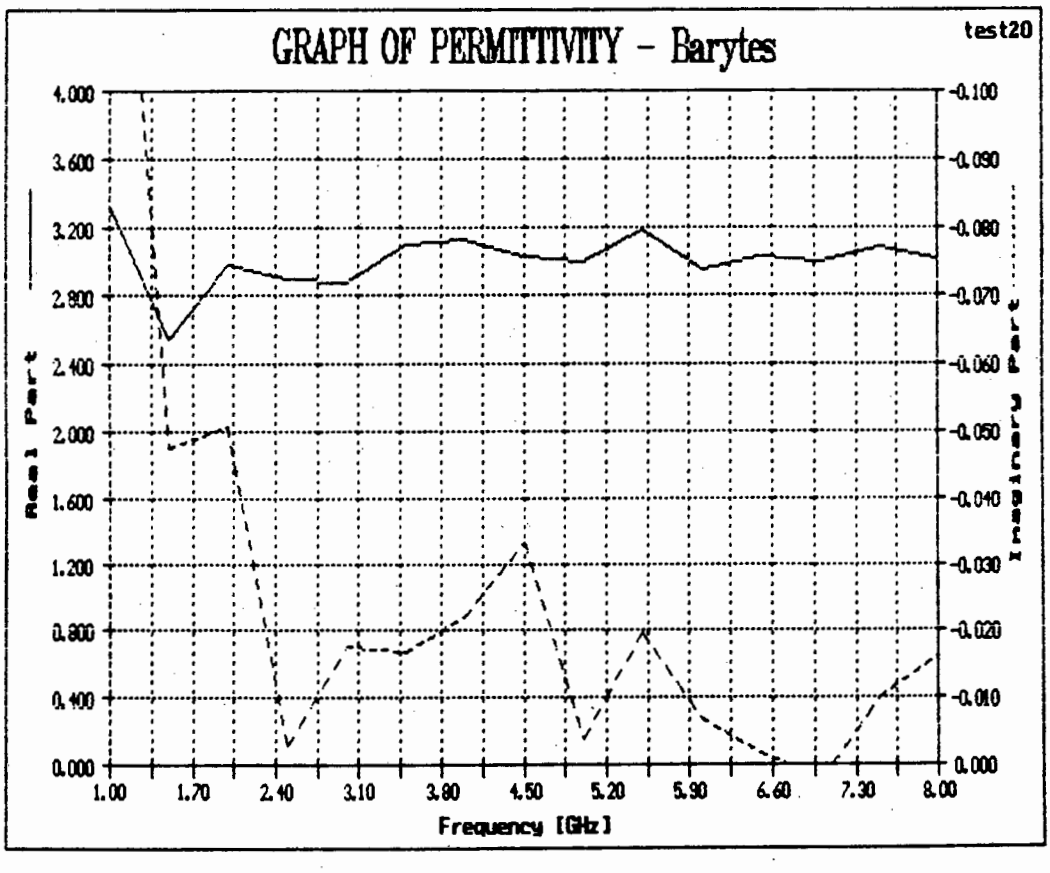

Figure 5.6.i) Permittivity Curves for some of the Minerals Measured

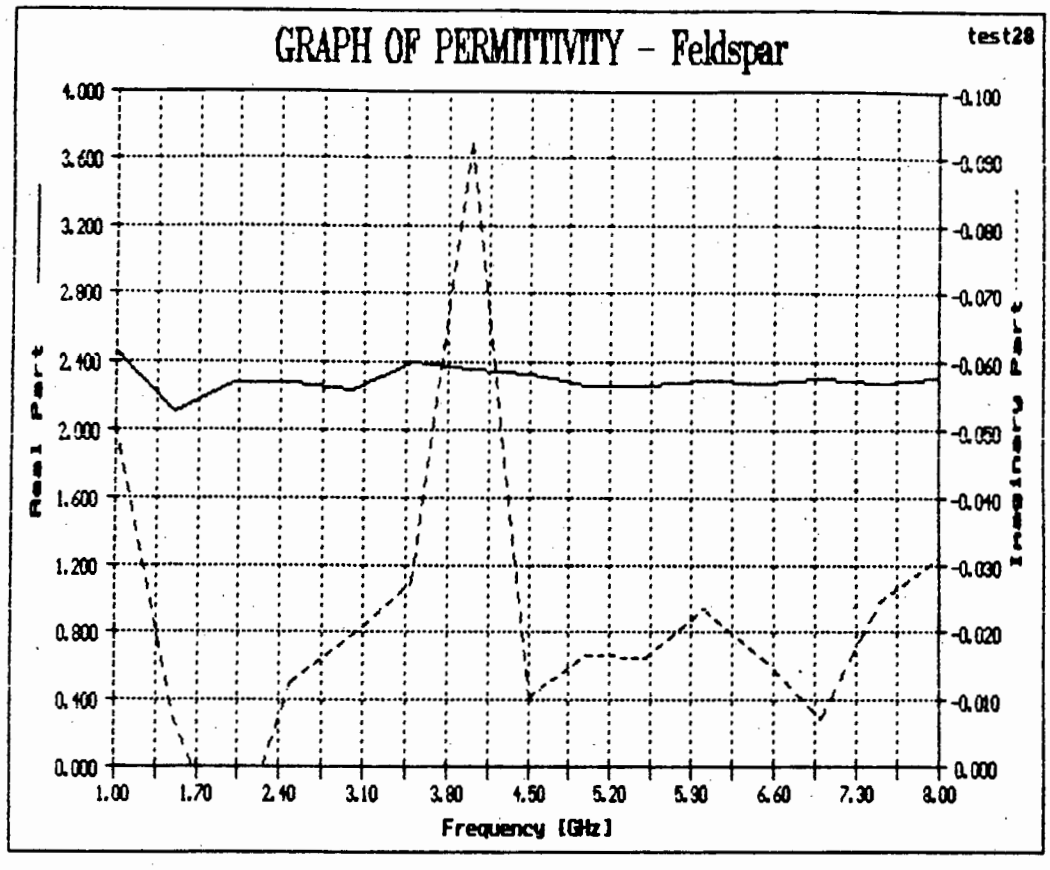

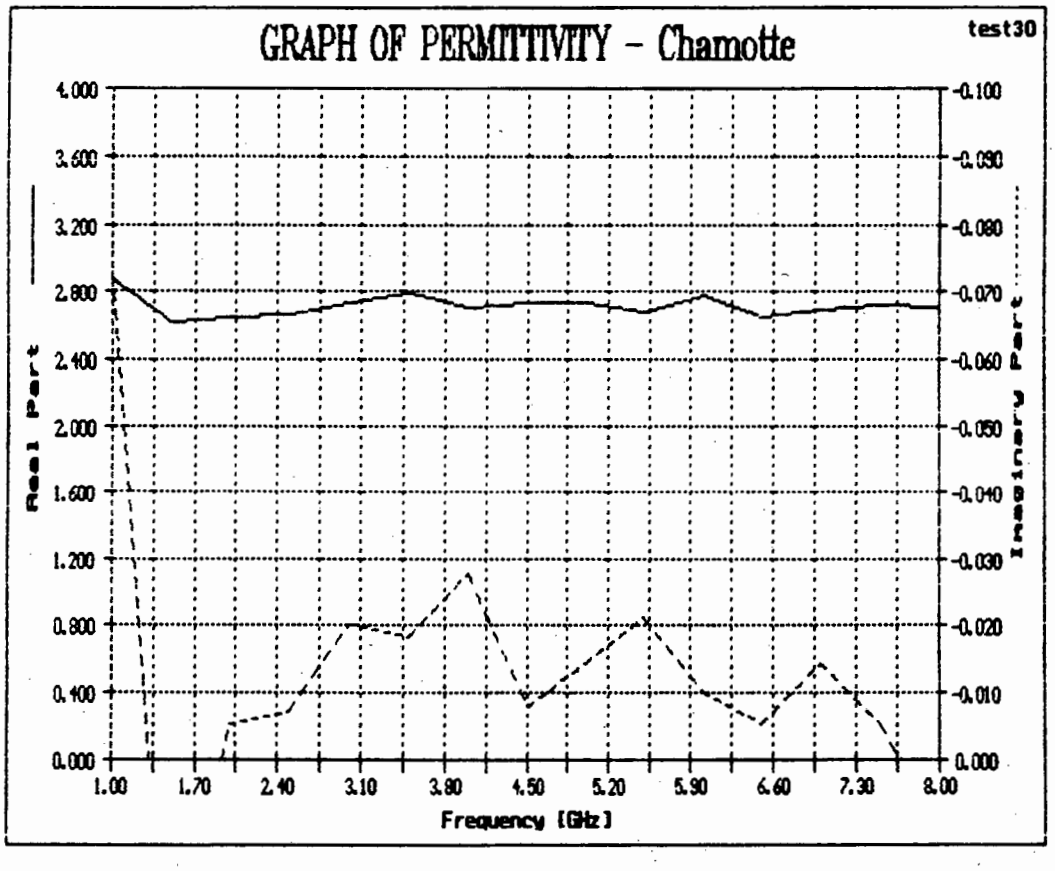

Figure 5.6.ii) Permittivity Curves for some of the Minerals Measured

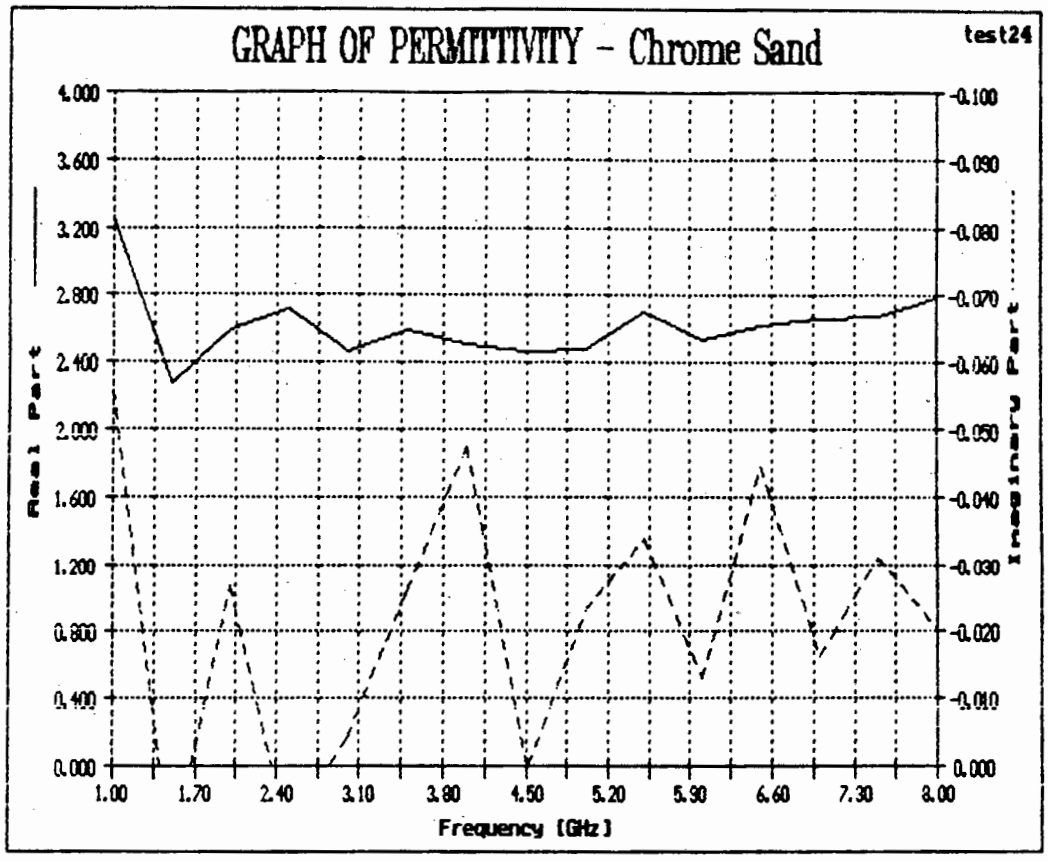

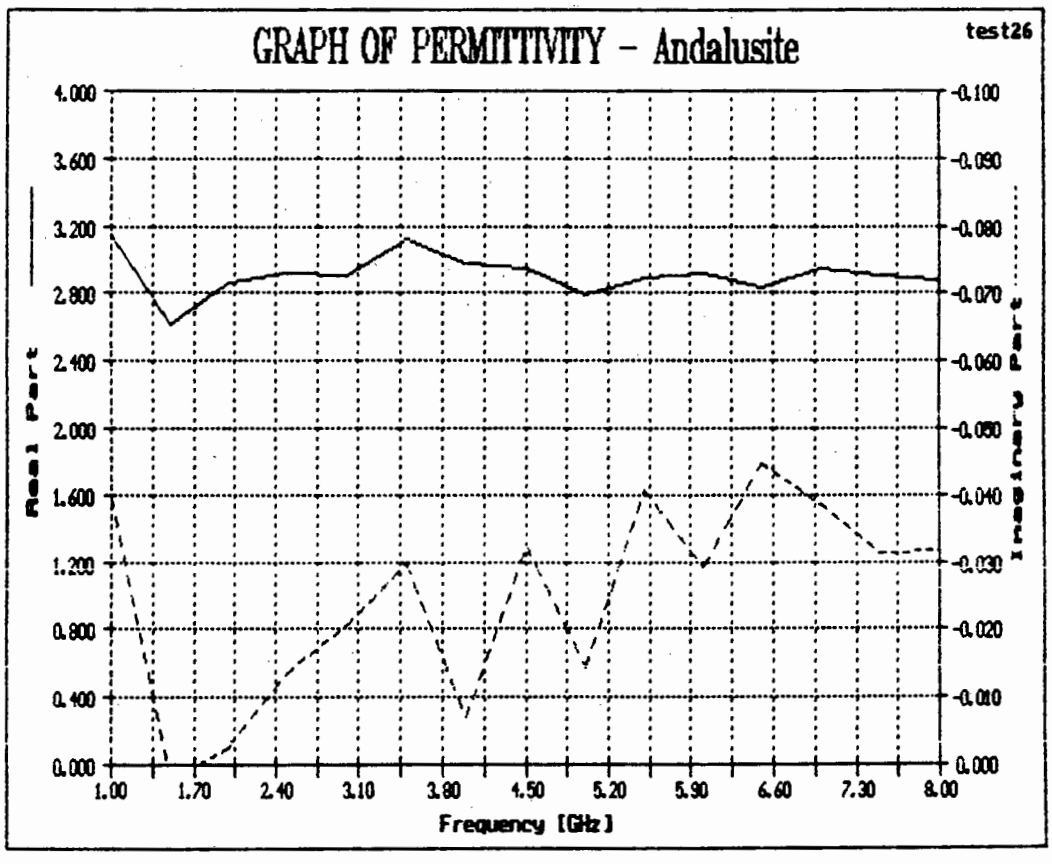

Figure 5.6.iii) Permittivity Curves for some of the Minerals Measured

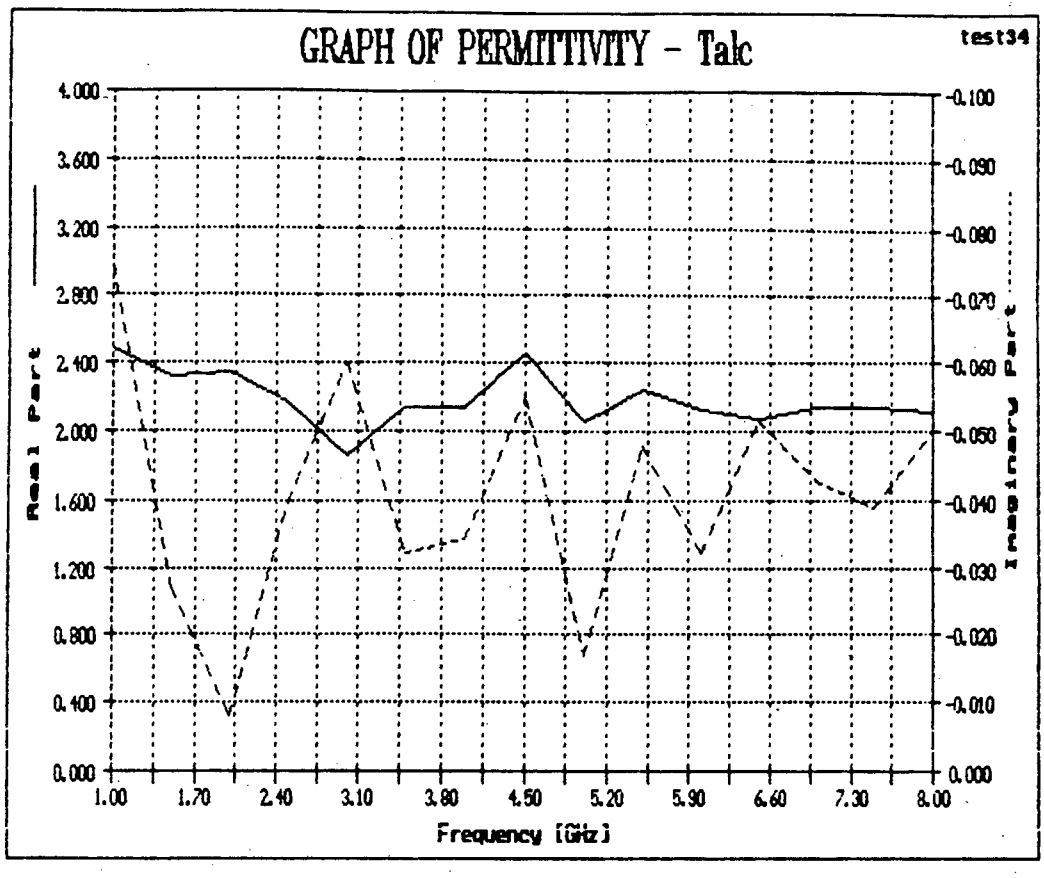

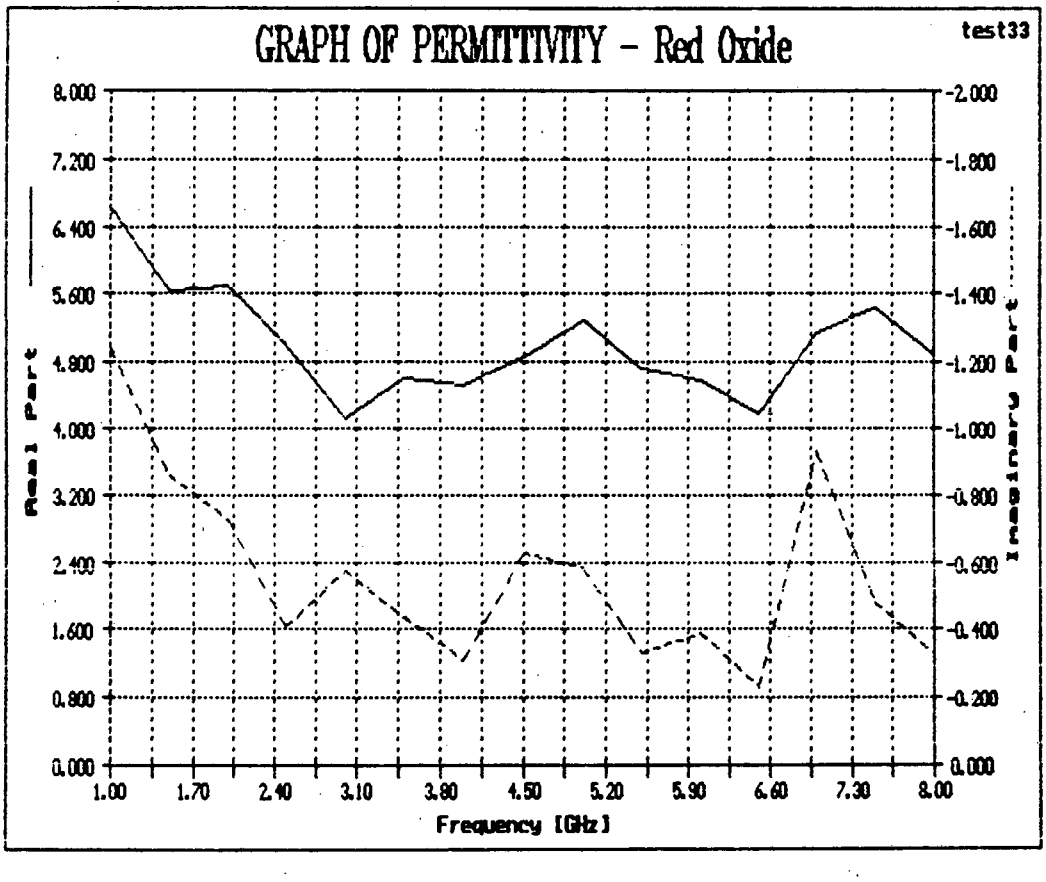

Figure 5.6.iv) Permittivity Curves for some of the Minerals Measured

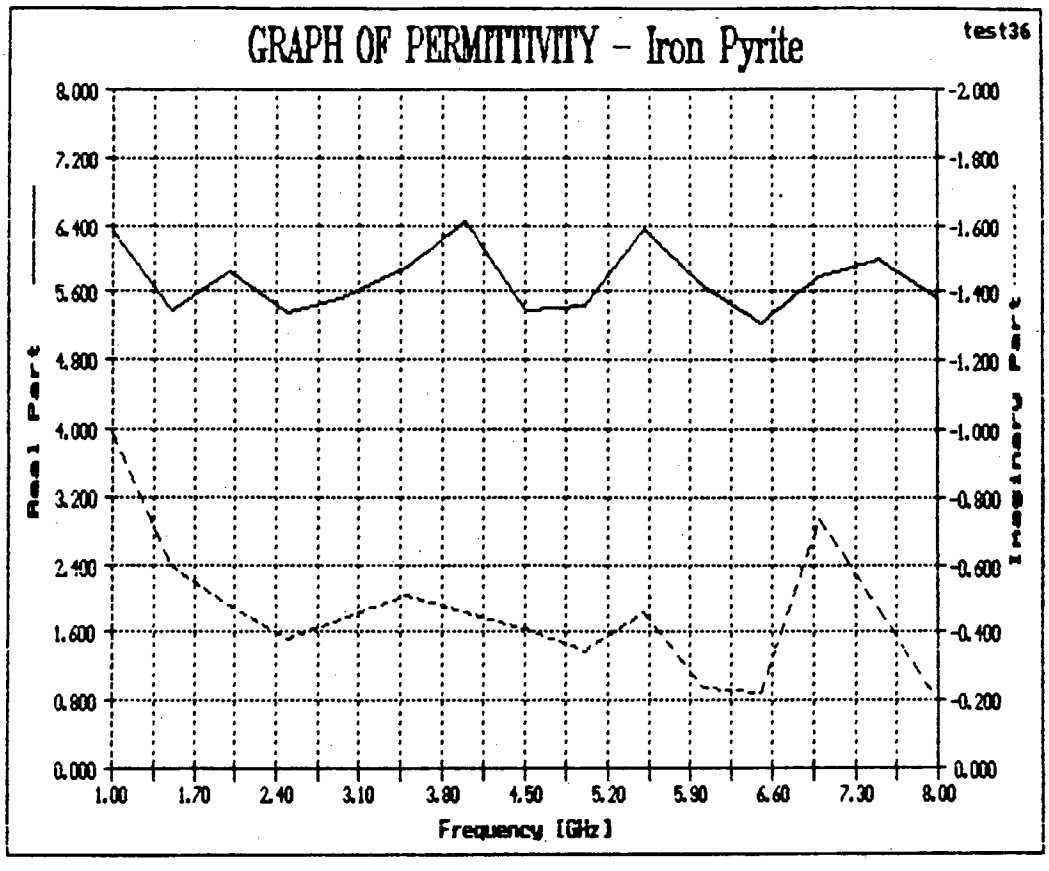

Figure 5.6.v) Permittivity Curves for some of the Minerals Measured

unclear since little analysis on the accuracy and errors was given and the tests were performed with the minerals in alcohol mixtures.

More accurate results should be possible by using a network analyser of higher accuracy and more carefully machined test cells. Better error modelling of the coaxial test cell discontinuities and imperfections may also help improve the accuracy.

The cavity perturbation method and its results are now covered in the next chapter.

6. CAVITY PERTURBATION METHOD

6.1. INTRODUCTION TO CAVITY PERTURBATION

A closed volume bounded by a conductive (metal) surface will exhibit only eigenvalue solutions to Laplace's equation $\nabla^2\Phi = 0$ (Maxwell's equation in free space with Φ the electric potential). Such a system can thus only sustain specific electromagnetic field patterns at specific frequencies - ie. it acts as a resonant structure. The field patterns are referred to as 'modes', with each mode being able to exist only at its resonant frequency. Such closed metallic resonant structures are termed 'cavities'.

Since Laplace's equation is separable in cartesian and cylindrical coordinates, this results in clear, analytical field solutions for both rectangular and cylindrical cavities. This advantage (plus mechanical simplicity) has resulted in both of these shapes being popular for resonant structures.

Because resonant cavities have discrete frequencies of oscillation, with corresponding field modes, it follows that it should only be possible to excite the cavity at exactly these resonant frequencies. In practice, however, there will be a narrow continuous band of frequencies, centred around the resonant frequency, at which resonant excitation may occur [31] - resulting in a typical lumped resonant shape response (cf. LRC lumped resonant circuit.).

The two parameters which characterise a particular resonant response of such cavities are therefore :

1) Resonant frequency. The frequency at which peak resonance occurs. There may be several resonant frequencies, each associated with a particular mode. These depending on the shape and size of the cavity.

2) Quality factor or Q. This determines the purity or sharpness of resonance, and accounts for energy losses within the cavity.

The Q (as in the case of a classic lumped resonant circuit), determines the 3 dB bandwidth of the resonant response. Energy losses within the cavity are mainly due to :

1) Finite conductivity and skin effect of the metal walls.

2) Power losses occurring due to any dielectric filling within the cavity.

3) Radiative losses from poor joints in the cavity walls.

4) Power coupled out into a resistive load.

Cavity perturbation methods measure both the resonant frequency and Q of the cavity both when empty and containing a sample of the dielectric to be measured. The introduction of the dielectric sample into the cavity has two effects [23] (see figure 6.1.) :

1) The resonant frequency will decrease. The dielectric will increase the stored energy of the cavity due to its higher dielectric constant. The wavelength in the dielectrically filled section becomes longer and thus the cavity will resonate at a lower frequency. This decrease in resonant frequency is thus mainly a function of the dielectric constant ϵ' of the dielectric sample.

2) The Q will decrease. This is due to increased energy losses within the cavity resulting from the dielectric. The decrease in resonant Q is thus mainly a function of the dielectric loss factor ϵ''.

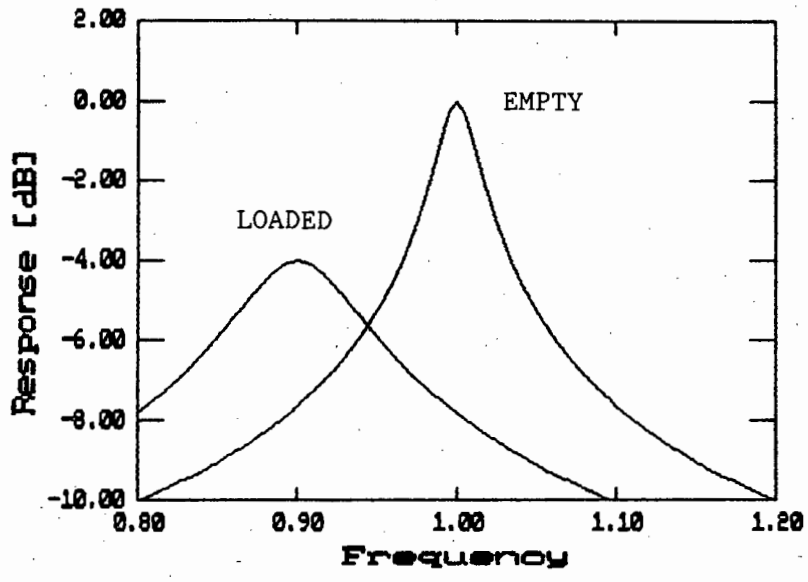

Figure 6.1. Resonant Changes due to a Cavity Perturbation

Hence by measuring the changes in resonant frequency and Q, and by knowing the system and field geometry, it is possible (in principle at least) to determine the complex permittivity of the dielectric sample.

The cavity type chosen for this study was a cylindrical cavity. The motivation for this choice, design, field distribution, and perturbation theory are covered in the following section.

6.2. CYLINDRICAL RESONANT CAVITY

The main motivation in choosing a cylindrical cavity (over other shapes, eg. rectangular) is in the advantages offered by the radial symmetry. Many of the modes have fields that are circularly symmetric, and by correct choice of sample position the perturbed field will retain its circular symmetry, only changing in radial distribution. This has led to its popularity since such radial field perturbations are easier to analyse than for those of other cavity types. These factors will become apparent in the following sub-sections. Such advantages are not available with rectangular configurations. Comparison of the dominant

(lowest frequency) field modes in rectangular and cylindrical cavities, shown in figure. 6.2., clearly illustrate this. The cylindrical shape also offers a more rigid mechanical construction.

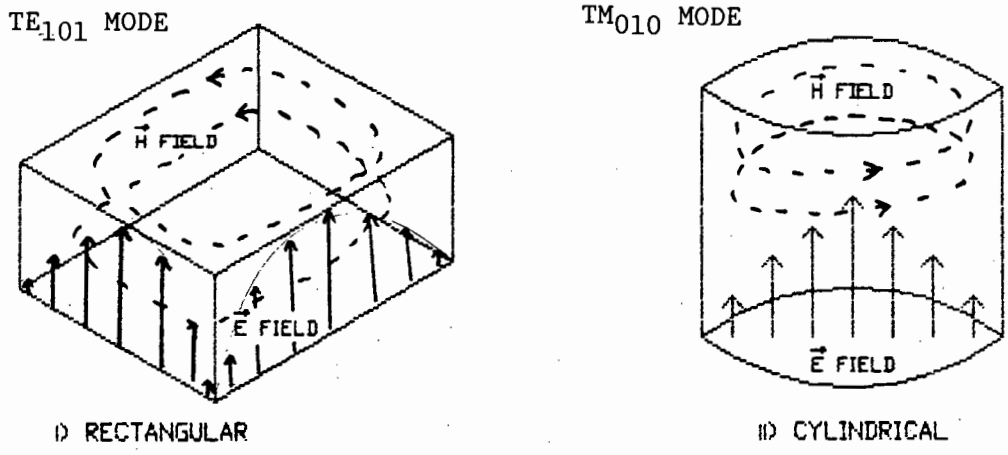

i) RECTANGULAR ii) CYLINDRICAL

Figure 6.2. Comparison between Field Symmetry in a Rectangular and Cylindrical Cavity

6.2.1. Choice of Mode and Field Distribution

The cylindrical cavity resonant mode chosen was the TM_{010} mode. For short length cavities this is the dominant mode (lowest resonant frequency) and well away from higher order modes. The TM_{010} mode has a resonant frequency given by [32] as :

$$f_o = \frac{c \cdot x_{01}}{\pi \cdot D} \qquad (1)$$

where D is the diameter of the cylinder and x_{01}=2.4048255 is the first root of $J_0(x) = 0$. This resonant frequency is independent of the length of the cavity L, however it does affect the Q and the resonant frequencies of the higher order modes. For convenience, a brief summary of the different mode patterns that occur in cylindrical cavities is given in **Appendix D**.

A resonant frequency of 1 GHz was chosen. There was no specific reason for using 1 GHz, it was mainly chosen to give a convenient physical size. For 1 GHz operation equation (1) gives a diameter of D = 23 cm. As mentioned above, although the resonant frequency of the TM_{010} mode is independent of length, it cannot be indiscriminately chosen, since it does affect higher order modes. The greater L, the higher the Q, but the lower the resonant frequencies of the higher modes. These higher order modes must be placed sufficiently far away. A height of L = 12 cm was chosen, this giving a resonant frequency for the closest mode (TE_{111}) of f_0 = 1.5 GHz.

The TM_{010} mode has a field distribution whose components are given by [32] (see appendix D) :

$$E_z = A \cdot J_0(2x_{01}r/D)$$

$$E_r = 0$$

$$E_\theta = 0$$

$$H_\theta = -J_1(2x_{01}r/D)$$

$$H_r = 0$$

$$H_z = 0$$

where r is the radial distance from the centre axis, and J_0 and J_1 the first and second order Bessel functions of the first kind. The field can be seen to be circularly symmetric since it has no dependence on θ.

These field distributions are shown diagrammatically in figure 6.3. The electric field occurs along the z axis, having its maximum at the centre and decreasing to zero at the circumference. The magnetic field occurs in radial shells, being zero at the axis and increasing to its maximum a little before the circumference.

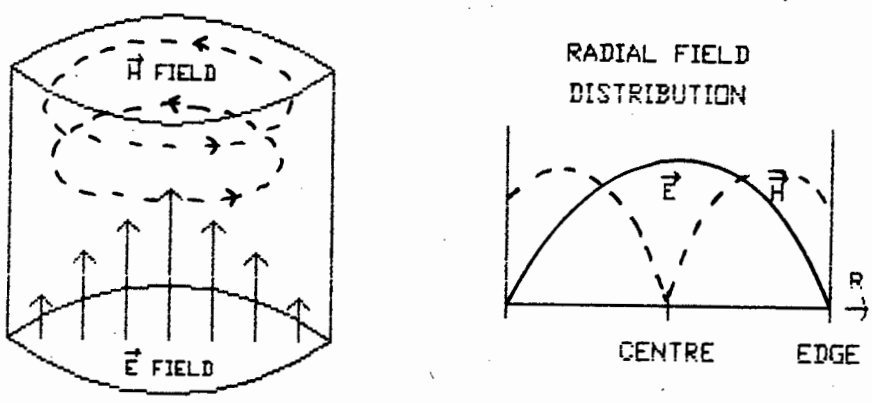

Figure 6.3. TM_{010} Field Pattern in a Cylindrical Cavity

6.2.2 Positioning of Dielectric Sample

Due to the radial symmetry of the fields, it can be seen that the most suitable position for placing a dielectric sample into the cavity is to mount a cylindrical specimen of the dielectric through the axis (see figure 6.4.) - ie. in a position of maximum electric field. This configuration still preserves the circular symmetry of the perturbed field and only alters its radial distribution. This positioning of the sample is commonly used.

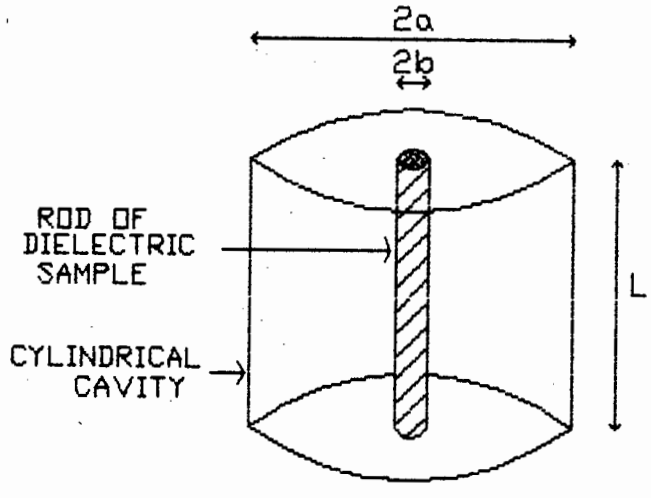

Figure 6.4. Cylindrical Cavity with Concentric Dielectric Sample

The effect of such a perturbation configuration was first studied by Horner et al [23]. Only the major points of interest will be presented here.

The resonant frequency of the cavity, as mentioned previously, is given by

$$f_o = c/(2.6125 \cdot a) \qquad (1)$$

where **a** is the radius of the cavity. In practice f_o will be slightly different due to resistive losses, frequency pulling by the coupling and finite Q. It is thus preferable to measure f_o and then calculate the 'effective' radius **a** (using (1)), that gives this resonance. The dielectric sample rod, of radius b, is now inserted, and the cavity found to resonate at a lower frequency of f_1. The dielectric constant ϵ' is then given by [23] :

$$\epsilon' = 1 + \frac{[aJ_0(\beta a)]/[bJ_1(\beta b)]}{F \cdot [1+(\beta b)^2/8]+[(\beta b)^2 aJ_0(\beta a)]/[8bJ_1(\beta b)]} \qquad (2)$$

where $F \equiv [Y_0(\beta a)J_0(\beta b)-Y_0(\beta b)J_0(\beta a)]\pi\beta a/2$

and $\beta = 2\pi f_1/c$.

If $b/a < 20$ then equation (1) can be approximated by

$$\epsilon' = 1 + 0.539 \cdot \frac{a^2}{b^2} \cdot \frac{(f_0-f_1)}{f_0} \qquad (3)$$

The above derivation assumes that the dielectric is of fairly low loss $\epsilon'' \ll 1$, the frequency shift is small $(f_0 - f_1)/f_0 \ll 1$ and that the Q is high.

The decrease in quality factor Q is used to determine the imaginary part of the permittivity. Suppose the cavity has a loaded $Q = Q_s$ with the sample enclosed. The imaginary part ϵ'' is then given by

$$\epsilon'' = \frac{a^2/b^2+F^2[\epsilon'-1)}{F^2\cdot[1+J_1^2(\beta_1 b)/J_0^2(\beta_1 b)]}\cdot[1/Q_s-1/Q'] \qquad (4)$$

where $\beta_1 = \epsilon'\beta$

and Q' is the cavity Q when the dielectric sample is replaced by a supposed loss-free specimen of the same dielectric constant and dimensions. Obviously it is not practical to use these 'equivalent loss-free dielectrics', and in practice Q' is calculated from

$$Q' = \frac{L}{d}\cdot\frac{a^2/b^2 + F^2\cdot(\epsilon'-1)}{a(a+L)/b^2 + F^2\cdot(\epsilon'-1)} \qquad (5)$$

where *d* is the 'effective skin depth' of the conducting walls of the cavity. It can be determined from $Q = Q_0$ of the empty cavity

$$Q_0 = \frac{L}{d(a+L)} \qquad (6)$$

Since, in practice, measured Q's are far lower than the theoretical values (due to numerous reasons mentioned previously), d is not the actual skin depth, but is simply used to model all the combined losses.

Again if $a/b < 20$ then (4) can be approximated by

$$\epsilon'' = J_1^2(x_{01})\cdot(1/Q_s-1/Q')\cdot a^2/b^2 \qquad (7)$$

The above theory has been shown to be very accurate. However, factors arising from necessary practical implementation will cause deviations from it. The practical implementation for a cylindrical cavity is covered in the next section.

6.3. PRACTICAL IMPLEMENTATION

This section covers construction details of the cavity, ways of inserting the powdered sample into the cavity and its effects, and resonant frequency and Q measurement techniques.

6.3.1 Construction

As mentioned in section 6.2.1, a 1 GHz cavity was chosen for study. This had a diameter of 2a = 23 cm and a height of L = 12 cm, and was fabricated from brass plate. All joints were soldered, except for the one end plate where a flange, onto which the end-plate is bolted, was provided in order to allow access inside the cavity. The use of metals with higher conductivities (copper, silver plating) would result in higher Q's being obtained.

Several methods of exciting the TM_{010} mode in the cavity were investigated. The most successful method found (achieved the highest Q) was that using two small loops of copper wire ('H-loops') each mounted half way down the opposite sides of the cavity (see figure 6.5.). The loops were both about 1 cm in diameter and soldered onto female BNC connectors. These connectors were then mounted through holes in the cavity side walls and held in a position by small tightening screws. This allowed the loops to be rotated in order to optimise the coupling, and hence Q. The loops were placed in these positions, so as to couple the circumferential loops of magnetic field through them. These coupling loops should be kept small so as minimise the distortion of the field

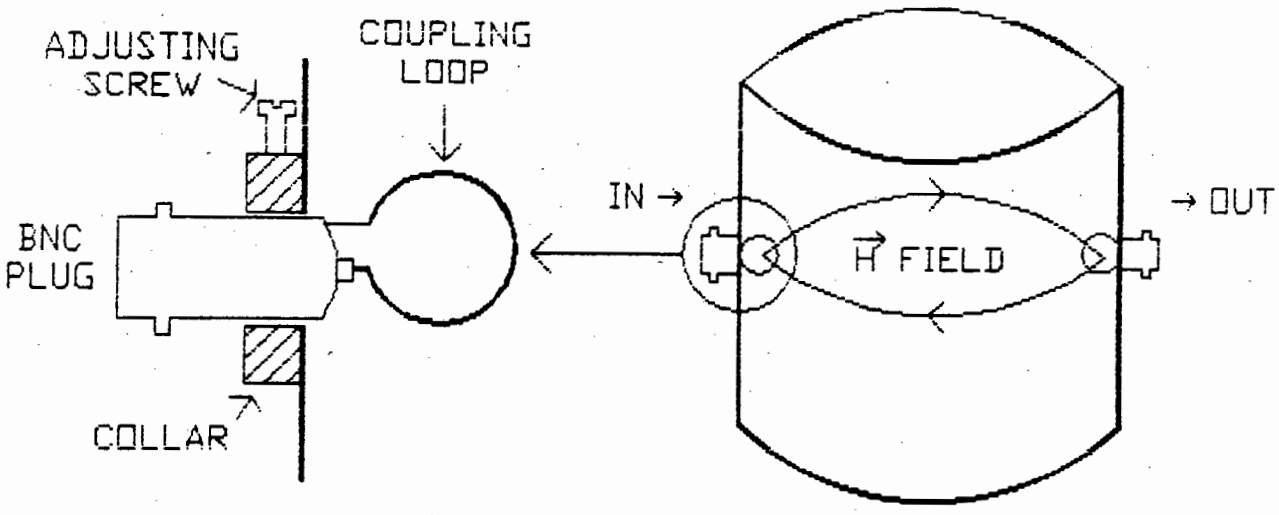

Figure 6.5. Cavity Coupling Loop Arrangement

The measured response of the cavity using the HP 8410 Network Analyser is shown in figure 6.6.. The resonance frequency was f_0 = 1.00262 GHz and the Q about 4730.

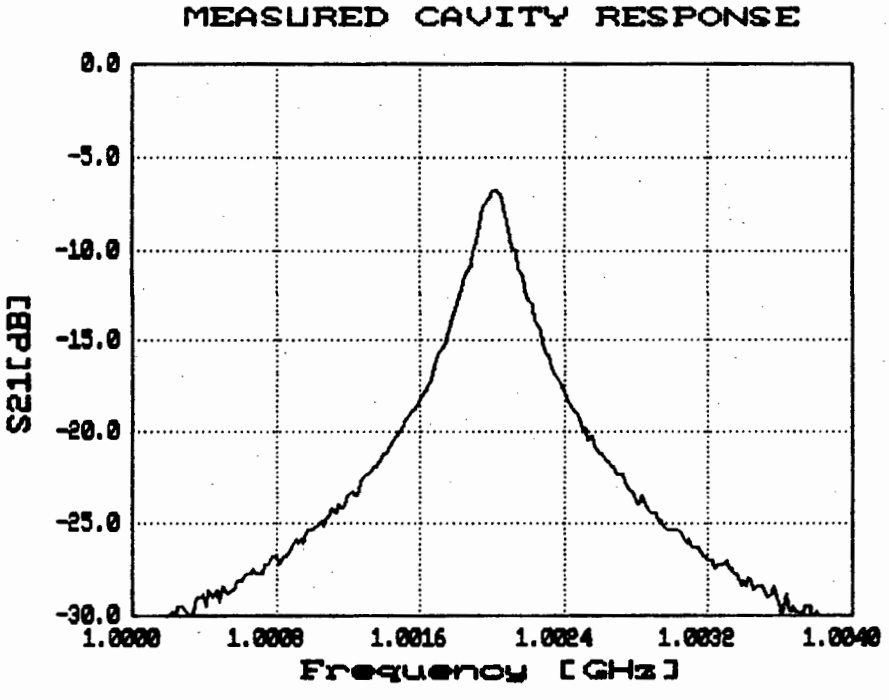

Figure 6.6. Measured Resonance Response of Cavity

A high Q is desirable since it provides a higher sensitivity in measuring loss, ie. the higher the unloaded Q, the larger will be the reduction in Q for a small change in ϵ''. This can be seen from equation 7, section 6.2.2.

To facilitate easy introduction of the powdered mineral samples into the cavity, a thin walled glass-pyrex or plastic tube is to be mounted along the axis through two holes in the end-plates (see figure 6.7.). Two brass tubes at the end-holes provide mechanical support, and also 'contain' the field, since they are below cut-off for 1 GHz and hence act as effenecent waveguides. This prevents radiation loss.

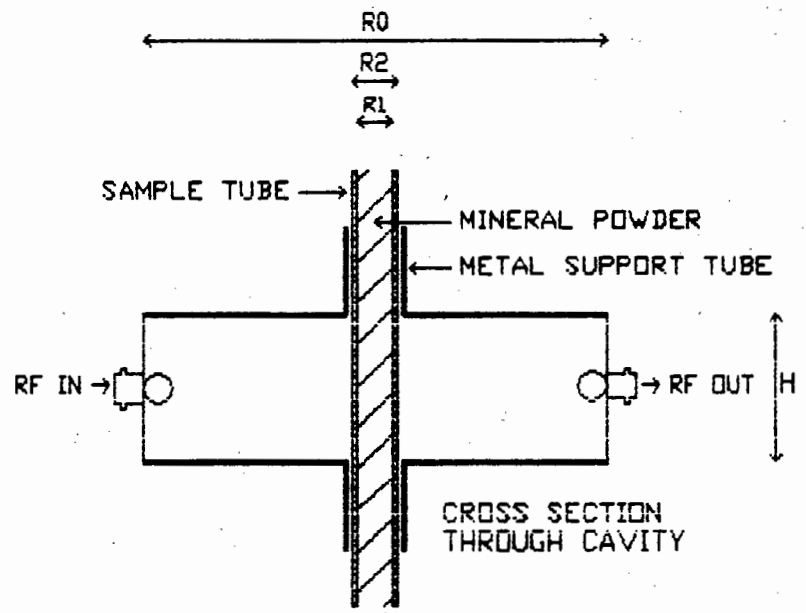

Figure 6.7. Sample Tube through End Holes and Support Tubes

The factors governing the dimensions and effects of this sample tube are discussed below.

6.3.2. Effect of Sample Tube and Insertion Hole

The use of a glass tube and its insertion holes will cause deviations from Horner's perturbation theory [23] as presented above in section 6.2.2. These effects have been studied extensively in the literature [33], [34], [35], [36] and [37], and are briefly presented here.

6.3.2.a). Effect of Sample Tube

Since the mineral samples are powdered they must be contained. Thin walled glass tubes were chosen for this. Although glass is fairly lossy, there is a wide range of glass tube sizes and the complex permittivity of glass is easily measured or found from references [27]. The effects of this sample tube would have to be removed anyway, so the use of glass is not detrimental.

Choice of the sample tube size is a trade-off between two factors:

1) The larger the tube (ie. sample diameter) the larger the frequency shift will be, and hence higher the sensitivity in measurement of ϵ'.

2) The sample size cannot be too large since this would reduce the Q too much and hence reduce the sensitivity in ϵ'' measurement.

A glass tube of outer diameter 1 cm, and wall thickness 1 mm, was selected on the basis of empirical tests on SiO_2 (a typical mineral to be measured). By using brass plugs, that screwed into the sample support tube, tubes of smaller diameters could be used. This was sometimes necessary for measurement of lossy substances, where a smaller sample volume was required in order not to overload the cavity. A thin walled plastic tube of 6 mm in diameter was used for these measurements.

Solutions for dielectric constant (accurate for $\tan\delta < 0.5$) accounting for the presence of a sampling tube (but ignoring hole effects) have been derived and presented by Lukác [34] and Gregory [35]. These equations must be solved numerically.

Exact equations that give both ϵ' and ϵ'' for dielectrics of both low loss and high loss have been derived by Li, Akyel and Bosisio [37]. Since many of the dielectrics to be measured were very lossy, their equations were selected for use as others would be less accurate. These equations are extremely involved and are listed in **Appendix E** together with a MathCAD programme listing used to solve them.

6.3.2.b). Effect of Sample Insertion Hole

The presence of the two axial insertion holes in the end plates will result in an infinite series of cylindrical TM_{0n} waveguide modes (n=1 to ∞) propagating down the dielectrically filled holes, with the metallic support tube acting as a circular waveguide ([33] & [36]). However, since these holes are far smaller in diameter than the resonant wavelength, all these modes evanesce rapidly. Although the higher order modes are weaker, they must also be considered since they evanesce less rapidly and hence propagate further than the low order modes. The presence of these tubes causes the cavity resonant frequency to increase slightly. This resultant frequency pulling effect, and the increased loss due to the added dielectric results in the fact that the measured ϵ' and ϵ'' values (using the formulae given above) are always found to be smaller and larger (respectively) than their true values. The effect of these holes have been studied by [33], [35] and [36], and it has been shown that correction factors can be used to correct for these differences :

$$\epsilon' = 1 + (\epsilon'_{unc} - 1) \cdot (1 + 4CR_1/H)$$

$$\epsilon'' = \epsilon''_{unc}(1 - 4DR_1/H)$$

where ϵ'_{unc} and ϵ''_{unc} are the uncorrected measured values and ϵ' and ϵ'' the new corrected values. The values of the correction factors C and D have a complex dependence on the ratio of inner to outer sample tube diameter R_1/R_2 and both sample tube and sample permittivities. Curves showing their values [36] are given in **Appendix E**. With no sample tube C = D = 0.327. These correction formulae are implemented in the MathCAD programme (mentioned in section 6.3.2.a.) of **Appendix E**.

6.3.3. Measurement Technique

Numerous techniques have been presented in the literature [38], [39], [40] and [41] for attempting accurate measurement of microwave cavity resonant frequency and Q. However, these methods tend to be either very complicated and involved or use equipment that was unavailable. A different measurement method was thus developed using the existing network analyser equipment, and found to be extremely accurate. This method is briefly described below :

The experimental set-up used is shown in figure 6.8. The computer sets the required frequency at the HP microwave signal generator via the HPIB interface. Since the frequency reading from the signal generator is not very accurate, a fraction of the output signal is coupled off through a -20dB coupler to a HP frequency counter. The actual frequency can then be read far more accurately by the computer via the HPIB bus. The rest of the signal is directed to the HP s-parameter test set to which the cavity is connected. The response of the cavity (s_{21}) can then be read from the analogue magnitude output of the network analyser, via signal conditioning circuitry, by a 12-bit ADC on-board the PC.

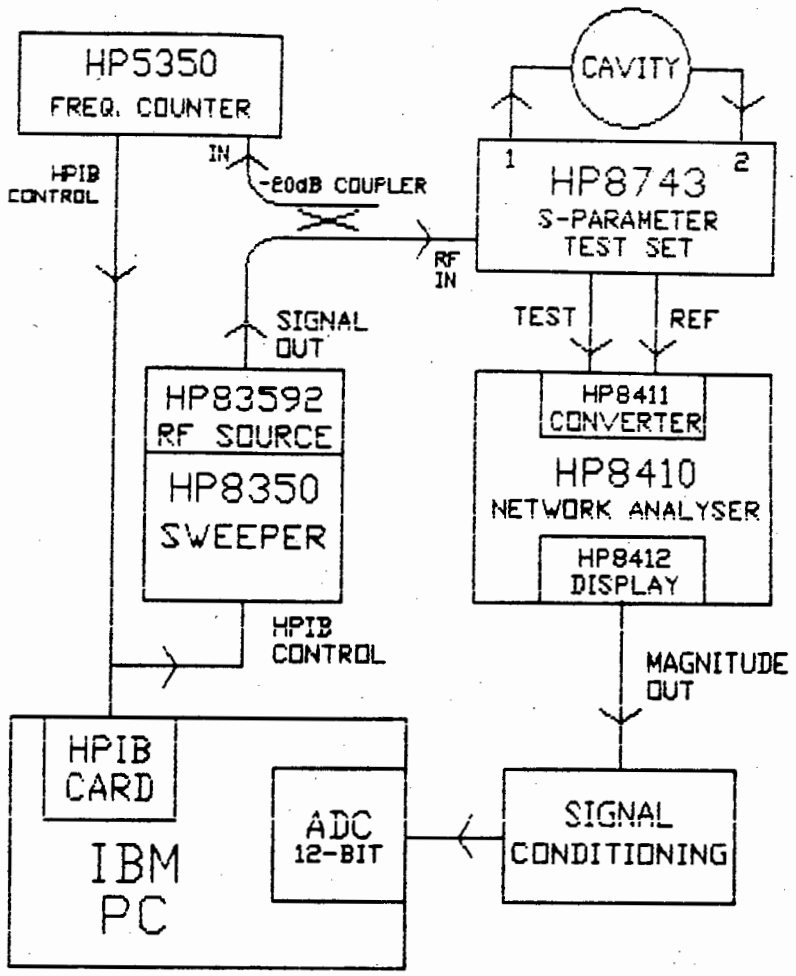

Figure 6.8. System used for Measuring Cavity Response

Since the HP microwave signal generator has a step resolution of about 100 KHz, it would seem that this would put the limit on the resolution attainable in measuring the resonant frequency and Q. However, by taking a series of readings at frequency intervals spanning the resonant peak (done automatically by computer), far more accurate values can be obtained by using the theoretical resonant response formula [31] :

$$S_{12}(w) = K \cdot \frac{1}{\sqrt{[(w-w_0)^2+(w_0/2Q)^2]}} \qquad (1)$$

Parameters w_0 (resonant frequency), Q and K (constant offset) are then optimised to provide a best least squares fit to the discrete measured data. This effectively performs an "optimum interpolation" between the measured data points (see figure 6.9.).By using this technique, the resolution and accuracy can be improved by about two orders of magnitude.

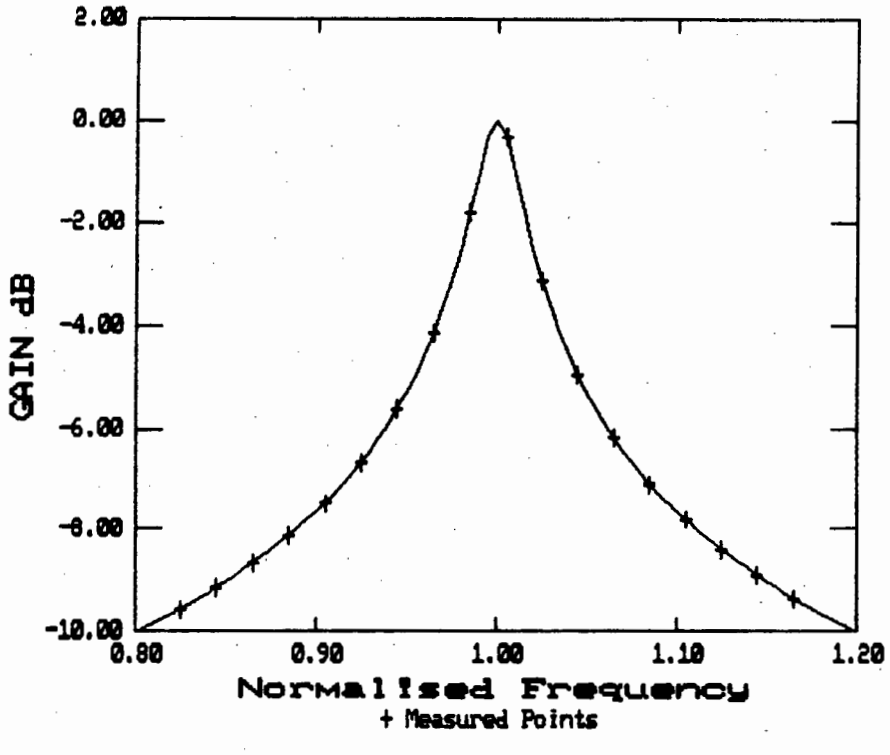

Figure 6.9. Fitting Theoretical Resonance Response to Measure Data

This system was capable of measuring resonant frequency accurately and repeatedly to six significant figures. The repeatability in Q measurement was better than 0.5 %. The mean square error between the theoretical response and the measured data points was consistently less than 0.0001.

More complete details of the interface, measurement method and computer routines are given in **Appendix F**.

6.4. PERTURBATION TESTS

Initial cavity perturbation tests were performed on known substances in order to test the accuracy of the measurement system and the calculations. These measured values of dielectric constant were then compared against their reference values. Very few referenced values for loss factor are available, so most of the comparisons were for dielectric constant. The initial tests were done on 1 cm diameter plastic rods with no sample tubes. The results are shown in table 2 below.

MATERIAL	MEASURED ϵ_r	REFERENCE ϵ_r [27]
Teflon	2.09+j0.00022	2.10+j0.0003
Polyethylene	2.34+j0.0000	2.33
Nylon	3.20+j0.052	3.14 - 3.13

Table 2. Comparison between Measured and Referenced Values of Some Solid Dielectrics

The difference between these values is small, indicating the accuracy of the measurement system and perturbation formulae used.

Since glass tubes were to be used to contain the powdered mineral samples, the permittivity of this glass was required. Because the permittivity of glass varies widely, depending on its grading [27], a solid glass rod of the same type as the tubes was measured. Its permittivity was found to be $\epsilon = 4.51 - j0.05$. To check this, and the validity of the equations accounting for the tube, air and liquid cyclohexane were measured. Table 3 gives the comparison between their measured and referenced values.

MATERIAL	MEASURED ϵ_r	REFERENCED ϵ_r
Air	0.997+j0.00006	1.000+j0.0000
Cyclohexane	2.016-j0.00012	2.015 [10]

Table 3. Comparison between Measured and Referenced Values of Dielectric Constant with Glass Sample Tube

The difference between these values is negligible, showing that the measurement of dielectrics contained in the sample tube, and the calculation of their permittivities, could be trusted.

For the lossy minerals, a smaller plastic tube (of outer diameter 6.07 mm and inner diameter 5.17 mm) was to be used. The permittivity of this tube was measured as ϵ=2.36-j0.04. Table 4 gives test results on air and cyclohexane using this tube.

MATERIAL	MEASURED ϵ_r	REFERENCED ϵ_r
Air	1.002+j0.00001	1.000+j0.0000
Cyclohexane	2.12-j0.00019	2.015 [10]

Table 4. Comparison between Measured and Referenced Values of Dielectric Constant with Plastic Sample Tube

The error in the dielectric constant of cyclohexane is slightly larger than previously (by 5%), but this is probably due to the difficulty in accurate measurement of the tube thickness (resolution of the micrometer).

Now that testing was complete, measurement on the powdered mineral samples could proceed. Measurements of these samples, and their results, are covered in the following section.

6.5. MINERAL MEASUREMENTS AND RESULTS

This section presents and discusses the permittivity measurements performed on the powdered mineral samples listed in **Appendix A**. The tests and results are presented in the following sub-sections.

6.5.1. Sample Preparation

As mentioned in section 3.2., small quantities of water would severely affect the measurement of permittivity. The samples were thus dried in a thermal oven (≈170°C for 1-2 hrs) prior to measurement. The powdered minerals were then loaded into the sample tubes. The two different sample tubes (the 1 cm diameter glass tube for the low loss minerals, and the smaller 6 mm diameter plastic tube for the very lossy minerals) as mentioned in the above tests were used.

Since the minerals were in powdered form (discussed in section 3.1.) they are essential mineral-air mixtures, and thus have a reduced effective permittivity compared to their solid form. The tighter the powders packs, the higher will be their measured effective permittivities. The powders' volume may vary by as much as 40 % depending on packing density, thus seriously affecting the permittivity reading if not accounted for. Methods have been used to allow the measurement of the actual permittivity of the solid by compressing and baking the powder into a 'cake', and also by mixing the powder with low-loss liquids of known permittivities [10] in order to 'fill the gaps' and allow extraction of the actual permittivity value independent of packing density. Many theoretical formulae relating the resultant permittivity of binary mixtures to the permittivities of their individual components exist [17]. Some of these were mentioned in

section 3.3. If Lichteniker's formula (which supposedly gives good correlation to actual experiment), see section 3.3., is applied to an air-mineral mixture, the resultant permittivity of the mixture becomes :

$$\epsilon = \epsilon_1 \cdot \exp(\theta)$$

where ϵ_1 is the permittivity of the solid material, and θ its volume fraction in the air mixture. This may help in obtaining an approximate value of the solid mineral alone, if the packing density θ can be determined. Other mixture formulae (eg. Bruggeman's) may also prove useful.

Because the minerals were to be encountered in their powdered form (eg. dried slurry), it was decided to investigate ways of obtaining a uniform packing density, yet retaining the minerals' powdered form. Surprisingly, the most successful method was found to be one in which the sample tube was repeatedly tapped until the powder settled under its own weight to a constant height. This was verified by weighing the sample (total weight minus glass tube weight) and measuring the sample height and then calculating a linear packing density (ie. g/cm). By monitoring this packing density, it was found that repeatabilities of better than 8 % could generally be obtained. Although this error is far greater than the measurement error (as seen from section 6.4.), it was felt to be sufficient in this study for these initial mineral comparisons.

The loaded sample tubes were then inserted into the cavity and readings taken (as described in section 6.3.3. and appendix F). The resonant frequency and Q perturbations were then processed (see section 6.3.2.b and appendix E) so as to calculate their complex permittivities.

6.5.2. The Measured Complex Permittivities of the Mineral Powders

The dielectric constant and loss factor results of the minerals measured are given in table 5 below.

MINERAL	DIELECTRIC CONSTANT	LOSS FACTOR
Andulasite	2.5	0.0056
Barytes	3.6	0.0024
Calcined Magnesite	2.0	0.0068
Chamotte	2.7	0.0058
Chrome Diopside	2.8	0.0066
Chrome Sand	3.2	0.0080
Coal	2.5	0.042
Feldspar	1.9	0.0037
Garnet	4.3	0.0036
Graphite	Conductor	
Ilmenite	7.5	0.91
Iron Pyrites	7.2	0.55
Manganese Dioxide	9.2	0.86
Ocean Bentonite	4.7	1.1
Red Oxide	4.7	0.53
Silica	1.9	0.0060
Talc	1.8	0.0089
Zircon	3.3	0.00081

Table 5. Complex Permittivity Results of the Measured Minerals

It is observed that there is an enormous range in the value of the loss factors. The minerals can be divided into two distinctly different groups : i) those of low loss, and ii) those of high loss. Of the high loss minerals, Ilmenite, Iron Pyrites and Red Oxide are obviously ferromagnetic. Their values of measured permittivity are thus probably not true due to there magnetic permeability μ_r being greater than unity (see section 3.4.). However, these values are still useful since they allow differentiation against the other minerals. Although Ocean Bentonite has the highest loss, its small content of Fe_2O_3 is unlikely the cause of this. It is probably due to its highly polar OH^- hydroxyl groups (see section 2.2.2).

Because these ferromagnetic minerals are very lossy, the loss factor of low loss dielectric minerals may be strongly affected by small parasitic quantities of such ferromagnetic or other high loss substances (eg. Talc containing 4.5 % Fe_2O_3). This may provide erroneous readings.

The effect of powdering the mineral on reducing the effective permittivity can clearly be seen by looking at the value for SiO_2. In this powdered state, SiO_2 had a dielectric constant of 1.9, whereas solid quartz crystal has a value of 3.85. This effect, as explained in section 3.3.4, is due to the presence of air. To achieve equivalent readings using a powdered form, other preparation methods suggested earlier would have to be used.

Plotting the positions of the minerals on a plane with axes of dielectric constant and loss factor provides useful visual insight into their distribution. Figure 6.10 shows such a plot, with dielectric constant on the horizontal axis and loss factor on the vertical axis with a logarithmic scale.

If certain minerals are positioned substantially far apart on the plane, then such data could be used for the identification and differentiation between these minerals. Such an idea has been successfully implemented

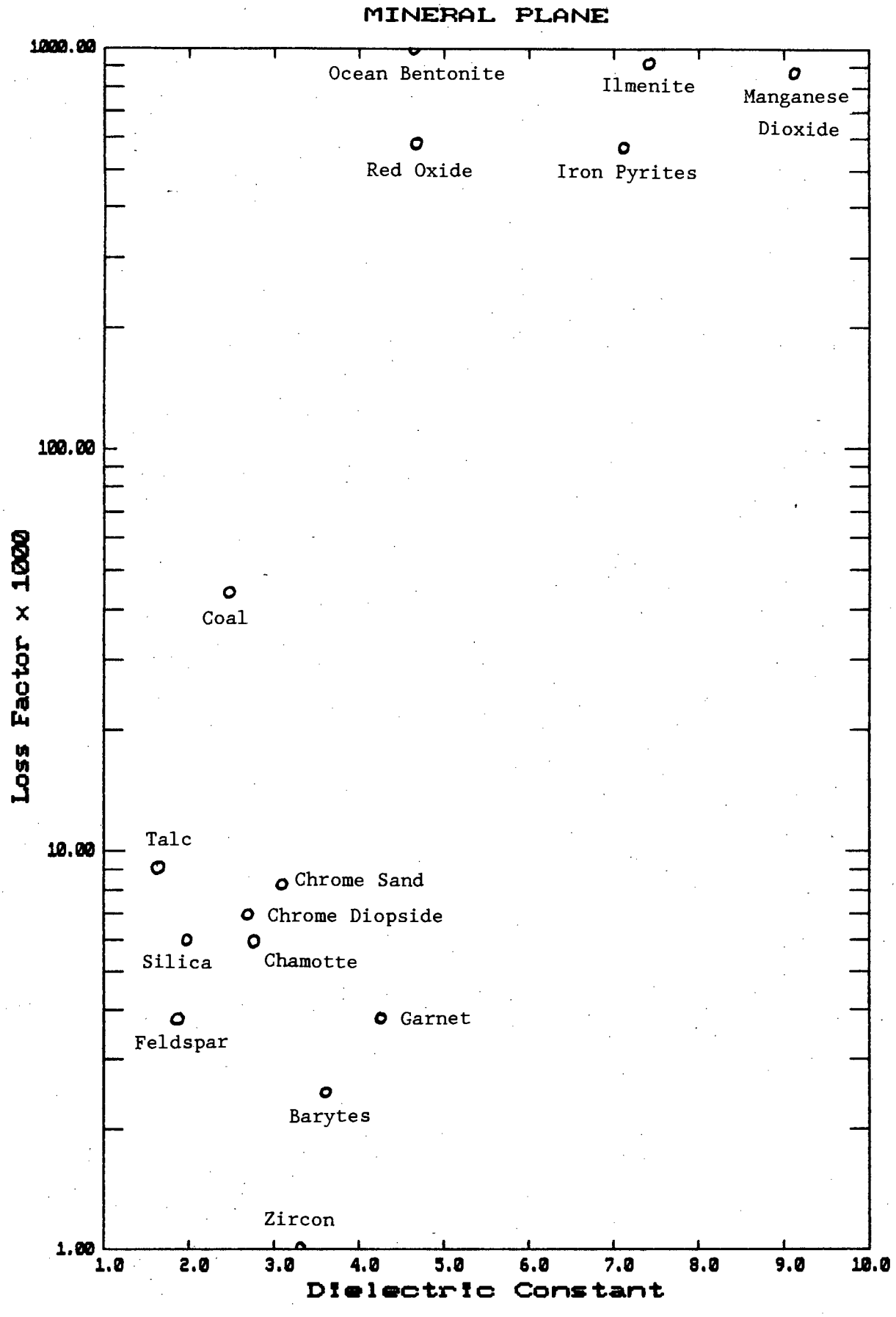

Figure 6.10. Position of the Minerals on a Complex Permittivity Plane

on far simpler scale [24]. Here, the greatly different degrees of loss for the two rock types, gabbro and kimberlite, were used to facilitate on-line separation of them.

Mono-mineralic minerals (ie. one compound only, eg. SiO_2) should show fairly consistent values of permittivity independent of their source of origin, provided the purity is high. However, polymineralic minerals (containing different minerals, eg. Andalusite) cannot be expected to have consistent permittivity values, since their permittivity will be highly dependent on the composition. Such minerals could be expected to show substantial variations in their permittivities for different sources. This effect, and possible applications of it, were briefly investigated and are covered in the following section.

6.5.3. Variation in Permittivity with Mineral Content

As mentioned above, small parasitic quantities of very high loss minerals could severely alter the measured permittivity of a low loss host material. This effect was tested by purposefully 'contaminating' silica with controlled amounts of high-loss iron pyrites and then measuring the permittivity of the resultant mixture. If the individual permittivities of the two components are known, then this could possibly be used as a crude analysis technique. Table 6 gives the results for such a test. The percentage of iron-pyrites in the silica base is by mass.

% IRON PYRITES	DIELECTRIC CONSTANT	LOSS FACTOR
0.0%	1.94	0.007
1.9%	2.00	0.0086
5.3%	2.02	0.0090
10.3%	2.13	0.013
15.0%	2.18	0.014
22.8%	2.44	0.020
30.8%	2.47	0.024
40.7%	2.56	0.027

Table 6. Variations in Complex Permittivity for a Silica-Iron Pyrites Mixture

As is expected, both the loss factor and dielectric constant increase with rising iron pyrites content. These variations in permittivity are graphically plotted in figure 6.11.

The major cause of deviations in the points from a smooth line is due to the problem of measurement repeatability caused by packing density variations. A more controlled method of obtaining a constant packing density (eg. see section 6.5.1.) would be necessary to enable accurate measurement of iron pyrites content to better than 5 % resolution. Such a method could then possibly be used for simple and rough 'concentration analysis'.

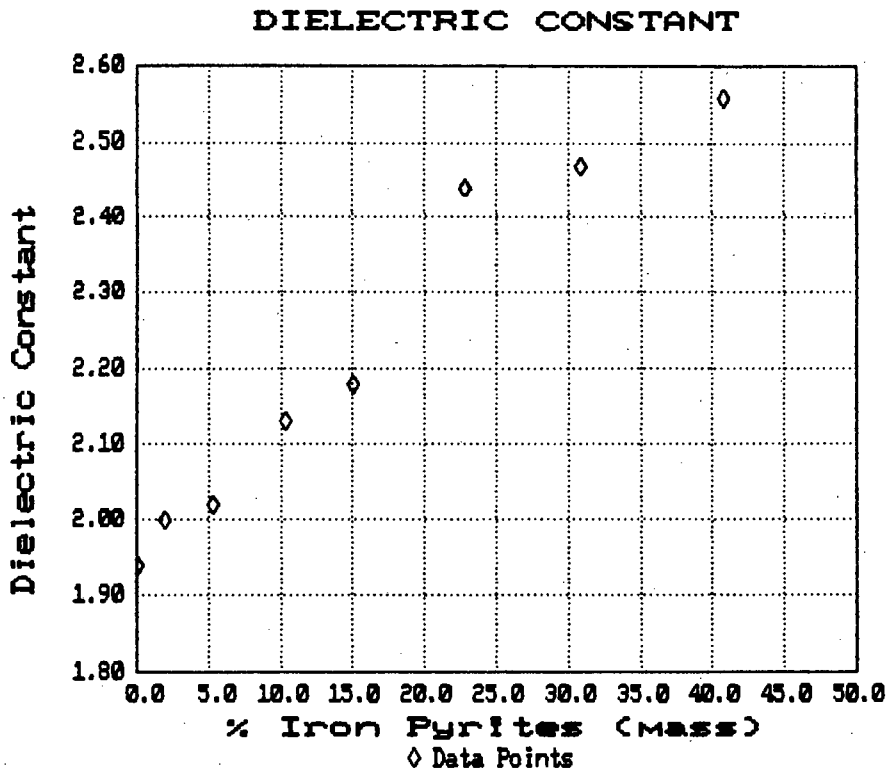

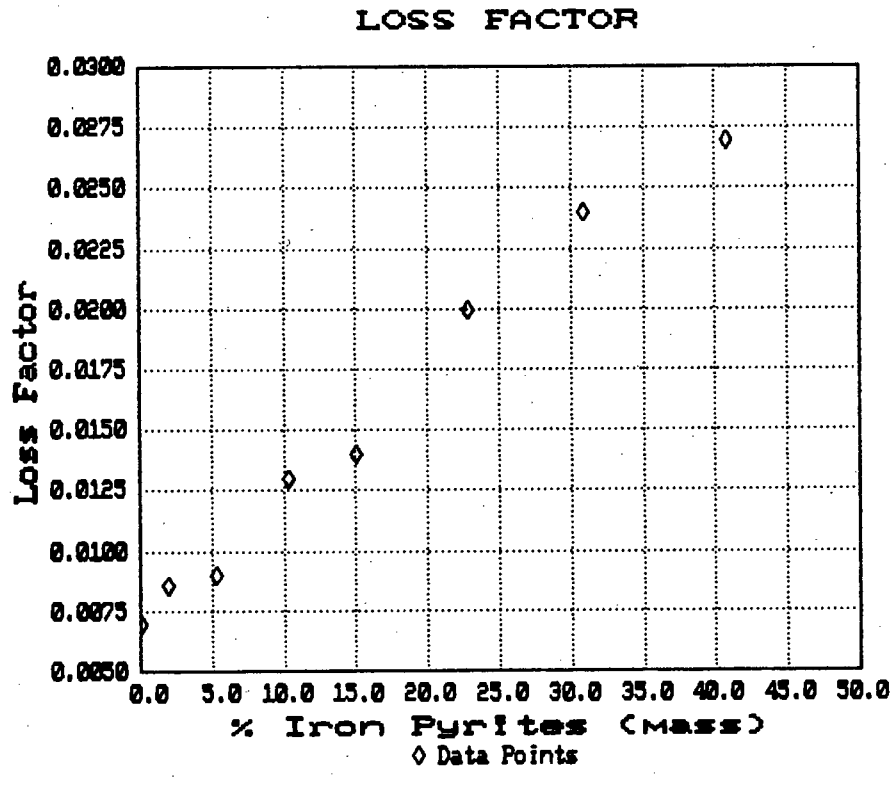

Figure 6.11. Graphs Showing Variations in Permittivity for a Silica/Iron Pyrites Mixture

6.6. CONCLUSION ON CAVITY PERTURBATION METHOD

The cavity perturbation method has been shown to be simple, accurate and fairly successful in the measuring of a wide variety of mineral powders. The main problem is that of repeatability when measuring powdered mineral samples. This, as explained, is due to variations in the packing density of the mineral, and hence its effective complex permittivity. The microwave measurement system side has been shown to be extremely accurate and consistent. Its contribution to the nett error being negligible. Possible techniques for increasing measurement repeatability of mineral powders have been suggested, but investigation of these is beyond the scope of this thesis. Such work may probably be studied at a later stage by MINTEK.

Final conclusions on this thesis, together with suggestions on possible future recommendations and uses for microwave mineral analysis, are presented in the next, and final, chapter.

7. SUMMARY, CONCLUSIONS AND RECOMMENDATIONS

This thesis has investigated the reasons for microwave loss in dielectrics, how minerals can often be considered as dielectrics and completely characterised (electrically) by their complex permittivity. Several microwave methods of measuring permittivity, and how these could be applied to minerals, were investigated. Two of these methods (the short circuited coaxial line method and cavity perturbation), were selected for testing on the various mineral powders chosen for this study.

The short circuited coaxial line method was considered suitable since it enables wide bandwidth permittivity measurements to be made. The theory, equations and measurement method were described. Unfortunately tests showed that this method was prone to large errors. These errors limited the success of this experiment. The errors resulted from equipment inaccuracies and poor sensitivity of the equations. However, it was seen that there were no significant variations in the mineral dielectric constants over the 1 GHz - 8 GHz frequency range swept.

The second method to be investigated was a cavity perturbation technique. This proved to be very successful. A 1 GHz cylindrical cavity operating in a TM_{010} mode was chosen. The theory behind cavity perturbation and the measurement system used were described. Tests on the system showed that complex permittivities could be measured repeatedly with good accuracy.

The powdered mineral samples were measured and the results presented and discussed. The minerals exhibited large ranges in permittivities, especially in loss factor. The main problem encountered with this method in measuring powdered samples was that of repeatability. This is caused by variations in the packing density of the powder; the denser the packing density, the higher the permittivity. Possible methods of overcoming this were suggested, but not tested. The effect of changes in composition on permittivity were briefly looked at.

The possible applications of such cavity perturbation techniques for mineral analysis by measuring complex permittivity could include :

a) On-line rock differentiation. This has been successfully applied to a simple differentiation between two distinctly different rock types [42]. Here, highly lossy kimberlite rocks were sorted from low loss gabbro rocks by dropping them through a 500 MHz TE_{101} rectangular cavity and noting the decrease in Q. The difference in loss was large enough to allow successful sorting with a 2:1 independence in rock size. However, by predetermining the positions of the different rocks of interest on a complex mineral plane, such as figure 6.10, and using a more advanced perturbation measurement system together with an on-line measure of rock volumes (eg. optical imaging) to obtain a approximate on-line measurement of permittivities, would enable the identification and sorting of several different rock types simultaneously.

b) Determining the complex permittivities of various solid rocks would help characterise the propagation of radio or microwaves underground. This may help in the design of ground penetrating radars (GPR's). Such radars have shown potential for geological use.

c) Measured values of complex permittivity will help predict the microwave heating of minerals without actually resorting to high power levels. This will help in the design of microwave digestion equipment. As mentioned in the introduction, chemical reactions using microwave heating instead of thermal heating have shown great promise.

Future work on the use of cavity perturbation for mineral study will involve the construction of a simple stand-alone unit to provide accurate measurement of cavity perturbations. This unit will be sent to MINTEK to enable them to continue this work with more extensive mineral testing and analysis.

REFERENCES

[1] K. CARR-BROWN, 'Radio and Microwave Techniques for On-Line Analysis', Trans. Inst. MC., vol. 9, No. 1, pp.3-7, Jan-March 1987.

[2] J. M. OSEPCHUK, 'A History of Microwave Heating Applications', IEEE Trans. Microwave Theory Tech., vol MTT-32, No. 9, pp.1200-1222, November 1984.

[3] J. ASMUSSEN, H. H. LIN, B. MANRING, R. FRITZ, 'Single-Mode or Controlled Multimode Microwave Cavity Applicators for Precision Materials Processing', Rev. Sci. Instrum. 58(8), pp.1477-1486, August 1987.

[4] P. KRUESI, 'Microwave Energy Promises to Improve the Efficiency of Metal Extraction', Chemical Engineering, pp.18, Nov. 1984.

[5] H. CHALOUPKA, O. OSTWALD, B. SCHIEK, 'Structure Independent Microwave Moisture Measurements', Journal of Microwave Power, 15(4), pp.221-231, 1980.

[6] S. R. MERCER, B. J. DOWNING, J. D. SALTER, L. NORDIN, 'Microwave Discrimination Techniques for Rock Sorting', ELEKTRON, November/December 1988.

[7] A. De WAAL, S. R. MERCER, B. J. DOWNING, 'On-Line Fruit Weighing using a 500 MHz Waveguide Cavity', Electronics Letters, February 1988.

[8] J. W. WALKIEWICZ, G. KAZONICH, S. C. McGILL, 'Microwave Heating Characteristics of Selected Minerals and Compounds', Minerals and Metallurgical Processing, pp.37-47, February 1988.

[9] P. SEN, W. CHEW, 'The Frequency Dependent Dielectric and Conductivity Response of Sedimentary Rocks', Journal of Microwave Power, 18(I), pp.95-105, 1983.

[10] R. CHURCH, W. WEBB, J. SALSMAN, 'Dielectric Properties of Low Loss Minerals', Report of Investigations 9194, Bureau of Mines, U.S.A.,1988.

[11] A. PRICE, G. WEGDAM, 'Dielectric Spectroscopy at Microwave Frequencies' Journal of Physics E: Scientific Instruments, Volume 10, pp.478-481, 1977.

[12] S. NELSON, G. E. FANSLOW, D. BLUHM, 'Frequency Dependence of the Dielectric Properties of Coal', Journal of Microwave Power, 5(4), 1980.

[13] J. C. ANDERSON, 'Dielectrics', Chapman & Hall, 1964.

[14] R. P. FEYNMAN, R. B. LEIGHTON, M. SAND, 'The Feynman Lectures on Physics', Addison Wesley, 1964.

[15] H. FROHLICH, 'Theory of Dielectrics', Oxford, 1949.

[16] B. K. P. SCHAIFE, 'Complex Permittivity', The English Universities Press, 1971

[17] E. I. PARKOMENKO, 'Electrical Properties of Rocks', Plenum Press, 1967.

[18] S. ROBERTS, A. VON HIPPEL, 'A New Method of Measuring Dielectric Constant and Loss in the Range of Centimeter Waves', Journal of Applied Physics, Vol. 7, pp.610-616, 1946.

[19] M. SUCHER, J. FOX, 'Handbook of Microwave Measurements - Volume 2', 3rd Ed., Polytechnic Press, 1963.

[20] M. du PLESSIS, J. H. CLOETE, 'Measurement of Complex Permittivity and Permeability of Homogeneous Materials at Microwave Frequencies', SAIEE Symposium on Antennas and Propagation, August 1988.

[21] M. C. DECRETON, G. E. FRED, 'Simple Non-Destructive Method for the Measurement of Complex Permittivity', IEEE Trans. Inst. and Measurement, vol. IM-23, No. 4, pp.434-438, December 1974.

[22] J. P. GRANT, R. N. CLARKE, G. T. SYMM, N. M. SPYROU, 'A Critical Study of the Open-Ended Coaxial Line Sensor Technique for RF and Microwave Complex Permittivity Measurements', University of Surrey, England.

[23] F. HORNER, T. A. TAYLOR, R. DUNSMUIR, J. LAMB, W. JACKSON, 'Resonance Methods of Dielectric Measurements at Centimeter Wavelengths', Proc. Inst. Elec. Eng., (London), vol. 93, pt.III, pp.53-68, 1946.

[24] M. LAKSHMINARAYANA, L. PARTAIN, W. COOK, 'Simple Microwave Technique for Independent Measurement of Sample Size and Dielectric Constant with Results for a Gunn Oscillator System', IEEE Trans. Microwave Theory Tech., vol. MTT-27, No.7, pp.661-664, July 1979.

[25] S. CHAO, 'An Uncertainty Analysis for the Measurement of Microwave Conductivity and Dielectric Constant by the Short Circuited Line Method', IEEE Trans. Inst. Measurement, vol. IM-35, No. 1, pp.36-41, March 1986.

[26] K. F. SANDER, 'Microwave Components and Systems', Addison-Wesley, 1987.

[27] 'Handbook of Chemistry and Physics', 68th Edition, CRC Press.

[28] HP Application Note, 'Vector Measurements of High Frequency Networks', pp.3.1-3.10.

[29] HP Application Note, 'Vector Measurements of High Frequency Networks', pp.3.1.-3.10.

[30] W. WILLIAMS, R. COMPTON, D. RUTLEDGE, 'Elf: Computer Automation and Error Correction for a Microwave Network Analyser', Trans. Inst. Measurement, vol. 37, March 1988.

[31] D. JACKSON, 'Classical Electodynamics', Wiley & Sons, 1975.

[32] C. MONTGOMERY, 'Techniques of Microwave Measurement', M.I.T. Radiation Laboratory Series, McGraw-Hill, 1947.

[33] A. ESTIN, H. BUSEY, 'Errors in Dielectric Measurement due to a Sample Insertion Hole in the Cavity', IRE Trans. Microwave Theory Tech., vol. MTT-8, pp.650-653, 1960.

[34] P. LUKAC, 'The Determination of Electron Density by Means of a Cylindrical TM_{010} Microwave Cavity', Brit. J. Appl. Phys. (J. Phy D), Ser. 2, vol. 1, pp.1495-1499, 1968.

[35] B. GREGORY, 'The Effects of End Holes and the Glass Tube on Average Electron Number Density Measurements in a TM_{010} Cavity', Canadian Journal of Physics, vol. 46, pp.2281-2286, 1968.

[36] S. LI, R. BOSISIO, 'Composite Hole Conditions on Complex Permittivity Measurements using Microwave Cavity Perturbation Techniques', IEEE Trans. Microwave Theory Tech., vol. MTT-30, No. 1, pp.100-103, January 1982.

[37] S. LI, C. AKYEL, R. BOSISIO, 'Precise Calculationsand Measurement on the Complex Dielectric Constant of Lossy Materials Using TM_{010} Cavity Perturbation Techniquesl, IEEE Trans. Microwave Theory Tech., vol. MTT-29, No.10, pp.1041-1047, October 1981.

[38] M. NEY, F. GARDIOL, 'Automatic Monitor for Microwave Resonators', IEEE Trans. Inst. Measurement, vol. IM-26, No.1, pp.10-13, March 1977.

[39] C. AKYEL, R. BOSISIO, G-E. APRIL, 'An Active Frequency Technique for Precise Measurements on Dynamic Microwave Cavity Perturbations', IEEE Trans. Inst. Measurement, vol. IM-27, No.4, pp.364-368, December 1979.

[40] M. RZEPEKA, M. HAMID, 'Automatic Digital Method for Measuring the Permittivity of Thin Dielectric Films', IEEE Trans. Microwave Theory Tech., vol. MTT-20, No.1, pp.30-37, January 1972.

[41] A. HIGGS, 'A System for Measuring Complex Permittivity at Microwave Frequencies', The Institute of Physics, pp.1019-1025, 1986.

[42] A. DE WAAL, 'Kimberlite/Gabbro Rock Discrimination Using a 500 MHz Resonant Waveguide Cavity', Undergraduate Thesis, Department of Electrical Engineering, University of Cape Town, 1987.

APPENDIX A - LIST OF MINERALS AND THEIR COMPOSITIONS

A table listing most of the minerals used in this study, and their compositions, is given below :

MINERAL	COMPOSITION
ANDALUSITE	60% Al_2O_3, 37% SiO_2, 0.88% Fe_2O_3
BARYTES	96% $BaSO_4$, 0.03%Fe_2O_3
CALCINED MAGNESITE	88.5% MgO, 6.6% SiO_2, 2.5% Fe_2O_3
CHAMOTTE	52% SiO_2, 46% Al_2O_3, 0.5% Fe_2O_3
CHROME DIOPSIDE	
CHROME SAND	47% Cr_2O_3, 26%FeO, 15%Al_2O_3,10%MgO
COAL	
FELDSPAR	66% SiO_2, 19% Al_2O_3, 12% K_2O 2.3% Na_2O_3
GARNET	
GRAPHITE	85% C, 10% SiO_2, 1.64% Al_2O_3, 0.54% Fe_2O_3
ILMENITE	$FeTiO_3$
IRON PYRITES	
MANGANESE DIOXIDE	72% MnO_2,MnO, 12.5% Fe_2O_3, 7% SiO_2
OCEAN BENTONITE	57% SiO_2, 23% Al_2O_3, 4% Fe_2O_3, 4% MgO, 2% CaO
RED OXIDE	92% Fe_2O_3, 3% SiO_2
SILICA	99.4% SiO_2, 0.2% Al_2O_3, 0.13% Fe_2O_3
TALC	59% SiO_2, 25% MgO, 4.5% Fe_2O_3
ZIRCON	$ZrSiO_4$

APPENDIX B - SOLUTION OF SHORT-CIRCUITED LINE EQUATION

This appendix takes a more detailed look at solving the short-circuited line equation given in chapter 5.2 :

$$\rho = \frac{\Gamma_o \cdot \tanh(\Gamma d) - \Gamma}{\Gamma_o \cdot \tanh(\Gamma d) + \Gamma} \qquad (1)$$

Γ_o is the propagation coefficient of the empty section of the coaxial line, and Γ is the propagation constant of the dielectrically filled section. ρ is the measured reflection coefficient at the dielectric-air interface and d the length of the dielectric sample (see figure 5.1. section 5.2). The equation (1) must thus be solved for Γ in order to determine the complex permittivity ϵ_r since

$$\Gamma = \omega\sqrt{\epsilon_r}/c \qquad (2)$$

As mentioned in section 5.2., equation (1) is transcendental and hence has no analytical solution. It is also complicated by the fact that the variables Γ, Γ_o, and ρ are all complex. Since the hyperbolic tangent of a complex number is periodic, equation (1) has a multiplicity of solutions and thus all the roots (up to a limit) must be found to be sure of selecting the correct permittivity using (2).

This equation was originally solved using graphical curves [18]. Simplification of equation (1) can be done by assuming that the dielectric is of low loss (eg. [19] and [10]). This simplification results in a simple analytic procedure. However, since the minerals measured in this study had a wide range of losses, a complete solution was desirable. Several methods were tried before a suitable one was found. These are discussed below:

a) Muller's Method. This method is specifically for complex equations. Whilst Muller's method always converged to a root, it did not always converge to the desired root. This resulted in the

correct solution often being missed. The method was also very slow.

b) Newton's Method. This has previously been used [25] to solve equation (1). The equation is split into real and imaginary parts, and Newton's method for a system of two simultaneous equations in two variables applied. Whilst convergence to roots was extremely rapid, it was difficult to control convergence to the desired root, or it did not converge at all. The method required to much operator interference and was hence unsuitable for solving for multiple solutions, as is required here for a frequency sweep.

c) Optimisation. An optimisation technique to solve (1) was developed by the author. This method was found to be very successful and was hence selected for use. Its operation is described below :

Substituting $z = \Gamma d$ into equation (1) and rearranging to obtain

$$d\Gamma_0(\rho-1)\tanh(z) + z(\rho+1) = 0 \qquad (3)$$

Now z is complex: $z = x + jy$

and $$\tanh(x + jy) = \frac{\tanh(x) + j\tanh(y)}{1 + j\tanh(x)\tan(y)} \qquad (4)$$

Substituting (4) into (3) and rearranging to get

$$G(x,y) + jH(x,y) = 0 \qquad (5)$$

where

$$G(x,y) = d\tanh(x)(\alpha_o(\rho_o-1)-\beta_o\rho_1) - d\tan(y)(\beta_o(\rho_o-1)+\rho_1\alpha_o) + x(\rho_o+1) - \rho_1 y - \tanh(x)\tan(y)(y(\rho_o+1)+\rho_1 x)$$

$$H(x,y) = d\tanh(x)(\beta_o(\rho_o-1)+\rho_1\alpha_o) + d\tan(y)(\alpha_o(\rho_o-1)-\beta_o\rho_1) + \tanh(x)\tanh(y)(x(\rho_o+1)-\rho_1 y) + y(\rho_o+1) + \rho_1 x$$

and $\Gamma_o = \alpha_o + j\beta_o$

and $\rho = \rho_o + j\rho_1$

For a solution, both the real and imaginary parts of (5) must be zero :

ie. x,y such that $G(x,y) = H(x,y) = 0$

This is equivalent to : $G(x,y)^2 + H(x,y)^2 = 0$ (6)

Written as $F(x,y) = G(x,y)^2 + H(x,y)^2$, this function now forms a two dimensional surface in three dimensions. Numerical search methods were then used to find minima of the surface. If the x,y found at the minima satisfy (6) then a solution to the equation has been found. The relative complex permittivity ϵ_r can then easily be calculated from these solutions.

A numerical minimisation programme (a simple alternate variable optimisation routine) was written to run on an personal computer (Turbo Pascal with math co-processor) and found to be very successful. All the solutions (ie. local minima) can easily be roughly located since they are known to lie near the y-axis (corresponding to dielectric constant) since ϵ'' is always much smaller than ϵ'. The optimisation routine then accurately calculates the roots. Although far slower than Newton's method, all the desired roots were automatically found with few problems due to convergence, etc.

Once x and y are calculated, Γ and hence ϵ_r can easily be found. The complex permittivity ϵ_r is plotted on a graph against frequency. A listing of the computer programme is given below:

Computer Programme:

```
{-------------------------------------------------------}
{ PROGRAMME TO SOLVE THE SHORT-CIRCUITED TRANSMISSION LINE }
{ EQUATION.          GRAEME PENDOCK - THESIS             }
{-------------------------------------------------------}

{$N+}                { compile for 8087 maths coprocesssor }

PROGRAM permittivity_calculations;

USES Dos,Crt,Graph,CompMath;      { units used}

VAR n,m,i,j,k,numread,count:integer;
    frequency,omega,l,length,dis,distance:double;
    samplelength,path,angle,maxperm:double;
    upperfreq,lowerfreq,freqstep:double;
    startsearch,zvaluenew,zvalueold,minimumvalue:double;
    rhol,rho,gamma0,gamma,permittivity,var1,var2,var3:complex;
    phase,magnitude:array[1..100] of double;
    data:array[-1..100,1..2,1..2] of double;
    solutions:array[1..100,1..15] of complex;
    answers:array[1..100] of complex;

{-------------------------------------------------------}
{calculate magnitude G(x,y)^2 + H(x,y)^2}
FUNCTION height(x,y:double):double;

VAR s,v,A,B,C,D,E,F,G,H:extended;

BEGIN
 A:=samplelength*(gamma0.Re*(rho.Re-1)-gamma0.Im*rho.Im);
 B:=samplelength*(gamma0.Im*(rho.Re-1)+rho.Im*gamma0.Re);
 C:=x*(rho.Re+1)-rho.Im*y;
 D:=y*(rho.Re+1)+rho.Im*x;

 s:=exp(x);v:=exp(-x);
 E:=(s-v)/(s+v);          { E=tanh(x) }
 F:=sin(y)/cos(y);        { F=tan(y) }

 G:=(E*A/F+C/F)-(E*D+B);       { function G(x,y) }
 H:=(E*B/F+D/F)+(E*C+A);       { function H(x,y) }

 height:=sqr(G)+sqr(H);
END;
{-------------------------------------------------------}
{find an approximate region of solution by}
{ searching along y axis}
PROCEDURE findhollow(var minvalue:double);

CONST deltay=0.01;                  {stepping along y axis}
```

```
VAR  y,yold,oldvalue,newvalue:double;
     uphill:boolean;

BEGIN
  uphill:=true;
  y:=startsearch;
  newvalue:=height(0,y);
  REPEAT
     yold:=y;
     oldvalue:=newvalue;
     y:=yold+deltay;
     newvalue:=height(0,y);
     if (uphill) and (newvalue<oldvalue) then uphill:=false;
  UNTIL NOT(uphill) AND (newvalue>oldvalue);
  startsearch:=yold;
  minvalue:=oldvalue;
END;
{-------------------------------------------------------}
{find accurate solution by optimising x&y to}
{ minimise magnitude function}
PROCEDURE optimisation;

CONST nearlyzero=1E-12;
      almostzero=1E-5;

VAR n,m,number,factor:integer;
    value,initialvalue,temp:double;
    step,coord,old,resolution:array[1..2] of double;

BEGIN
   coord[1]:=0;
   coord[2]:=startsearch;
   resolution[1]:=1E-9;
   resolution[2]:=1E-10;
   value:=minimumvalue;
   factor:=0;
   {alternate optimisation routine}
     REPEAT
       inc(factor);
       initialvalue:=value;
        FOR n:=1 to 2 DO
         BEGIN
           step[n]:=0.005/factor;  {shorten step}
           number:=0;
            REPEAT
              inc(number);
              temp:=value;
              old[n]:=coord[n];
              coord[n]:=coord[n]+step[n];
              value:=height(coord[1],coord[2]);
              if (value>temp) then step[n]:=-step[n]/2;
            UNTIL abs(step[n])<(resolution[n]/number);
         END; {for n}
```

```
        {stop when minimum found}
        UNTIL abs(initialvalue-value)<nearlyzero;
{is it a solution ?}
IF value<almostzero THEN
 BEGIN
  inc(count);
  gamma.Re:=coord[1]/samplelength;
  gamma.Im:=coord[2]/samplelength;   {propogation constant}
  permcalculate(gamma,omega,var2);   {evaluate permittivity}
  if var2.Re < maxperm then
    begin
       write(f,count:2,' : Er = ');    {print permittivity}
       print(var2);
       solutions[j,count].Re:=var2.Re;  {store in array }
       solutions[j,count].Im:=var2.Im;
    end
        else
    begin
     for m:=count to 15 do
      begin
     solutions[j,m].Re:=-99;     {if not a solution give
                                  dummy value}
     solutions[j,m].Im:=-99;
   end;
  count:=15;
  end;
END;    {end if}
END;  {procedure}
{-------------------------------------------------------}
{sweep through the data}
{and find all the permittivity solutions}
{up to a predefined limit}
PROCEDURE  solve;

VAR frequency:double;

BEGIN
 { calculate multiple solutions}
 clrscr;
 writeln;
 write('Enter the upper limit of the dielectric constant for the search
? ');
 readln(maxperm);
 writeln;
 writeln('Do you want to print the output ?');
 if upcase(readkey)='Y' then assign(f,'lptl') else assign(f,'');
 rewrite(f);
 clrscr;
 writeln('Solving......');

 writeln(f,'     Length = ',samplelength*1000:4:2,' mm');

freqstep:=(upperfreq-lowerfreq)/(numread-1); {freq interval}
  for j:=1 to numread do
```

```
    begin
      frequency:=lowerfreq+freqstep*(j-1); {calculate freq}
      omega:=frequency*1E+9*2*pi;
      gamma0.Re:=0;
      gamma0.Im:=omega/light;
      writeln(f,j:2,' :  FREQUENCY = ',frequency:4:4,' GHz');

       { convert polar coords to cartesian coords }
polar_cartesian(magnitude[j],phase[j]*pi/180,rho.Re,rho.Im);
        write(f,'     Refl. coeff.  = ');
        print(rho);
        writeln(f);
        startsearch:=0.01;
        count:=0;
           REPEAT
               findhollow(minimumvalue);
               optimisation;
           UNTIL count=15;           { 15 points found }
       { compare the two sets of data to obtain unique
                   solutions}
        write(f,'================================================');
  end;          {end j}

    writeln('Finished!');
    sound(880);    {beep}
    delay(200);
    nosound;
END;
{-------------------------------------------------------}
{select desired solutions}
PROCEDURE sort;

VAR n,m:integer;
    upper,lower:single;
    finished:boolean;

BEGIN
  finished:=true;
 REPEAT
  writeln;
  writeln('WINDOW FOR SELECTING RESULTS');
  writeln('============================');
  writeln;
  write('Enter upper dielectric limit : ');
  readln(upper);
  write('Enter lower dielectric limit : ');
  readln(lower);

  for n:=1 to numread do
    begin
       frequency:=lowerfreq+freqstep*(n-1);   {calculate frequency}
       write(n,': ',frequency:2:2,' GHz  : ');
       m:=0;
          repeat
```

```
            inc(m);        {m:=m+1}
          until (solutions[n,m].Re>lower) or (m=numread);
          answers[n].Re:=solutions[n,m].Re;
          answers[n].Im:=solutions[n,m].Im;
          write(f,' : Er = ');
          print(answers[n]);
    end; {for n}
  UNTIL finished=true;
  close(f);
END;
{ ------------------------------------------------------}
{ routine to retrieve reflection coefficient data off disk }
PROCEDURE retrieval;

VAR i,j,k,IOcode:integer;
    filename:string[64];
    fyle:text;

BEGIN
{$I-}                    { disable IO checking }
 clrscr;
 writeln('DATA RETRIEVAL');
 writeln('==============');
repeat
 writeln;
 write('Enter drive, path, name of file to retrieve data from. ');
 writeln('(eg. c:\perm\rock.dat) : ');
 readln(filename);
 assign(fyle,filename);
 reset(fyle);
 IOcode:=IOresult;
 if IOcode<>0 then writeln('Drive, path or file not found. Try again.');
until IOcode=0;
 writeln;
 writeln('Reading from disk.....');
  while not(eof(fyle)) do
  begin
    readln(fyle,lowerfreq);          {start frequency}
    readln(fyle,upperfreq);          {stop frequency}
    readln(fyle,numread);            {number of points}
    readln(fyle,samplelength);       {length of sample [m]}
    for n:=1 to numread do
     begin
       readln(fyle,magnitude[n]);       {magnitude}
       readln(fyle,phase[n]);           {phase}
       end;
    end; {while}
  close(fyle);
{$I+}                    { enable IO checking }
 END;
{------------------------------------------------------}
{ routine to plot graph of complex permittivity }
PROCEDURE DrawGraph;
```

```
VAR Gd,Gm,Xmax,Ymax,Xend,Yend,Xnumber,Ynumber:integer;
x,y,Xcoord,Ycoord,Xcoord0,Yreal,Yreal0,halfx,halfy:integer;
    Yimag,Yimag0:integer;
    Xspace,Yspace,freqinterval,frequency:single;
    permrealinterval,permimaginterval,deltapermreal,
    peltapermimag:single;
    color:word;
    permrealmax,permrealmin,permimagmax,permimagmin:single;
    permreal,permimag,GHz:string[6];
    title:string[70];
    reference:string[6];

BEGIN
 write('Enter substance for graph title - ');
 readln(title);
 writeln;
 write('Enter reference code - ');
 readln(reference);
 permrealmax:=2;permrealmin:=0;
 permimagmax:=-0.1;permimagmin:=0;
 Xnumber:=20; Ynumber:=10;   {number of intervals on grid}
REPEAT
 clrscr;
 writeln('PRESENT AXES SCALES SET AT :-');
 writeln;
 writeln('Real Axis Maximum = ',permrealmax:2:4);
 writeln('Real Axis Minimum = ',permrealmin:2:6);
 writeln;
 writeln('Imag Axis Maximum = ',permimagmax:2:6);
 writeln('Imag Axis Minimum = ',permimagmin:2:6);
 writeln;
 writeln('ENTER NEW VALUES :-');
 writeln;
 write('Real Axis Maximum = ');readln(permrealmax);
 write('Real Axis Minimum = ');readln(permrealmin);
 writeln;
 write('Imag Axis Maximum = ');readln(permimagmax);
 write('Imag Axis Minimum = ');readln(permimagmin);
 clrscr;
 Gd:=detect;
 InitGraph(Gd,Gm,'');
 color:=GetMaxColor;
 Xmax:=GetMaxX;
 Ymax:=GetMaxY;
 halfx:=round(Xmax/2);
 halfy:=round(Ymax/2);
 Rectangle(0,0,Xmax,Ymax);

{ labels }
 SetTextJustify(CenterText,TopText);
 SetTextStyle(DefaultFont,HorizDir,1);
 OutTextXY(Xmax-30,6,reference);
 SetTextStyle(TriplexFont,HorizDir,2);
 OutTextXY(halfx,4,'GRAPH OF PERMITTIVITY - '+title);
```

```
 SetTextStyle(DefaultFont,HorizDir,0);
 OutTextXY(halfx,334,'Frequency [GHz]');
 SetTextStyle(DefaultFont,VertDir,0);
 SetTextJustify(CenterText,CenterText);
 OutTextXY(17,halfy,'Real Part');
 OutTextXY(700,halfy,'Imaginary Part');

 SetLineStyle(SolidLn,0,NormWidth);
 Line(17,halfy-60,17,halfy-100);

 SetLineStyle(DottedLn,0,NormWidth);
 Line(700,halfy-60,700,halfy-100);

 SetViewPort(72,34,647,312,ClipOff);
 Xend:=575;Yend:=278;
 Rectangle(0,0,Xend,Yend);

{ ticks }
  Freqinterval:=(upperfreq-lowerfreq)/Xnumber; {frequency spacing on x
axis}
 Xspace:=Xend/Xnumber;Yspace:=Yend/Ynumber;
 SetTextStyle(SmallFont,HorizDir,0);
 for x:=0 to Xnumber do
   begin
     Xcoord:=Round(Xspace*x);
     if not(odd(x)) then
       begin
         frequency:=lowerfreq+Freqinterval*x;
         Str(frequency:2:2,GHz);
         OutTextXY(Xcoord,yend+10,GHz);
       end;
     SetLineStyle(SolidLn,0,NormWidth);
     Line(Xcoord,Yend-2,Xcoord,Yend+5);
     SetLineStyle(DottedLn,0,NormWidth);
     Line(Xcoord,0,Xcoord,Yend-2);
   end;

{plot curves of dielectric constant and loss factor}
permrealinterval:=(permrealmax-permrealmin)/Ynumber;
permimaginterval:=(permimagmax-permimagmin)/Ynumber;
for y:=0 to Ynumber do
   begin
     Ycoord:=Round(Yspace*y);
     Str((permrealmin+permrealinterval*(Ynumber-y)):2:3,permreal);
     Str((permimagmin+permimaginterval*(Ynumber-y)):2:3,permimag);
     OutTextXY(-26,Ycoord,permreal);
     OutTextXY(xend+25,Ycoord,permimag);
     SetLineStyle(SolidLn,0,NormWidth);
     Line(-5,Ycoord,2,Ycoord);
     Line(Xend-2,Ycoord,Xend+5,Ycoord);
     SetLineStyle(DottedLn,0,NormWidth);
     Line(2,Ycoord,Xend-5,Ycoord);
   end;
```

```
  { draw the traces }
  SetViewPort(72,34,647,312,ClipOn);
  deltapermreal:=Yend/(permrealmax-permrealmin);
  deltapermimag:=Yend/(permimagmax-permimagmin);
  Xcoord0:=0;
  Yreal0:=Yend-Round(deltapermreal*(answers[1].Re-permrealmin));
  Yimag0:=Yend-Round(deltapermimag*(answers[1].Im-permimagmin));
  for x:=2 to numread do
   begin
     Xcoord:=Round(Xend/(numread-1)*(x-1));
     Yreal:=Yend-Round(deltapermreal*(answers[x].Re-permrealmin));
     Yimag:=Yend-Round(deltapermimag*(answers[x].Im-permimagmin));
     SetLineStyle(SolidLn,0,NormWidth);
     Line(Xcoord0,Yreal0,Xcoord,Yreal);
     SetLineStyle(DashedLn,0,NormWidth);
     Line(Xcoord0,Yimag0,Xcoord,Yimag);
     Xcoord0:=Xcoord;
     Yreal0:=Yreal;
     Yimag0:=Yimag;
   end;

  readln;
  CloseGraph;
  RestoreCRTMode;
  writeln('Do you want to modify the graph parameters ? ');
UNTIL upcase(readkey)<>'Y';
END;

{-------------------------------------------------------------}
{MAIN PROGRAMME}
BEGIN
ClrScr;

writeln('CALCULATION OF PERMITTIVITY FROM SHORT-CIRCUITED LINE METHOD');
writeln('=========================================================');
  writeln;
  writeln('                    By Graeme Pendock');
  writeln;
  write('press enter to continue...');
  readln;

  retrieval;                {obtain data off disk}
  solve;                    {obtain solutions for data}
  sort;                     {select correct readings}
  writeln('Do you want to plot a graph ?');
  if upcase(readkey)<>'N' then DrawGraph;   {plot graph of permittivity
values}

END.

{-------------------------------------------------------------}
{ COMPMATH UNIT USED IN SHORT-CIRCUITED LINE EQUATION      }
{ PROGRAMME. PERFORMS COMPLEX CALCULATIONS AND CO-ORDINATE}
{ TRANSFORMATIONS.                                         }
```

```
{-------------------------------------------------------}

{$N+}          {compile for 8087 maths coprocessor}

UNIT compmath;

INTERFACE

TYPE complex=record
              Re,Im:double;
             end;

CONST light=2.9969E8;              { speed of light in air }

VAR f:text;

PROCEDURE print(number:complex); { to print complex number }
PROCEDURE add(a,b:complex; var c:complex);        {c=a+b}
PROCEDURE subtract(a,b:complex; var c:complex);   {c=a-b}
PROCEDURE scalarmultiply(a:complex;k:double;var b:complex);   {b=a*k}
PROCEDURE multiply(a,b:complex; var c:complex);   {c=a*b}
PROCEDURE divide(a,b:complex; var c:complex);     {c=a/b}
PROCEDURE power(a:complex; var b:complex);        {b=exp(a)}
PROCEDURE permcalculate(gammafinal:complex;omega:double;
                        var dielectric:complex); {calculate complex ε}
          { convert cartesian coords to polar coords }
PROCEDURE cartesian_polar(x,y:double;var r,theta:double);
          { convert polar coords to cartesian coords }
PROCEDURE polar_cartesian(r,theta:double;var x,y:double);


IMPLEMENTATION
{-------------------------------------------------------}
{ procedure to print complex number }
PROCEDURE print(number:complex);

BEGIN
 write(f,number.Re:3:3);
 if number.Im<0 then write(f,'-j') else write(f,'+j');
 writeln(f,abs(number.Im):3:4);
END;
{-------------------------------------------------------}
{ complex addition }
PROCEDURE add(a,b:complex; var c:complex);         {c=a+b}

BEGIN
 c.Re:=a.Re+b.Re;
 c.Im:=a.Im+b.Im;
END;
{-------------------------------------------------------}
{ complex subtraction }
PROCEDURE subtract(a,b:complex; var c:complex);    {c=a-b}

BEGIN
```

```
 c.Re:=a.Re-b.Re;
 c.Im:=a.Im-b.Im;
END;

{-------------------------------------------------------}
{ scalar multiplication }
PROCEDURE scalarmultiply(a:complex;k:double;var b:complex);  {b=a*k}

BEGIN
 b.Re:=a.Re*k;
 b.Im:=a.Im*k;
END;

{-------------------------------------------------------}
{ complex multiplication }
PROCEDURE multiply(a,b:complex; var c:complex);  {c=a*b}

BEGIN
 c.Re:=a.Re*b.Re-a.Im*b.Im;
 c.Im:=a.Im*b.Re+a.Re*b.Im;
END;
{-------------------------------------------------------}
{ complex division }
PROCEDURE divide(a,b:complex; var c:complex);       {c=a/b}

VAR d:double;

BEGIN
 d:=sqr(b.Re)+sqr(b.Im);
 c.Re:=(a.Re*b.Re+a.Im*b.Im)/d;
 c.Im:=(a.Im*b.Re-a.Re*b.Im)/d;
END;

{-------------------------------------------------------}
{procedure to calculate complex exponent}
PROCEDURE power(a:complex; var b:complex);      {b=exp(a)}

BEGIN
 b.Re:=exp(a.Re)*cos(a.Im);
 b.Im:=exp(a.Re)*sin(a.Im);
END;
{-------------------------------------------------------}
{ calculate complex permittivity from gamma }
PROCEDURE permcalculate(gammafinal:complex;omega:double;
                        var dielectric:complex);

VAR temp:complex;
    factor:double;

BEGIN
 multiply(gammafinal,gammafinal,temp);
 factor:=-sqr(light)/sqr(omega);
     scalarmultiply(temp,factor,dielectric);          {     dielectric=-
c*c/(w*w)*sqr(gamma) }
```

```
END;
{-------------------------------------------------------}
{ convert cartesian coords to polar coords }
PROCEDURE cartesian_polar(x,y:double;var r,theta:double);

BEGIN
 r:=sqrt(sqr(x)+sqr(y));
 theta:=arctan(y/x);
 if (x<0) and (y>=0) then theta:=theta+pi; {second quadrant}
 if (x<0) and (y< 0) then theta:=theta-pi; {third  quadrant}
END;
{-------------------------------------------------------}
{ convert polar coords to cartesian coords }
PROCEDURE polar_cartesian(r,theta:double;var x,y:double);

BEGIN
 x:=r*cos(theta);
 y:=r*sin(theta);
END;
{-------------------------------------------------------}
END.
```

APPENDIX C - DETAILS OF SHORT-CIRCUITED LINE EXPERIMENTAL SET-UP

This appendix gives details on the PC - HP 8410 Network Analyser interface used in the short circuited line experimental set-up. A description of the control and operation provided by the computer programme is given.

C.1. INTERFACE DESCRIPTION

Figure 5.3. (section 5.3) shows the block diagram of the overall system. The HPIB card in the PC allows (via the HPIB bus) control of the HP sweep generator. By appropriate HPIB codes this sets :

1) Power level of the generator.
2) Sweep range and rate.
3) CW frequency of operation.

as defined by the computer programme.

The reflection coefficient is displayed by the Network Analyser Magnitude-Phase display. At the rear of the display are analogue outputs that are fed via a signal conditioning unit to a PC26 12-bit Analogue-to-Digital converter on board the PC. This allow accurate and automatic measurement of the reflection coefficient. The specifications of the analogue outputs on the network analyser display are:

1) Magnitude. 50 mV/dB wrt. reference.
2) Phase. 10 mV/deg. 0 deg = 0 mV

These are scaled and filtered and the fed to channel 1 (magnitude) and channel 2 (phase) of the ADC. The scaling is necessary to bring the signal to the full -5 to 5 V range of the ADC. The filtering helps remove noise from the network analyser, and is well within the sampling rate. The signal conditioning circuitry is shown in figure C.1. The front stages are unitary gain differential amplifiers to provide common-mode noise rejection from the interface lines (two-core shielded coax).

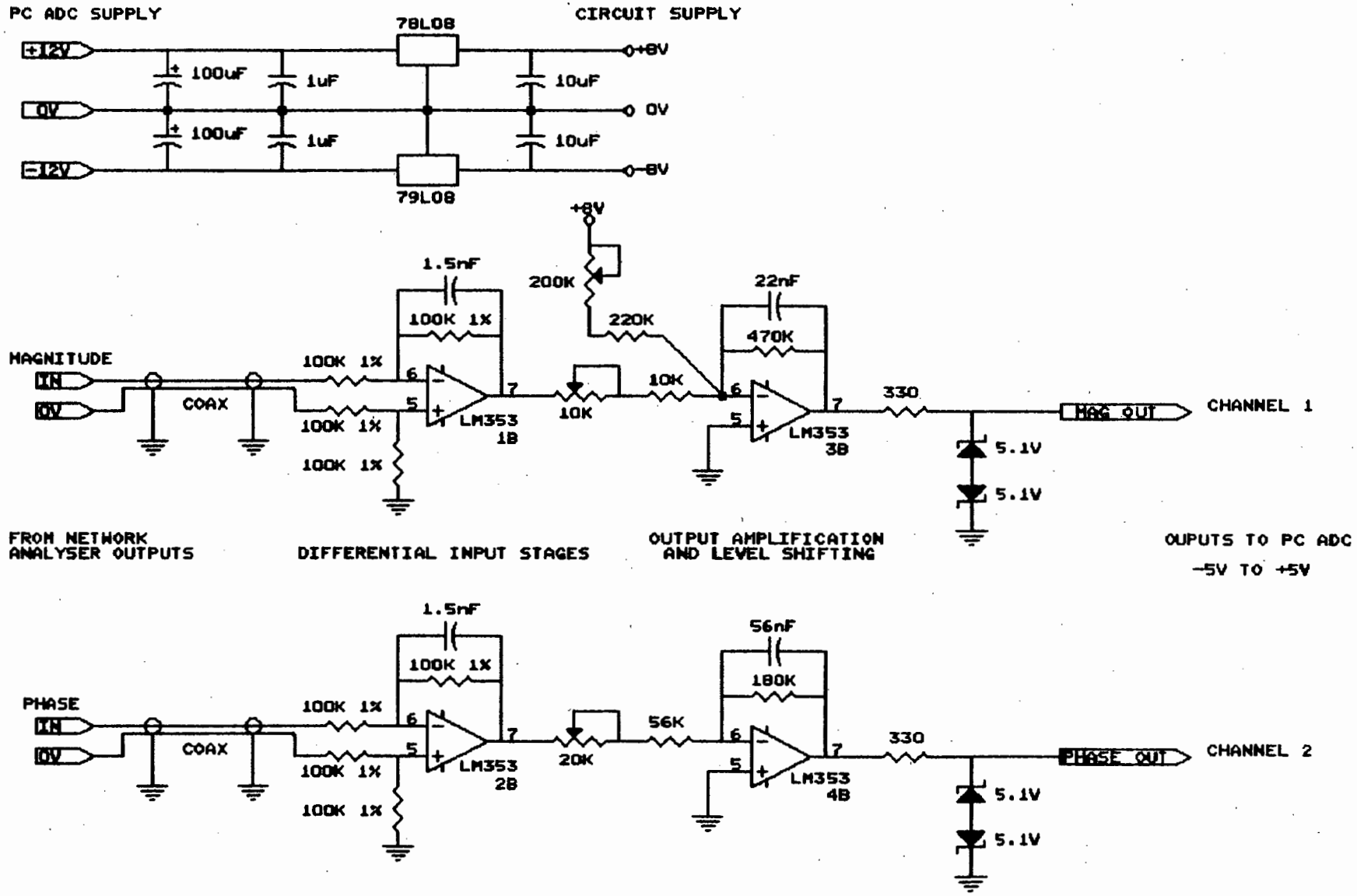

Figure C.1. Circuit Diagram of PC - HP 8410 Interface Circuitry

This is followed by the appropriate amplification and level-shifting. The inputs to the ADC card are protected by the zener diodes at the output should the signal exceed ±5 V. The ±8 V supply is obtained (through regulators and filter capacitors) from the ±12 V supply of the PC 26 card.

C.2. TEST PROCEDURE AND COMPUTER PROGRAMME

The upper and lower frequencies and number of steps in the sweep are entered into the computer. The empty coaxial test-cell is then connected to the network analyser port. Reflection coefficient readings are then taken across the prescribed range. These are then stored for use in later error correction, since it is known that they should be that for a perfect short circuit. The sample of powdered mineral is then loaded into the test-cell and its length measured. Measurements on the test-cell are then performed. This is followed by the error correction calculations in order to enhance measurement accuracy. Since after correction the measurements would be with reference to the short-circuit, their phases must be reduced by twice the phase difference (through & back) of that through a section of air of equal length of the sample, in order to obtain the desired reflection coefficients at the sample-air interface. These readings are then stored on disk for later processing.

A listing of the control programme (Turbo Pascal) is given below :

```
{-------------------------------------------------------}
{ Programme to sweep network analyser and sample response. }
{ Written by Graeme Pendock. Thesis - Coaxial Line method. }
{-------------------------------------------------------}

{$N+}                    {Compile for 8087 maths-coprocessor}

PROGRAM network_analyser_control;

{$M $4000, 0, $4000}          {Compiler option nescessary for
                                    HPIB operation}

USES dos,crt;
```

```
TYPE data=array[1..100] of double;  {for measured data file}

CONST scalemag=564;          {ADC divisions per dB}
      phasescale=10.7;       {ADC divisions per degree phase}

VAR frequency,freqstep,lowerfreq,upperfreq:double;
    samplelength,average:double;
    n,numread,IOcode,answer:integer;
    lower,upper:string[8];
    thetascale,magscale,theta,magnitude:data;
    GPIO:text;
{------------------------ ------------------------------}
{take a ADC reading for channel}
FUNCTION adcsample(channel:integer):integer;

VAR i,out:integer;

BEGIN
  port[$702]:=(channel SHL 4)+2;  {Clear SC,select channel}
  port[$702]:=(channel SHL 4)+3;  {Start Conversion channel}

  {loop until end of conversion-40 us}
    for i := 1 to 10 do
       begin
           inline($90/$90/$90/$90/$90);  {delay for EOC}
       end;
   {Read word from ADC}
    adcsample:=((port[$701] and $0F) SHL 8)+port[$700];
END;
{-------------------------------------------------------}
{take count readings of magnitude and phase from network  analyser}
{Channel 0 = Phase, Channel 1  = Magnitude }

PROCEDURE readings(count:integer;var
                                  phase,magnitude:double);

VAR sample,channelnumber:integer;
    total:longint;
    channel:array[0..1] of double;

BEGIN
 for channelnumber:=0 to 1 do       {Sample channels 1&2}
   begin
     total:=0;
      for Sample := 1 to count do    {Collect count samples}
       begin
          {tally ADC conversions}
          total:= total+adcsample(channelnumber);
       end;
    channel[channelnumber]:=total/count;         {average}
 end;
   phase:=channel[0];              {phase and mag. readings}
   magnitude:=channel[1];
END;
```

```
{-------------------------------------------------------}
{select HP device, ie. sweep generator}
PROCEDURE SelectHPIB(code:integer);

VAR  Addr : String[8];

BEGIN
  Str(code,Addr);
  Addr := 'HPIB='+Addr;
  Exec('HPIBMODE.COM',Addr);
END;
{-------------------------------------------------------}
{setup HPIB interface to sweep generator & ADC card }
PROCEDURE setup;

BEGIN
  port[$703] := $92;              {initialize ADC card}
  Assign(GPIO,'HPIBDEV');         {initialise HPIB interface}
  ReWrite(GPIO);                  {open HPIB interface file}
  SelectHPIB(719);       {select sweep generator: address=19}
END;
{---------------------- ---------------------------------}
{Maintains phase angle in cyclic range -180 to +180 degrees}
PROCEDURE modulus(var theta:double);

BEGIN
 theta:=theta-INT(theta/360)*360;
 if (theta>0) and (theta>180)  then theta:=theta-360;
 if (theta<0) and (theta<-180) then theta:=theta+360;
END;
{-------------------------------------------------------}
{ routine to store data on disk for future retrieval }
PROCEDURE storage;

VAR i,j,k:integer;
    filename:string[64];
    fyle:text;

BEGIN
 {$I-}                    {disable IO checking}
 clrscr;
 writeln('DATA STORAGE');
 writeln('============');
 writeln;
 repeat
   repeat
      writeln('Enter drive, path and name of file to be created for
storage');
      writeln('( eg. c:\perm\rock.dat )');
      readln(filename);
      IOcode:=IOresult;
      if IOcode<>0 then writeln('Invalid format. Try again.');
   until IOcode=0;
   writeln;
```

```
   write('Writing to disk....');
   assign(fyle,filename);                    {open storage file}
   rewrite(fyle);
   IOcode:=IOresult;
    if IOcode<>0 then writeln('Can't find directory. Try again.');
 until IOcode=0;

  {write data to disk file}
     writeln(fyle,lowerfreq:2:3);            {start frequency}
     writeln(fyle,upperfreq:2:3);            {stop frequency}
     writeln(fyle,numread:3);                {number of points}
     writeln(fyle,samplelength:1:5);         {sample length[m]}
     for n:=1 to numread do
      begin
         writeln(fyle,magnitude[n]:1:3);     {write magnitude}
         writeln(fyle,theta[n]:3:1);         {write phase}
      end;
 close(fyle);                                {close file}
 writeln('Finished.');
 {$I+}                                      {enable IO checking}
END;
{-------------------------------------------------------}
{to sweep over frequency range and take reflection coefficient readings}
PROCEDURE measurements;

VAR freqcode:string[8];

BEGIN
 frequency:=lowerfreq;                      {sweep from low freq}
   FOR n:=1 to numread do                   {to high frequency}
     BEGIN
      Str(frequency:4:2,freqcode);
      freqcode:='cw'+freqcode+'gz';         {convert to codes}
      write(GPIO,freqcode);                 {set sweep oscillator}
      delay(400);                           {allow YIG to settle}
      {take average of 400 ADC readings}
      readings(400,theta[n],magnitude[n]);
      frequency:=frequency+freqstep;        {increment frequency}
  END;
  write(GPIO,lower,' ',upper);              {reset sweep oscillator}
END;
{-------------------------------------------------------}
{procedure to take measurements and remove errors }
PROCEDURE correct;

BEGIN
 writeln('Reading....');
   measurements;                {sweep and take measurements}
 frequency:=lowerfreq;
   for n:=1 to numread do
     begin
     {convert to dB}
        magnitude[n]:=(magnitude[n]-average)/scalemag;
      {convert to linear}
```

```
        magnitude[n]:=exp((magnitude[n]/20)*2.30259);
      {correct error}
        magnitude[n]:=magnitude[n]/magscale[n];
      {phase in degrees}
        theta[n]:=theta[n]/phasescale;
      {correct error}
        theta[n]:=theta[n]-thetascale[n];
      {maintain in range -180 to 180}
        modulus(theta[n]);
       frequency:=frequency+freqstep;  {increment frequency}
     end;
END;
{-------------------------------------------------------}
{calculate error correction coefficients}
PROCEDURE calibration;

VAR n:integer;
    reference:double;

BEGIN
 clrscr;
 write(GPIO,'pl5.0dm st0.05sc');     {set power level=5dBm}
                                     {sweep=0.05ms}
 write(GPIO,lower,' ',upper);        {set sweep oscillator}

 writeln('** CALIBRATION PROCEDURE **');
 writeln('============================');

 writeln;
 writeln('Settings :-');         {prompt user to set correct }
 writeln;                        {Network Analyser settings}
 writeln('1: Amp gain at 23dB');
 writeln('2: Amp vernier fully ccw');
 writeln('3: Phase vernier fully cw');
 writeln('4: 0 deg offset');
 writeln('5: 90 deg/div');
 writeln('6: 2.5 dB/div');
 writeln;

 writeln('Calibration');
 writeln('-----------');
 writeln;
 writeln('1: Connect empty tube to port');
 writeln;
 write('Press return to start calibration -');
 readln;
 writeln;
 write('Calibrating....');

 measurements;                {take measurements over range}

{ find average }
 average:=0;
 for n:=1 to numread do average:=average+magnitude[n];
```

```
 average:=average/numread;

{ scale to linear reading}
for n:=1 to numread do
  begin
    {give dB}
    magnitude[n]:=(magnitude[n]-average)/scalemag;
    {give linear reading}
    magnitude[n]:=exp((magnitude[n]/20)*2.30259);
    {phase - degrees}
    theta[n]:=theta[n]/phasescale;

    {calculate coefficients to do error correction}
    thetascale[n]:=180+theta[n];
    modulus(theta[n]);                          {-180 to 180}
    magscale[n]:=magnitude[n];
  end;

END;
{-------------------------------------------------------}
{take a sample reading}
PROCEDURE takesample;

CONST light=2.9969E+8;                  {speed of light }

VAR  wavelength,deltatheta:double;
     n:integer;

BEGIN
 clrscr;
 write(GPIO,lower,' ',upper);          {set sweep oscillator}

 writeln('--- LOAD SAMPLE ---');
 writeln;
 write('Enter sample length [mm] - ');
 readln(samplelength);
 samplelength:=samplelength/1000;       {convert to metres}

 write('To take readings press return -');
 readln;
 correct;         {take measurements and provide necessary error
correction}

 { adjust phase to that at interface}
  frequency:=lowerfreq;
   for n:=1 to numread do
     begin
        wavelength:=light/(frequency*1E+9);
        deltatheta:=720*samplelength/wavelength;
        theta[n]:=theta[n]-deltatheta;
        modulus(theta[n]);              {range -180 to 180}
        frequency:=frequency+freqstep; {increment frequency}
     end;
 storage;                          {store data on disk file}
```

```
 clrscr;
END;
{-------------------------------------------------------}
{ routine to get parameters from user}
PROCEDURE getinfo;

VAR n:integer;

BEGIN
  clrscr;
  writeln('SHORT-CIRCUIT LINE FOR ε MEASUREMENT');
  writeln('=====================================');
  writeln;

{ get frequency sweep range }
 {$I-}                          {disable IO checking}
  REPEAT
    writeln('Enter frequency range to be swept:');
     repeat
        write('  Lower limit [GHz] = ');
        readln(lowerfreq);
        IOcode:=IOresult;
        if IOcode<>0 then writeln('Invalid format. Try again.');
     until IOcode=0;

     repeat
        write('  Upper limit [GHz] = ');
        readln(upperfreq);
        IOcode:=IOresult;
        if IOcode<>0 then writeln('Invalid format. Try again.');
     until IOcode=0;
   UNTIL lowerfreq<=upperfreq;

   Str(lowerfreq:4:2,lower);
   Str(upperfreq:4:2,upper);
   lower :='fa'+lower+'gz';   {convert to HPIB sweep codes}
   upper :='fb'+upper+'gz';

 REPEAT
     REPEAT
       repeat
        write('How many readings do you want to take ? [1-100] ');
        readln(numread);
        IOcode:=IOresult;
        if IOcode<>0 then writeln('Invalid format. Try again.');
       until IOcode=0;
     UNTIL (numread>=1) and (numread<=100);
  if numread>1 then
                freqstep:=(upperfreq-lowerfreq)/(numread-1)
              else freqstep:=0;
  if numread>1 then
   writeln('That gives ',freqstep*1000:6:4,' MHz steps');
   writeln('Is that OK ? [Y/N] ');
 UNTIL upcase(readkey)<>'N';
```

```
END;
  {$I+}                              {enable IO checking}
{-------------------------------------------------------------}
{ MAIN PROGRAMME }
BEGIN

 setup;       {initialise HPIB interface to sweep generator}
 getinfo;     {get frequency sweep parameters from user}
 calibration; {calibration procedure}

repeat
  takesample;    {take readings of sample}
  writeln('Do you want to take another reading [Y/N] ?');
until upcase(readkey)<>'Y';
END.
{-------------------------------------------------------------}
```

APPENDIX D - CYLINDRICAL RESONANT CAVITY FIELD MODES

This appendix, for convenience, gives a brief summary of field modes (and their resonant frequencies) that occur in right cylindrical cavities (figure D.1.).

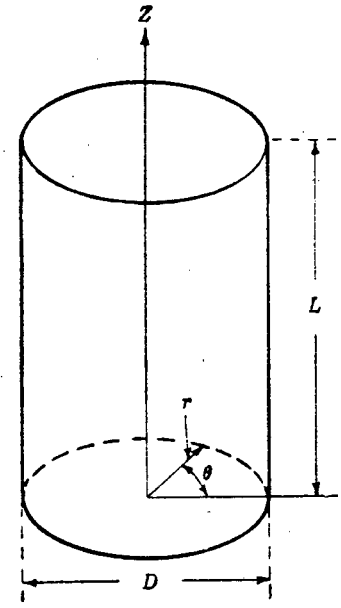

Figure D.1. Right Circular Cylinder

As in cylindrical waveguides, the normal modes may be divided into TE and TM classes. These are specified by the integers, *l*, *m*, and *n*, which define :

l ≡ number of full-period variations of E_r with respect to θ
m ≡ number of half-period variations of E_θ with respect to r
n ≡ number of half period variations of E_r with respect to z

for TE modes. For TM modes these correspond to components of **H** instead of **E**.

The resonant frequencies of the modes are all given by the equation [32] :

$$f_{lmn} = \tfrac{1}{2} \cdot c \cdot \sqrt{\{(2x_{lm}/\pi D)^2 + (n/L)^2\}},$$

where $x_{lm} \equiv m^{th}$ root of $J'_l(x) = 0$ for the TE-modes,
$x_{lm} \equiv m^{th}$ root of $J_l(x) = 0$ for the TM-modes.

The different resonant frequencies and their respective dependences on L and D are shown graphically in the mode chart in figure D.2.

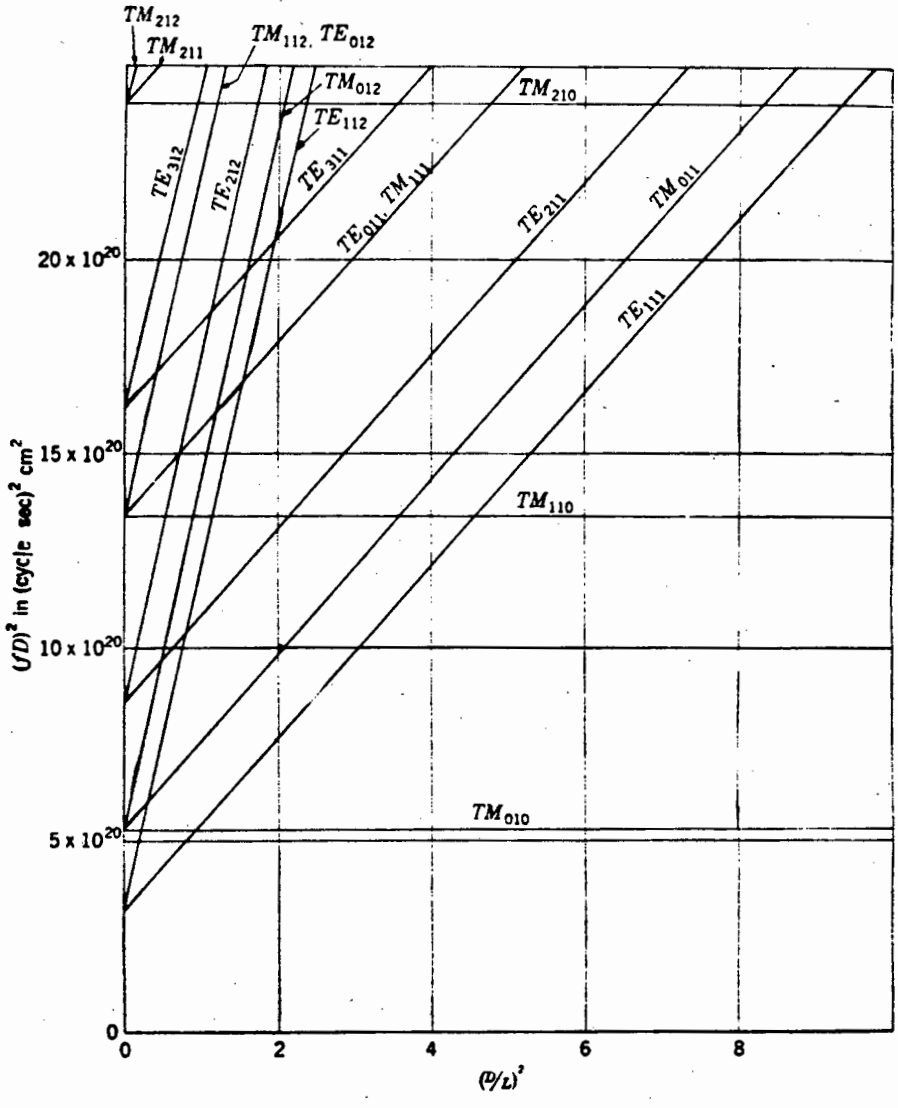

Figure D.2. Mode Chart for Right Circular Cylinder

The field modes are given by the following equations :

For TE modes :

$$E_r = -l\frac{J_l(k_1 r)}{k_1 r}\sin(l\theta)\sin(k_3 z)$$

$$E_\theta = -J'_l(k_1 r)\cos(l\theta)\cos(k_3 z)$$

$$E_z = 0$$

$$H_r = \frac{k_3}{k} J'_l(k_1 r)\cos(l\theta)\cos(k_3 z)$$

$$H_\theta = -l\frac{k_3}{k}\frac{J_l(k_1 r)}{k_1 r}\sin(l\theta)\cos(k_3 z)$$

$$H_z = \frac{k_1}{k} J_l(k_1 r)\cos(l\theta)\sin(k_3 z)$$

And for the TM modes :

$$E_r = -\frac{k_3}{k} J'_l(k_1 r)\cos(l\theta)\cos(k_3 z)$$

$$E_\theta = l\frac{k_3}{k}\frac{J_l(k_1 r)}{k_1 r}\sin(l\theta)\cos(k_3 z)$$

$$E_z = \frac{k_1}{k} J_l(k_1 r)\cos(l\theta)\sin(k_3 z)$$

$$H_r = -l\frac{J_l(k_1 r)}{k_1 r}\sin(l\theta)\cos(k_3 z)$$

$$H_\theta = -J'_l(k_1 r)\cos(l\theta)\cos(k_3 z)$$

$$H_z = 0$$

where $k_1 = 2x_{lm}/D$, $k_3 = n\pi/L$, $k^2 = k_1^2+k_2^2$, and $f = kc/2\pi$

If the modes have no dependence on θ they will be circularly symmetric.

APPENDIX E - CALCULATION OF PERMITTIVITY FOR CAVITY PERTURBATION

This appendix presents the formulae that were used in obtaining the complex permittivity values from measured resonant frequency and Q cavity perturbations. As mentioned in section 6.3.2.a), numerous solutions to this field problem have been published in the literature. The equations used in this study are those presented by S. Li, C. Akyel, and R. Bosisio [37]. Unlike other solutions that rely on approximations, these are complete and are valid for both low-loss and high-loss dielectrics. The equations are presented and briefly described. The curves of correction factors to compensate for end-hole effects [36] (as mentioned in section 6.3.2.b.) are also presented and discussed. To solve all these equations the computer package MathCAD was used. A listing of the MathCAD programme is also provided.

E.1. CAVITY PERTURBATION FORMULAE

The dimensions of the cavity are (see figure 6.7, section 6.3.2a) :

Cavity Radius = R_0
Inner Tube Radius = R_1
Outer Tube Radius = R_2
Height of Cavity = H

If the empty cavity resonates at f_u, then the effective Cavity Radius can be calculated from :

$$R_0 = \frac{c \cdot x_{01}}{2 \cdot \pi \cdot f_u} \qquad \text{where } x_{01} = 2.4048255$$

The dielectric constant of the measuring tube is:

$$\epsilon_2 = \epsilon_2' - j\epsilon_2''$$

Let the dielectric constant of the dielectric to be measured be:

$$\epsilon_1 = \epsilon_1' - j\epsilon_1''$$

When loaded the cavity resonates at the new frequency f_s.

The quality factors from the perturbation are:

Unloaded $Q = Q_0$

Loaded $Q = Q_s$

The wave-numbers in the relevant sections of the cavity are:

$$k_0 = 2\cdot\pi\cdot f_s/c \qquad k = k_0\cdot[1 + j\tfrac{1}{2}(1/Q_s - 1/Q_0)]$$

$$k_2 = \sqrt{\epsilon_2'}\cdot k_0 \qquad k_1^2 = k^2\cdot\epsilon_1 = \alpha^2 - j\beta^2 \qquad (1)$$

The equation to be solved is a complex series differential equation that arises from the electric field boundary conditions at the surface of the sample $r = R_1$. The equation is :

$$-\left.\frac{dE_z}{E_z\cdot dE_z}\right|_{r=Ro} = F^*(k,\epsilon_2,R_1,R_2,R_0) \qquad (2)$$

The field E_z is complex, ie. $E_z = E_z' + jE_z''$
where :

$$E_z' = J_0(\alpha r) - \frac{\beta^4 r^2}{8\alpha^2}\cdot J_2(\alpha r) + \frac{\beta^8 r^4}{384\alpha^4}\cdot J_4(\alpha r) \ldots.$$

$$E_z'' = \frac{r\beta^2}{2\alpha}\left[J_1(\alpha r) - \frac{\beta^4 r^2}{24\alpha^2}\cdot J_3(\alpha r) + \frac{\beta^8 r^4}{1920\alpha^4}\cdot J_5(\alpha r) \ldots.\right]$$

The right hand side of the field equation is a complex constant:

$$F^* = \sqrt{\epsilon_2}\cdot k\cdot\frac{F_1 - AF_2}{F_3 - AF_4}$$

where

$$B = \frac{Y_{000} - j\eta_o Y_{100}}{J_{000} - \tfrac{1}{2}\cdot\eta_o^2 J_{200} - j\eta_o J_{100}}$$

$$A = \sqrt{\epsilon_2}\cdot\frac{Y_{002} - j\eta_2 Y_{102} - B\cdot(J_{002} - j\eta_2 J_{102})}{Y_{102} + j\eta_2 Y'_{102} - B\cdot(J_{102} + j\eta_2 J'_{102})}$$

$$F_1 = J_{121}Y_{022} - Y_{121}J_{022} + j[\xi_1(Y_{022}J'_{121} - J_{022}Y'_{121}) + \xi_2(Y_{121}J_{122} - J_{121}Y_{122})]$$

$$F_2 = J_{121}Y_{122} - Y_{121}J_{122} + j[\xi_1(Y_{122}J'_{121} - J_{122}Y'_{121}) + \xi_2(Y'_{121}J_{121} - J'_{122}Y_{121})]$$

$$F_3 = J_{021}Y_{022} - Y_{021}J_{022} + j[\xi_1(Y_{121}J_{022} - J_{121}Y_{022}) + \xi_2(Y_{021}J_{122} - J_{021}Y_{122})]$$

$$F_4 = J_{021}Y_{122} - Y_{021}J_{122} + j[\xi_1(Y_{121}J_{122} - J_{121}Y_{122}) + \xi_2(Y'_{122}J_{021} - J'_{122}Y_{021})]$$

$$\eta_m = \frac{k_0 R_m}{2}\cdot(1/Q_s - 1/Q_0)$$

$$\xi_m = \sqrt{\epsilon'_2}\cdot\eta_m \qquad ,m = 1,2$$

and $J_{npq} = J_n(k_p R_q)$ & $Y_{npq} = Y_n(k_p R_q)$

$J'_{npq} = J'_n(k_p R_q)$ & $Y'_{npq} = Y'_n(k_p R_q)$

Equation (2) is solved iteratively for α and ß. These values are then substituted into (1) to obtain ϵ_1, the complex permittivity of the dielectric.

Once this value of permittivity has been determined, it must be corrected for the effects of the sampling tube holes. The formulae from [36], as described in section 6.3.2.b), can be used for this:

$$\epsilon_1' = 1 + (\epsilon'_{unc} - 1)\cdot(1 + 4CR_1/H)$$

$$\epsilon_1'' = \epsilon''_{unc}\cdot(1 - 4DR_1/H)$$

where ϵ'_{unc} and ϵ''_{unc} are the uncorrected measured values determined from above. The correction constants C and D have a complex dependence on ϵ'_1, ϵ'_2, and R_1/R_2. Rough values were used from the curves presented by [36], see figure E.1.

For $R_1/R_2 = 1$, ie. no glass tube, $C = D = 0.323$.

These are now the final values of permittivity for the dielectric.

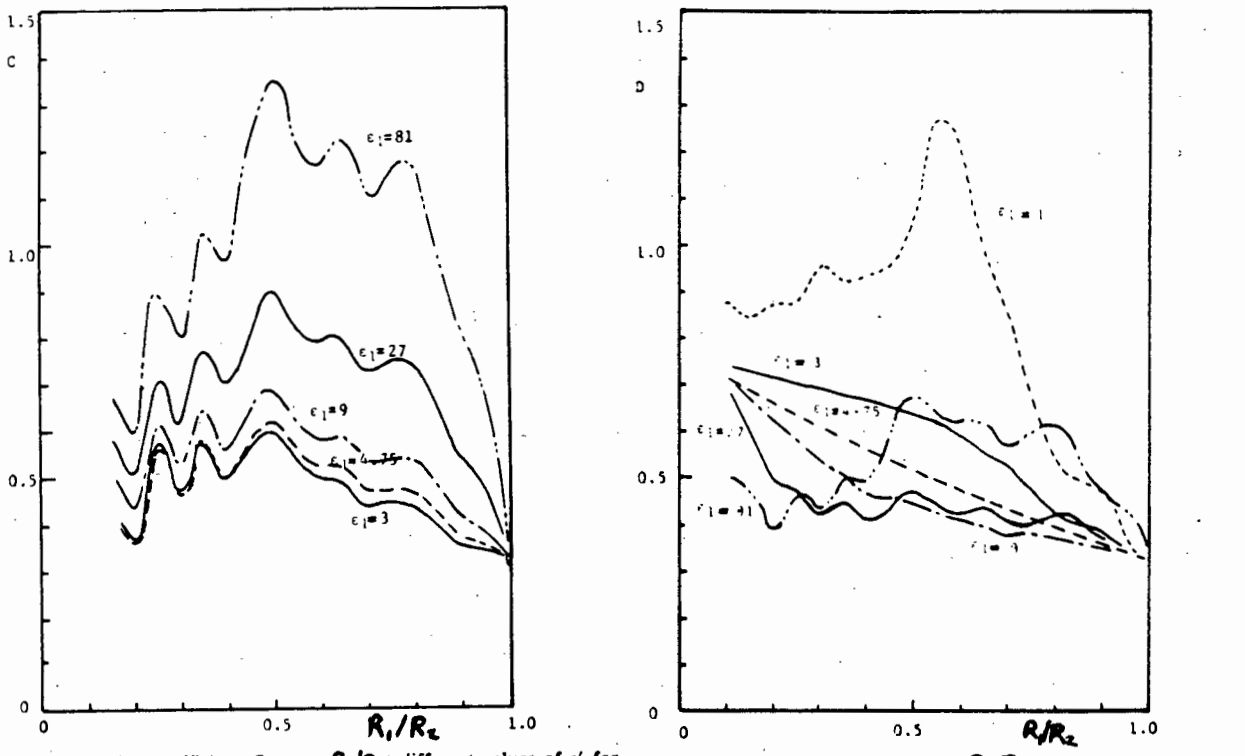

The correction coefficient C versus R_1/R_2 at different values of ϵ'_1 for $\epsilon_2 = 4.75$.

The correction coefficient D versus R_1/R_2 at different values of ϵ'_1 ($\epsilon_2 = 4.75$).

Figure E.1. Hole Correction Coefficients for ϵ' and ϵ''

E.2. NUMERICAL CALCULATION

The above equations were solved on MathCAD. A listing of the programme used is given below :

CALCULATION OF COMPLEX PERMITTIVITY FROM CAVITY PERTURBATION MEASUREMENTS

-USING MATHCAD PROGRAM

The MathCad program below uses the formulae presented in the paper:

S. Li, C. Akyel, R. Bossisio, "Precise Calculations and Measurements on the Complex Dielectric Constant of Lossy Materials Using TM0101 Cavity Perturbation Techniques," IEEE Trans. Microwave Theory Tech., Vol. MTT-29, No. 10, October 1981, pp1041-1048.

For convenience the below formula are referrenced to those in the above paper.

Resonant frequency of empty cavity : $f0 := 1.002703 \cdot 10^{9}$ [GHz]

Resonant frequency of loaded cavity : $f1 := 0.993353 \cdot 10^{9}$ [GHz]

Q of empty cavity : $Q0 := 4676$

Q of loaded cavity : $Q1 := 3126$

Speed of light : $c := 2.9979 \cdot 10^{8}$

Bessel root : $x01 := 2.4048255$

Effective radius of cavity : $R0 := \left[\frac{c \cdot x01}{\pi \cdot f0 \cdot 2}\right]$

$R0 = 0.114432$ [m]

Outer radius of tube : $R2 := 0.005$ [m]

Inner radius of tube : $R1 := 0.004$ [m]

Height of Cavity : $H := 0.12$ [m]

Complex permittivity of tube : $\epsilon 2c := 4.51 - 0.05 \cdot j$

Equations (14.11) : $\epsilon 2r := Re(\epsilon 2c)$ (Split into real and imaginary parts)

$\epsilon 2i := -Im(\epsilon 2c)$

Define higher order Bessel Functions :

$J2(x) := Jn(2,x)$ $J3(x) := Jn(3,x)$ $Y2(x) := Yn(2,x)$

Define Bessel function derivatives :

$\delta J1(x) := \frac{1}{2} \cdot (J0(x) - J2(x))$ $\delta Y1(x) := \frac{1}{2} \cdot (Y0(x) - Y2(x))$

$k0 := 2 \cdot \pi \cdot \frac{f1}{c}$ Free space wave number - equ. (6.3)

$k2 := \sqrt{\epsilon 2r \cdot k0}$

$\delta Q := \left[\frac{1}{Q1} - \frac{1}{Q0}\right]$

Equations (14.3) :

$$eta0 := \left[k0 \cdot \frac{R0}{2}\right] \cdot \delta Q \qquad eta2 := \left[k0 \cdot \frac{R2}{2}\right] \cdot \delta Q \qquad eta1 := \left[k0 \cdot \frac{R1}{2}\right] \cdot \delta Q$$

Equations (14.10) :

$$zeta0 := \sqrt{\epsilon 2r} \cdot eta0 \qquad zeta2 := \sqrt{\epsilon 2r} \cdot eta2 \qquad zeta1 := \sqrt{\epsilon 2r} \cdot eta1$$

$$k := k0 \cdot \left[1 + \frac{\delta Q}{2} \cdot j\right] \qquad \text{Equation (14.12)}$$

Define functions Jnpq and Ynpq :

```
J000 := J0(k0·R0)    J001 := J0(k0·R1)    J002 := J0(k0·R2)    J022 := J0(k2·R2)
Y000 := Y0(k0·R0)    Y001 := Y0(k0·R1)    Y002 := Y0(k0·R2)    Y022 := Y0(k2·R2)
J100 := J1(k0·R0)    J102 := J1(k0·R2)    J121 := J1(k2·R1)    J122 := J1(k2·R2)
Y100 := Y1(k0·R0)    Y102 := Y1(k0·R2)    Y121 := Y1(k2·R1)    Y122 := Y1(k2·R2)
J021 := J0(k2·R1)    Y021 := Y0(k2·R1)    J200 := J2(k0·R0)
```

Define functions J'lpq and Y'lpq :

```
δJ101 := δJ1(k0·R1)   δJ121 := δJ1(k2·R1)   δJ122 := δJ1(k2·R2)
δY101 := δY1(k0·R1)   δY121 := δY1(k2·R1)   δY122 := δY1(k2·R2)
δY102 := δY1(k0·R2)   δJ102 := δJ1(k0·R2)
```

Equations (14.6) to (14.9) :

```
F1 := J121·Y022 - Y121·J022
F2 := J121·Y122 - Y121·J122
F3 := J021·Y022 - Y021·J022
F4 := J021·Y122 - Y021·J122

F1 := F1 + (zeta1·(Y022·δJ121 - J022·δY121) + zeta2·(Y121·J122 - J121·Y122))·j
F2 := F2 + (zeta1·(δJ121·Y122 - J122·δY121) + zeta2·(δY122·J121 - δJ122·Y121))
F3 := F3 + (zeta1·(Y121·J022 - J121·Y022) + zeta2·(J122·Y021 - Y122·J021))·j
F4 := F4 + (zeta1·(J122·Y121 - J121·Y122) + zeta2·(J021·δY122 - Y021·δJ122))·j
```

$$B := \left[\frac{Y000 - eta0 \cdot Y100 \cdot j}{J000 - \frac{eta0^2}{2} \cdot J200 - eta0 \cdot J100 \cdot j}\right] \qquad \text{Equation (14.4)}$$

$$B = 43.786355 + 0.246764j$$

$$A := \sqrt{\epsilon 2c} \cdot \left[\frac{Y002 - j \cdot eta2 \cdot Y102 - B \cdot (J002 - j \cdot eta2 \cdot J102)}{Y102 + j \cdot eta2 \cdot \delta Y102 - B \cdot (J102 + j \cdot eta2 \cdot \delta J102)}\right] \qquad \text{Equation (14.5)}$$

$$Fb := \sqrt{\epsilon 2c} \cdot k \cdot \left[\frac{F1 - A \cdot F2}{F3 - A \cdot F4}\right] \qquad \text{Equation (14.2) and RHS of (13)}$$

$$Er(\alpha, \beta, r) := J0(\alpha \cdot r) - \left[\frac{\beta^4 \cdot r^2}{8 \cdot \alpha^2}\right] \cdot J2(\alpha \cdot r) \qquad \text{Equation (10.1)}$$

$$Ei(\alpha,\beta,r) := \left[\frac{r^2\cdot\beta^2}{2\cdot\alpha}\right]\cdot\left[J1(\alpha\cdot r) - \left[\frac{\beta^4\cdot r^2}{24\cdot\alpha^2}\right]\cdot J3(\alpha\cdot r)\right] \qquad \text{Equation (10.2)}$$

$$Ec(\alpha,\beta,r) := Er(\alpha,\beta,r) + Ei(\alpha,\beta,r)\cdot i \qquad \text{Equation (10)}$$

$$LHS(\alpha,\beta,r) := \left[\frac{-1}{Ec(\alpha,\beta,r)}\right]\cdot\frac{d}{dr}Ec(\alpha,\beta,r) \qquad \text{LHS of equation (13)}$$

Split equation (13) into real and imaginary parts :

$LHSr(\alpha,\beta) := Re(LHS(\alpha,\beta,R1))$
$LHSi(\alpha,\beta) := Im(LHS(\alpha,\beta,R1))$

$Fbr := Re(Fb)$
$Fbi := Im(Fb)$

$\alpha 1 := 30 \qquad \beta 1 := 0.5$ Initial starting values

Given

$LHSr(\alpha 1,\beta 1) \approx Fbr$ Solve equation (13)
$LHSi(\alpha 1,\beta 1) \approx Fbi$

$\begin{bmatrix}\alpha\\ \beta\end{bmatrix} := Find(\alpha 1,\beta 1)$ Solutions α and β

$$\epsilon c := \frac{\alpha^2 - \beta^2\cdot i}{k^2} \qquad \text{Equation (8.1)}$$

Calculated Complex Permittivity : $\epsilon c = 3.080242 - 0.008499j$

THE PROGRAMME NOW CORRECTS FOR THE EFFECTS OF THE HOLE :
==========

The method used is described in the paper :

S. Li, R. Bossisio, "Composite Hole Conditions on Complex Permittivity Using Microwave Cavity Perturbation Techniques", IEEE Trans. Microwave Theory Tech., Vol. MTT-30, No. 1, January 1982, pp.100-103.

The correct correction factors should be obtained from curves Fig. 2 & 3 in the above paper. Hints: if no tube is used C=D=0.327. If a glass tube with R1/R2=0.8 is used and ϵ is about 3 to 9 use C=0.45 to .55 resp., and D=0.4

eg. Rough Approx. : $c := 0.43 + (Re(\epsilon c) - 3)\cdot 0.02$

$$C := 0.323 + (c - 0.323)\cdot 5\cdot\left[1 - \frac{R1}{R2}\right]$$

$$D := 0.323 + \left[1 - \frac{R1}{R2}\right]\cdot 5\cdot 0.077$$

$C = 0.431605$ Accept these approx. values, or
$D = 0.4$ define new ones !

Correction Formulae :

$$\epsilon r := 1 + (Re(\epsilon c) - 1) \cdot \left[1 + 4 \cdot C \cdot \frac{R1}{H}\right] \qquad \text{Equation (13)}$$

$$\epsilon i := -Im(\epsilon c) \cdot \left[1 - 4 \cdot D \cdot \frac{R1}{H}\right] \qquad \text{Equation (14)}$$

THE FINAL VALUE FOR THE COMPLEX PERMITTIVITY IS:

Dielectric Constant : $\epsilon r = 3.199955$
Loss Factor : $\epsilon i = 0.008045$

THE END

APPENDIX F - DETAILS OF CAVITY PERTURBATION EXPERIMENTAL SET-UP AND MEASUREMENT

This appendix describes the cavity test set-up interface and the measurement procedure, calculations and computer programme used. These are discussed under their separate headings below.

F.1. INTERFACE DESCRIPTION

The block diagram of the overall system is shown in figure 6.8, section 6.3.3. The frequency counter enables accurate measurement of the signal generator frequency to be made by sampling the signal through a -20 dB coupler. The HPIB interface thus allows the PC to step the frequency on the signal generator and to accurately measure it through the frequency counter.

The cavity is connected to the HP s-parameter test set and its transfer characteristic (s_{21}) is measured by the PC from the magnitude analogue output of the network analyser, via signal conditioning circuitry, by a 12-bit ADC on-board the PC.

The signal conditioning circuitry is shown in figure F.1. This scales the network analyser's 50 mV/dB signal output to the required ±5 V range for the ADC. The input stage is a simple unitary gain differential amplifier used to provide common-mode noise rejection from the interface lines (two-core shielded coax.). This is followed by a simple Butterworth 2nd order low-pass 100 Hz filter to suppress noise prior to sampling. The output stage provides the necessary amplification. The output is limited to ±5 V (by zener diodes) to protect the ADC input. The ±8 V supply is obtained (through regulators and filter capacitors) from the ±12 V supply of the ADC PC26 card.

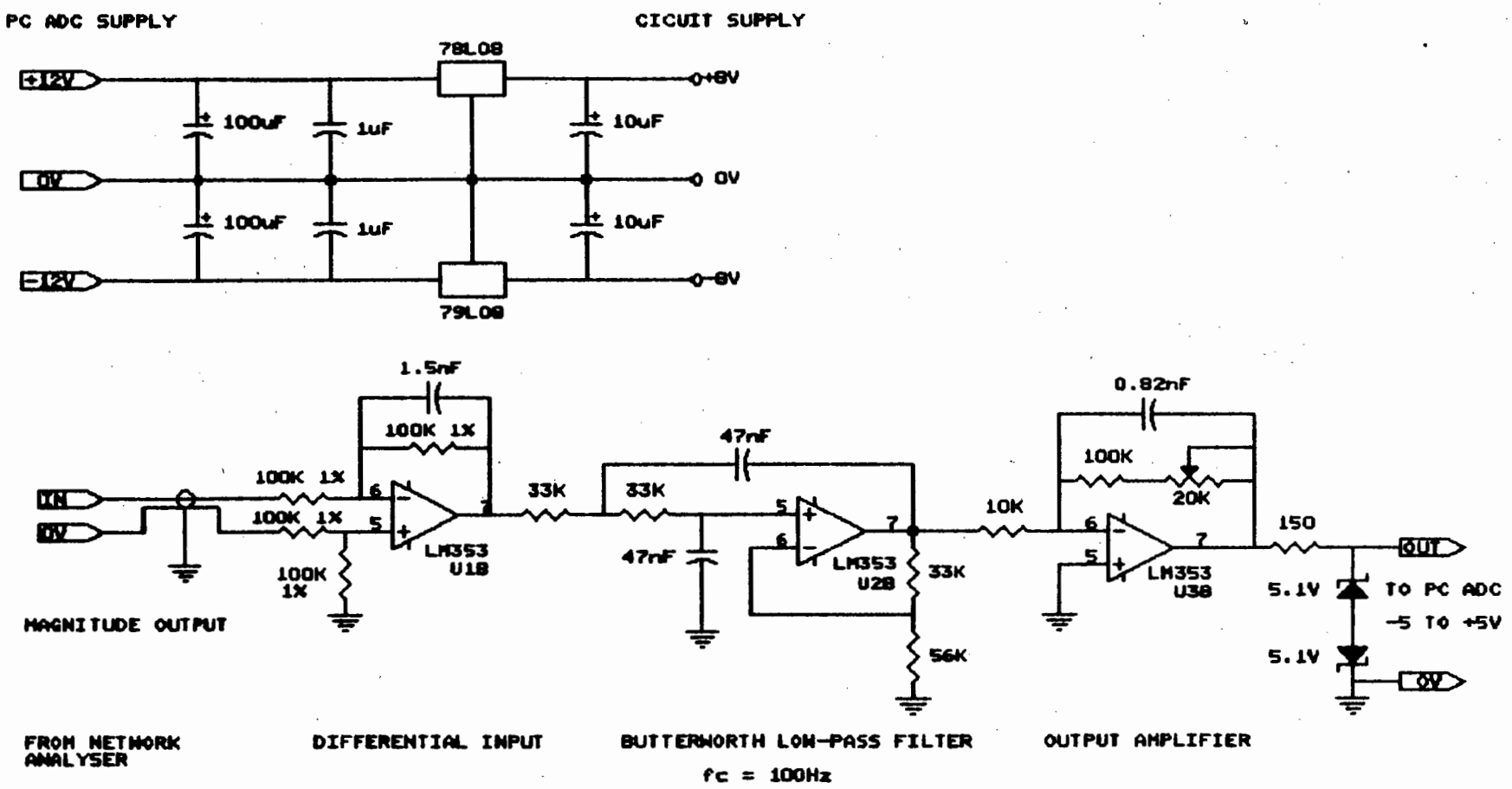

Figure F.1. Interface Circuitry for Cavity Measurement Setup

F.2. MEASUREMENT PROCEDURE

As described in section 6.3.3., the computer steps the signal generator in 100 KHz steps across the resonant response. At each point the frequency and magnitude are recorded. The computer then finds a least-squares fit between these measured data points and the theoretical response formula (see figure 6.9, section 6.3.3.). Using a logarithmic scale the mean square error between the theoretical curve and measured data is :

$$\text{Error} = \frac{1}{N} \cdot \Sigma\{S_{21(db)i} - 20\log[K/\sqrt{((w_i - w_o)^2 + (w_o/2Q)^2)}]\}^2$$

where i = 1...N are the data point indices with the measured data points $S_{21(dB)i}$ at their corresponding frequencies w_i.

Where $S_{21(db)i}$ are the measured data points (in dB's) corresponding to the frequencies w_i. The three parameters: w_o the resonant frequency, Q and K (offset) are then optimised in order to minimise this error. A simple alternate variable optimisation routine was used. These optimised values provide an "optimum best fit"; w_o and Q thus being the measured resonant frequency and quality factor of the cavity. The fit between the theoretical and measured responses was extremely good; a mean square error of less than 0.0001 being consistently achieved.

A listing of the computer programme subroutines used to perform the measurements and optimisation calculations are given below.

F.3. COMPUTER PROGRAMME

```
'***   QBASIC4 PROGRAMME TO TAKE CAVITY MEASUREMENTS ***'
'***   AND DETERMINE W0 AND Q BY OPTIMISATION        ***'
'***   G. PENDOCK - THESIS                           ***'
'***   USES QBASIC4 HPIB LIBRARY                     ***'

'ROUTINES :- '

DECLARE SUB difference (f0!, Q!, C!, number%, count!(), magnitude!(),
delta!)
DECLARE SUB theory (f!, f0!, Q!, C!, loss!)
DECLARE SUB evaluate (pnt%, number%, count!(), magnitude!(), Q!,
Resonance!, delta!)
DECLARE SUB scale (pnt%, number%, count!(), magnitude!())
DECLARE SUB storage (number%, count!(), magnitude!())
DECLARE SUB rate (Reading!)
DECLARE SUB delay (pause%)
DECLARE SUB measure (number%, count!(), magnitude!())
DECLARE SUB welcome ()
DECLARE SUB initialise ()
DECLARE SUB sample (Reading!)

'******** MAIN PROGRAMME *********
OPTION BASE 0
DIM magnitude!(200), count!(200)
CLS                              'clear screen
isc& = 7                         'HPIB interface code
sweeper& = 719                   'sweep generator address
counter& = 714                   'frequency counter address
CALL initialise                  'initialise interfaces
CALL welcome                     'prompt user to set N.A.
'take measurements across frequency
CALL measure(number%, count!(), magnitude!())
CALL initialise                 'reset interface
CALL scale(pnt%, number%, count!(), magnitude!())
'solve for resonant freq. and Q
CALL evaluate(pnt%, number%, count!(), magnitude!(), Q!, Resonance!,
delta!)
CLS
PRINT
PRINT "Measured Q = "; Q!
PRINT "Measured Resonance = "; Resonance!
PRINT "Mean Square Error = "; delta!
PRINT
PRINT "Frequency", "", "Measured", "Best Fit"
PRINT "---------", "", "--------", "--------"
FOR n% = 0 TO number%
 CALL theory(count!(n%), Resonance!, Q!, C!, loss!)
 PRINT count!(n%); "GHz", magnitude!(n%); "dB", loss!; "dB"
NEXT n%
END
```

```
'** PROGRAMME SUBROUTINES :-

'*********************************************************
SUB delay (pause%) STATIC ' routine to provide a delay

FOR n = 1 TO pause%       ' delay
NEXT n
END SUB

'*********************************************************
SUB difference (f0!, Q!, C!, number%, count!(), magnitude!(), delta!)
STATIC
'calculate mean square diff between theory and measured

total! = 0!
FOR n% = 0 TO number%
  CALL theory(count!(n%), f0!, Q!, C!, loss!)
  total! = total! + (magnitude!(n%) - loss!) ^ 2
NEXT n%
 delta! = total! / (number% + 1)
END SUB

'*********************************************************
SUB evaluate (pnt%, number%, count!(), magnitude!(), Q!, Resonance!,
delta!) STATIC
'routine to calculate the resonant frequency and Q

Q! = 4800!                  'STARTING VALUES
Resonance! = count!(pnt%)
C! = 0!
PRINT
PRINT "SORTED DATA"
PRINT "============"
PRINT
PRINT "Point", "Frequency", "", "Loss (S21)"
PRINT "-----", "---------", "", "----------"
FOR n% = 0 TO number%
 CALL theory(count!(n%), Resonance!, Q!, C!, loss!)
 PRINT n%, count!(n%); "GHz", magnitude!(n%); "dB"
NEXT n%
CALL difference(Resonance!, Q!, C!, number%, count!(), magnitude!(),
delta!)
PRINT "Error="; delta!

'******* NOW TO OPTIMISE! *******
PRINT "Optimising......";
Qresolution! = 1!           '1
resonanceresolution! = 500!   '500
Cresolution! = .0005        '.0005
terminate! = .0001 '.00005
CALL difference(Resonance!, Q!, C!, number%, count!(), magnitude!(),
delta!)
newvalue! = delta!
```

```
n% = 0

WHILE ABS(value! - newvalue!) > terminate!
  value! = newvalue!
  n% = n% + 1

'** optimise Q **
   Qstep! = 50 / (n% * n%)
   WHILE ABS(Qstep!) > (Qresolution! / (n% * n%))
     temp! = newvalue!
     Q! = Q! + Qstep!
     CALL difference(Resonance!, Q!, C!, number%, count!(),
     magnitude!(), delta!)
     newvalue! = delta!
     IF newvalue! > temp! THEN Qstep! = -Qstep! / 2
     PRINT ".";
   WEND

'** optimise resonance **
  resonancestep! = 10000 / n%
  WHILE ABS(resonancestep!) > (resonanceresolution! / n%)
  temp! = newvalue!
  Resonance! = Resonance! + resonancestep!
  CALL difference(Resonance!, Q!, C!, number%, count!(),
    magnitude!(), delta!)
  newvalue! = delta!
 F newvalue!>temp! THEN resonancestep! = -resonancestep!/2
  PRINT ".";
WEND

'** optimise offset **
  Cstep! = .01 / n%
  WHILE ABS(Cstep!) > (Cresolution! / n%)
  temp! = newvalue!
  C! = C! + Cstep!
  CALL difference(Resonance!, Q!, C!, number%, count!(),
    magnitude!(), delta!)
  newvalue! = delta!
  IF newvalue! > temp! THEN Cstep! = -Cstep! / 2
  PRINT ".";
WEND
WEND
PRINT
BEEP
END SUB

'*********************************************************
SUB initialise STATIC
SHARED sweeper&, counter&
' subroutine to initialise all interfaces

 OUT &H703, &H92              'set ADC 8255
 CALL ioremote(sweeper        'place sweeper in remote mode
 CALL ioremote(counter&)      'place counter in remote mode
```

```
 CALL iooutputs(counter&, "smooth,off", 10)  'filter off
 CALL iooutputs(counter&, "resol,3", 7)      '1kHz resolution
 CALL iooutputs(counter&, "sample,hold", 11) 'triggered mode
 CALL iooutputs(sweeper&, "tl", 2)           'internal trigger
 CALL iooutputs(sweeper&, "pl9.0dm", 7)      'power level 9dBm
 CALL iooutputs(sweeper&, "st0.02sc", 8)     'swweep time 0.1s
 CALL iooutputs(sweeper&, "fbl.003gz", 9)    'stop at 1.004GHz
 CALL iooutputs(sweeper&, "fa990mz", 9)      'start at 1.00GHz
END SUB

'*************************************************
SUB measure (number%, count!(), magnitude!()) STATIC
'sweep frequency and measure response
SHARED sweeper&, counter&

 decrease! = .0001          'freq decrement interval
 beginning! = 1.006         'beginning of sweep
 decrement% = 4
 m% = -1
 n% = 0
 limit! = 200               'take points above limit!
 flag% = 1                  'flag to check for termination
 PRINT "MEASURED DATA"
 PRINT "=============="
 PRINT
 PRINT "Point", "Frequency", "", "ADC Reading"
 PRINT "-----", "---------", "", "-----------"
 WHILE flag% = 1
  frequency! = beginning! - n% * decrease! 'calc freq
    code$ = STR$(frequency!)    'convert to string
    code$ = RIGHT$(STR$(frequency!), LEN(code$) - 1)
    code$ = "cw" + code$ + "gz"   'convert to HPIB code
    CALL iooutputs(sweeper&, code$, LEN(code$))  'send to
         sweeper
    CALL delay(700)                'allow sweeper to settle
    CALL sample(magnitude!(n%))   'measure magnitude via ADC
    IF magnitude!(n%) > limit! THEN
        m% = m% + 1
        decrement% = 1
        magnitude!(m%) = magnitude!(n%)
        CALL rate(count!(m%))            'measure frequency
        PRINT m%, count!(m%); " GHz", magnitude!(m%)
    END IF
    IF magnitude!(n%) < magnitude!(0) AND decrement% = 1 THEN flag% = 0

n% = n% + decrement%
WEND
number% = m%            'number of data points collected
END SUB

'*****************************************************
SUB rate (Reading!)
'subroutine to take frequency measurement from counter
SHARED counter&
```

```
total! = 0
number% = 8                    'take 8 readings
FOR n% = 1 TO number%
  CALL iotrigger(counter&)     'trigger counter to measure
  CALL ioenter(counter&, count!)     'get reading
  total! = total! + count!           'total readings
NEXT n%

 Reading! = total! / number%           'take average
END SUB

'*******************************************************
SUB sample (Reading!) STATIC
' subroutine to take ADC reading of magnitude

channel% = 1         'ADC channel 1 to be sampled
number% = 500        'number of samples to be taken
total& = 0
FOR i = 1 TO number%
 OUT &H702, 2                'clear ADC
 OUT &H702, channel% * &H10 + 3 'start conversion
   FOR d = 1 TO 5
     'delay for EOC
   NEXT d
 value% = (INP(&H701) AND &HF) * 256 + INP(&H700)  'total samples
 total& = total& + value%
NEXT i
Reading! = total& / number%   'take average
END SUB

'*******************************************************
SUB scale (pnt%, number%, count!(), magnitude!()) STATIC
'calculate maximum value and scale to dB

scaling! = 204                  'points per dB
maximimum! = 0
pnt% = 0
FOR n% = 0 TO number%
  IF magnitude!(n%) > maximum! THEN   'find maximum
    maximum! = magnitude!(n%)
    pnt% = n%
  END IF
NEXT n%

'scale to dB
FOR n% = 0 TO number%
 magnitude!(n%) = (magnitude!(n%) - maximum!) / scaling!
NEXT n%

m% = -1
FOR n% = 0 TO number%
 IF magnitude!(n%) > -10 THEN
  m% = m% + 1
```

```
  magnitude!(m%) = magnitude!(n%)
  count!(m%) = count!(n%)
END IF
NEXT n%
number% = m%
maximum! = -10
pnt% = 0
FOR n% = 0 TO number%
  IF magnitude!(n%) > maximum! THEN    'find maximum
    maximum! = magnitude!(n%)
    pnt% = n%
  END IF
NEXT n%

END SUB

'*****************************************
SUB theory (f!, f0!, Q!, C!, loss!) STATIC
' calculate theoretical resonance response

a! = (f0! / (2 * Q!)) ^ 2
loss! = -4.34294 * LOG(((f! - f0!) ^ 2 + a!) / a!) + C!
END SUB

'*******************************************************
SUB welcome STATIC
 'prompt user to set Network Analyser to required settings

 PRINT "AUTOMATIC RESONANT CAVITY MEASUREMENTS"
 PRINT "======================================="
 PRINT
 PRINT "                      by Graeme Pendock"
 PRINT
 PRINT "Network analyser settings:"
 PRINT
 PRINT " 1: Channel Gain = 30 dB"
 PRINT " 2: Amplitude Adjust Fully Counter-Clockwise"
 PRINT " 3: Screen Gain at 2.5 dB/div"
 PRINT
 PRINT
 PRINT "To continue press return"
 INPUT a$          'wait for return
 CLS               'clear screen
END SUB
'*****************************************
```